2011

Fabrication Of Pd-Cu Membranes By Surfactant Induced Electroless Plating (Siep)

Md. Saiful Islam
North Carolina Agricultural and Technical State University

FABRICATION OF Pd-Cu MEMBRANES BY SURFACTANT INDUCED ELECTROLESS PLATING (SIEP)

by

Md. Saiful Islam

A thesis submitted to the graduate faculty
in partial fulfillment of the requirements for the degree of
MASTER OF SCIENCE

Department: Chemical & Bioengineering
Major: Chemical Engineering
Major Professor: Dr. Shamsuddin Ilias

North Carolina A&T State University
Greensboro, North Carolina
2011

School of Graduate Studies
North Carolina Agricultural and Technical State University

This is to certify that the Master's Thesis of

Md. Saiful Islam

has met the thesis requirements of
North Carolina Agricultural and Technical State University

Greensboro, North Carolina
2011

Approved by:

Dr. Shamsuddin Ilias Major Professor	Dr. Vinayak N. Kabadi Committee Member
Dr. Debasish Kuila Committee Member	Dr. Leonard C. Uitenham Department Chairperson

Dr. Sanjiv Sarin
Dean of Graduate Studies

DEDICATION

To

My Mother Jobeda Begum

My Father Md. Shafiq Ullah

My Sister Sabrina Shafiq

My Brother Faisal Mahmud

And

My Nephew Raian Jawad Khan

BIOGRAPHICAL SKETCH

Md. Saiful Islam was born on December 25, 1980, in Noakhali, Bangladesh. He received the Bachelor of Science degree in Chemical Engineering from Bangladesh University of Engineering and Technology (BUET) in November, 2004. Then he worked for H. P. Chemicals Bangladesh, Chevron Bangladesh, Unilever Bangladesh and Bangladesh Development Bank Limited for almost four years in different responsible positions. He joined in the Master of Science program in Chemical Engineering in fall, 2008 as a research assistant. He is a candidate for Master of Science in Chemical Engineering.

ACKNOWLEDGMENT

I am blessed to have the trust and support of a number of people and organizations while working on this research.

I express my sincere gratitude to my advisor Dr. Shamsuddin Ilias, for his encouragement, financial support and guidance with formulating and advancing this research. He has provided me with useful guidelines and suggestions at various steps and kept trust in me all the way.

I would like to thank Analytical Instrumentation Facility (AIF), North Carolina State University, for allowing me to use the VPSEM and AFM instrument. Specially, I thank them for their valuable opinion during the characterization of my research materials.

Special thanks to North Carolina A&T State University for its financial support without which, I couldn't carry out this research.

Special gratitude goes to my parents Md. Shafiq Ullah and Jobeda Begum for inspiring me all through my life. Their continuous inspiration has given me enthusiasm and courage at all walks of the life.

Thanks to my beloved country Bangladesh, for its promise to educate and raise me. She has given me the strong foundation to face the world.

Finally, my heartfelt gratitude goes to Almighty Allah, for giving me this life and ability to conduct this research.

TABLE OF CONTENTS

LIST OF FIGURES

FIGURES **PAGE**

LIST OF TABLES

TABLES **PAGE**

LIST OF SYMBOLS

N_H	Flux (mol/m^2-s)
Q_H	Permeability (mol/m-s-psi^n)
Q_{Ho}	Pre-exponent factor (mol/m-s-psi^n)
P_f	Feed side pressure (psi)
P_p	Permeate side pressure (psi)
t	Membrane thickness (μm)
n	Pressure exponent/Power index
E	Activation energy (KJ/mol)
R	Universal gas constant (KJ/mol-K)
2θ	X-ray beam incident angle
d	Lattice spacing (Å)
a	Lattice parameter (Å)
nm	Nanometer (10^{-9} meter)
pm	Picometer (10^{-12} meter)
μm	Micrometer (10^{-6} meter)
Å	Angstrom (10^{-10} meter)
P_{H_2}	Partial pressure of hydrogen (MPa)
η	Hydrogen to Palladium ratio (H_2: Pd)
wt%	Weight percent
L	Liquid phase

αFe	α Iron phase
βFe	β Iron phase
γFe	γ Iron phase
K	1000x magnification
kV	Kilo electron volt
KJ	Kilo Joule
MPa	Mega Pascal
T_{Tamman}	Tamman temperature (K)
Pd_{Tamman}	Tamman temperature of Pd
Cu_{Tamman}	Tamman temperature of Cu

ABSTRACT

Islam, Md. Saiful. FABRICATION OF Pd-Cu MEMBRANES BY SURFACTANT INDUCED ELECTROLESS PLATING (SIEP). **(Major Advisor: Dr. Shamsuddin Ilias)**, North Carolina Agricultural and Technical State University.

Pd-Cu composite membranes on microporous stainless steel substrate (MPSS) were fabricated by novel electroless plating (EP) process. In conventional Pd-EP process, the oxidation-reduction reactions between Pd-complex and hydrazine result in evolution of NH_3 and N_2 gas bubbles. When adhering to a substrate surface and in the pores, these gas bubbles can hinder uniform Pd-film deposition, which results in dendrite growth leading to poor film formation. We addressed this problem by introducing cationic surfactant in the electroless plating process known as surfactant induced electroless plating (SIEP). The unique features of this innovation provide control of (1) Pd- and Cu-deposition rate, and (2) Pd- and Cu-grain size distribution. The surfactant molecules play a key role in the plating process in tailoring grain size and the process of agglomeration by removing tiny gas bubbles through adsorption at the gas-liquid interface. The water soluble surfactants which have near neutral hydrophilic-lipophilic balance (HLB) value, apparently have a stronger capability of removing gas bubbles from the substrate surface and the pores. To verify the improvement of membrane performance after introducing surfactant in bath solution, Pd-Cu membranes are fabricated by both conventional electroless plating (CEP) and surfactant induced electroless plating (SIEP). The pre- and post-annealing characterizations of these membranes (Pd-Cu on MPSS substrate) were carried out by SEM, XRD, EDX, and AFM studies. The SEM images showed a

significant improvement of the membrane surface morphology, in terms of metal grain structures and grain agglomeration compared to the membranes fabricated by conventional EP process. The SEM images and helium gas-tightness studies indicated that dense and thinner films of Pd-Cu membranes can be produced with shorter deposition time using surfactant. From cross-sectional SEM and EDX studies, the alloying of Pd-Cu was confirmed at the annealing condition of about 773 K with different annealing time in hydrogen environment. These membranes were also studied for hydrogen perm-selectivity as a function of temperature and feed pressure. Finally, long term thermal stability of Pd-Cu membrane fabricated by SIEP method was tested as a function of H_2 flux.

CHAPTER 1
Introduction

Recent international concerns regarding the climate change has prompted carbon cap and trade agreements and sparked interest in emission free energy productions. In addition to its many uses in the chemical and petrochemical industries, hydrogen (H_2) has the potential of being a sustainable "emission free" energy carrier. In recent years, there has been growing demand for high-purity H_2 in electronics manufacturing industries. Another important, not yet fully capitalized aspect of hydrogen is its enormous potential as energy carrier. Currently, various fuel cell technologies are at various stages of development, which offer a promise of green energy. For automotive and stand-alone power-generation applications, PEMFC (Proton-Exchange Membrane Fuel Cell) technology is being considered a serious contender. In PEMFC, high-purity hydrogen is a fuel of choice. For successful implementation of PEMFC in these applications, availability of high-purity hydrogen at a competitive price has to be assured. This has opened new opportunities in developing technologies for production and separation of hydrogen with 99.99% purity.

Hydrogen (H_2), although the most abundant element in the universe, on earth hydrogen (H_2) is mostly found chemically bonded. Chemical reactions are then necessary to break apart those bonds and free the hydrogen. Commercial bulk hydrogen is generally produced by the steam reforming or partial oxidation of alcohol or natural gas (methane or ethane) at high temperature and pressure. However, in doing so, several other gases are

formed, creating multi-component gas stream known as synthesis gas (syngas). Typically, this syngas contains H_2, CO, CO_2, CH_4, and N_2. Regardless of the production procedure, H_2 needs to be separated from syngas for its end use. Depending on the application, there are different technologies available among which cryogenic separation, pressure swing adsorption, polymeric membrane and so on, are at various stages of commercial exploitation. However, technologies for high-purity (99.9999%) separation of H_2 at process conditions are not yet available. In this regard, inorganic membranes are thought to be a strong contender.

Metal membranes with high perm selectivity for hydrogen and having good thermal, chemical and mechanical properties are widely used. Of these metals, Palladium (Pd) is predominantly used because of its high hydrogen permeability and compatibility with other gases in the mixture, for inorganic membranes [1-10]. Preparing the membrane involves deposition of the Pd or Pd-alloy film onto a substrate. This Pd- or Pd-alloy has high hydrogen solubility that allows high hydrogen throughput. The diffusivity of other gases is extremely small and can be ignored. Thus, theoretically, these membranes have infinite hydrogen selectivity and can function as a filter. Also, Pd- or Pd-alloy membranes are stable at high temperature and pressure. Production of H_2 by steam reforming or partial oxidation of alcohols or natural gas is thermodynamically rate limiting. Reforming reactions are also energy intensive. Currently, all the technologies for H_2 production require a reformer followed by a separation unit. Syngas is cooled in a condenser before allowing the gas mixture into the separator. The use of membrane based reactor allows tremendous flexibility for simultaneous production and separation of

hydrogen. It is easy to configure Pd-membranes into membrane-reactor. As Pd membranes are highly selective to hydrogen compared to other gases (CO, CO_2, N_2), the use of a membrane reactor facilitates the removal of hydrogen during reforming reaction from both unreacted and produced gases. Removal of H_2 from the reaction mixture shifts the equilibrium to the right, which increases the conversion of the reaction. Thus, membrane reactor eliminates the cooling and separation units. These advantages of Pd and Pd-alloy based membranes drew researchers' attention to fabricate robust membranes with high throughput of hydrogen. However, fabrication of thermally stable, defect-free robust membrane is still a challenge.

Palladium and its alloy, as well as, Ni, Pt and the metals in Groups III-V in the periodic table are all permeable to hydrogen [11]. However, pure Pd membranes suffer from embrittlement due to the α-phase to β-phase transition during hydrogen absorption, which often causes destruction of the membrane structure [11]. They also suffer from poisoning due to hydrogen sulfide, sulfur contaminants and carbon monoxide, when exposed to sulfur based gases. For these reasons, Pd membranes were alloyed with other metals such as silver (Ag), copper (Cu), gold (Au) or nickel (Ni) [11]. Palladium alloys often possess higher hydrogen permeability than pure palladium. In particular, alloy membranes, such as, Pd-Ag and Pd-Cu membranes have higher H_2 permeability than pure palladium, are unaffected by thermal cycling, and are resistant to sulfur poisoning [11-14]. Apart from the thermal stability, fabrication of defect free membranes and its reproducibility always remains obscured. Numerous synthesis procedures were investigated by different research groups for last two decades. However, membranes end

up with few defects causing to reduce the hydrogen selectivity. Sometimes the Pd films peel off from the substrate. Synthesis of dense and pinhole free Pd-membrane requires thicker Pd film which ultimately reduces the hydrogen throughput. To address all these issues, gaining control over the microstructure (grain size distribution) of Pd or Pd-alloy during fabrication is most important factor for future success of membrane application in hydrogen production and separation [15]. The control over the microstructure will allow one to synthesize pinhole free dense membrane with relatively thinner films.

In developing defect free Pd and Pd-alloy (Pd-Ag and Pd-Cu) membranes for hydrogen separation and membrane reactor application, our research group has patented a newly invented process called surfactant induced electroless plating (SIEP) for fabrication of thin Pd film membranes [16]. The use of a surfactant in SIEP provides better control on the grain size distribution, thinner film, better H_2 flux, as well as, its reproducibility. Membranes fabricated by surfactant induced electroless plating (SIEP) demonstrate better hydrogen flux compared to membranes fabricated by conventional electroless plating (CEP). In our previous works, we fabricated thin film Pd and Pd-Ag alloy membranes [15, 17]. On those studies, we also did detailed characterization and long term thermal study test for Pd and Pd-Ag alloy membranes. The results of previous studies were satisfactory and gave us confidence to extend this invented method to fabricate other Pd-alloy membranes, such as, Pd-Cu membranes. Pd-Cu membranes are more stable in toxic environment; especially, when sulfur based compounds are present, compared to other Pd-alloy membranes. In comparison to other Pd-alloy membranes, the Pd-Cu membrane is also less expensive to fabricate.

Using the patented SIEP process as a platform, this research will cover the following fundamental issues:

1) Using the SIEP process for the fabrication of Pd-Cu membranes making the assumption that the same surfactant will work effectively for copper (Cu) deposition as well. The target metal composition in the film is 35-45% of Cu which is the optimum for suppressing distortion [18]. The fabricated Pd-Cu alloy membranes were investigated for microstructure and film cross-section; thus, proving that the SIEP is a comprehensive process for fabricating Pd and Pd-based alloy membranes.
2) The use of a surfactant in electroless plating enhances the uniformity of the deposited film and produces finer grains of metals in the film. It is expected that SIEP process should achieve thinner film thickness for Pd-Cu alloy membrane than conventional EP process. In this work, the film thickness of Pd-Cu alloy membrane fabricated by SIEP process was investigated and found thinner in comparison with that of Pd-Cu membranes fabricated by the conventional EP process during helium gas tightness study.
3) For this work, we took a simple geometry of disc type micro-porous stainless steel (MPSS) substrate to establish the SIEP efficacy for Pd-Cu alloy membranes. After fabrication, Pd-Cu alloy membranes were characterized in terms of film properties, effect of heat treatment on microstructures of films by SEM, XRD, EDX, and AFM studies. Finally, H_2 transport behavior, H_2/N_2 selectivity and thermal stability of Pd-Cu membranes were also studied.

This thesis is comprised of five chapters, including the introduction, Chapter 1. A critical review of pertinent literature is presented in Chapter 2 followed by synthesis of membranes in Chapter 3. Chapter 4 presents a discussion on microstructure analysis of the Pd-Cu membranes along with full characterization. The later part of chapter 4 presents an evaluation of the performance of Pd-Cu membranes, in terms of H_2 transport behavior, in terms of gas separation and in terms of thermal stability criterion. Lastly, Chapter 5 gives the conclusion and recommendations for future works.

CHAPTER 2
Literature Review

2.1 Introduction

The hydrogen separating capability of Pd alloy membranes is well known [1-2, 6, 19-25]. Over the last two decades, there has been a growing interest in utilization of Pd membranes to separate H_2 produced in hydrocarbon reforming and coal gasification for power generation in fuel cell. Still development of high temperature sustainable inorganic membrane for H_2 separation and purification remains a real challenge. Palladium and its alloy have strong affinity for hydrogen and are being considered as barrier (membrane) material for hydrogen separation at high temperatures. Polymeric membranes are suitable for hydrogen separation at lower temperature (< 473 K). Many of the important reforming reactions for production of hydrogen are equilibrium limited and are usually carried out at elevated temperature. Pd-based inorganic membranes provide an option to integrate both reaction and separation in a single unit operation. This configuration, potentially, can eliminate the thermodynamic equilibrium limitations by simultaneous removal of product hydrogen from the reaction side.

This Chapter presents a brief review of organic and inorganic membranes for separation applications with a particular emphasis on hydrogen separation using Pd-based membrane for high temperature applications. A critical review is given on the Pd-H system, criteria for selection of membrane support materials; and finally, Pd and Pd alloy membrane fabrication techniques by electroless plating are presented.

2.2 Background of Hydrogen Separation

In response to the escalating energy crisis and related pollution problems, hydrogen has tremendous potential for the future energy security. An economic and efficient separation of hydrogen (H_2) from mixed gas stream is the precursor of its actual realization into the energy portfolio. Several techniques for hydrogen purification have been developed for last few decades, such as, catalytic purification, metal hydride separation, pressure swing adsorption, cryogenic separation, polymer membrane diffusion, solid polymer electrolyte cell and so on. Some of these are at various stages of commercial exploitation. The choice of the separation processes depends on the requirement of hydrogen purity, percent recovery, feed gas compatibility and flexibility of processes. A comparison of different separation processes are summarized in Table 2.1 [26]. Further, these processes are not suitable for high temperature application and can barely yield moderately high-purity hydrogen (H_2). Since all of the hydrogen production techniques involved high temperature, most of these technologies mentioned above require an additional cooling step. Thus, it requires an additional unit operation in the cascade to separate H_2 from other synthesis gases (H_2, CO, CO_2, CH_4, and N_2), results higher cost of operation. From Table 2.1 it is clear that at high temperature applications compared to other technologies to separate H_2, palladium based membranes, which are highly selective to hydrogen; offer higher purity of H_2 (almost ≥ 99.9999%), higher recovery of H_2 and durability during process operations in extreme conditions. Therefore, to facilitate the production and purification (either simultaneous or in series) of hydrogen in high temperature processes, Pd and Pd-alloy membranes are suitable contenders.

Table 2.1. Comparison of H_2 separation technologies [26]

Comparison of Hydrogen Purification Techniques						
Technique	**Principle**	**Typical Feed Gas**	**Hydrogen Output Percent**		**Scale of Use**	**Comments**
			Purity	**Recovery**		
Cryogenic Separation	Partial condensation of gas mixture at low temperatures	Petrochemical and refinery off-gases	90-98	95	Large scale	Pre purification step necessary to remove CO_2, H_2S and water
Polymer Membrane Diffusion	Differential rate of diffusion of gases through a permeable membrane	Refinery off-gases and ammonia purge gas	92-98	>85	Small to large	He, CO_2 and H_2O may also permeate the membrane
Metal Hydride Separation	Reversible reaction of hydrogen with metals to form hydrides	Ammonia purge gas	99	75-95	Small to medium	Hydrogen absorption poisoned by O_2, N_2, CO and S
Solid Polymer Electrolyte Cell	Electrolyte passage of hydrogen ions across a solid polymer membrane	Purification of hydrogen produced by thermochemical cycles	99.8	95	Small	Sulfur-containing compounds poison the electro-catalysts
Pressure Swing Adsorption	Selective adsorption of impurities from gas stream	Any hydrogen rich gas	99.999	70-85	Large	The recovery is relatively low as hydrogen is lost in the purging step
Catalytic Purification	Removal of oxygen by catalytic reaction with hydrogen	Hydrogen streams with oxygen impurity	99.999	Up to 99	Small to large	Usually used to upgrade electrolytic hydrogen, Organics, Pb-, Hg-, Cd- and S-compounds poison the catalyst. H_2O produced
Palladium Membrane Diffusion	Selective diffusion of hydrogen through a palladium alloy membrane	Any hydrogen containing gas stream	≥99.9999	Up to 99	Small to medium	Sulfur-containing compounds and unsaturated hydrocarbon impair permeability

The most important property that makes palladium unique from the other metals is its ability to take large quantity of hydrogen into solid solution. At the same time, it retains a high degree of ductility. Most significantly, hydrogen has a very high diffusion rate through the lattice of palladium. These properties of palladium help the palladium or palladium based membranes to be used as a separation unit for separating hydrogen from mixed process gases. Apart from hydrogen permeability in Pd- and Pd-alloy membranes, the permeability of all other gases (CO, CO_2, CH_4, and N_2) is so low that they are negligible in practice. Therefore, these membranes act as a highly specific filter for the production of ultra pure hydrogen. Hydrogen transport through the Pd membranes takes place via solution diffusion. When H_2 comes in contact with the Pd film of the membrane, Pd acts as a catalyst and H_2 dissociates to hydrogen atom. Molecular hydrogen chemisorptions take place on the membrane surface followed by reversible dissolution of atomic hydrogen in the bulk layers of the metal. Due to the trans-membrane partial pressure gradient atomic hydrogen diffuses through the bulk metal to the other side of the membrane and reassociates to H_2 molecule. The H_2 transport mechanism through the membrane is depicted in Figure 2.1 [11].

However, the use of pure palladium for fabrication of membranes encounters some problems, such as, hydrogen embrittlement, cracking of films, fabrication defects, poor stability and short lifetime of membranes in real process operations. Besides reproducibility of pinhole free Pd- and Pd-alloy (Pd-Ag and Pd-Cu) films, membrane fabrication with consistent permeability and selectivity is an issue in different conventional membrane fabrication processes.

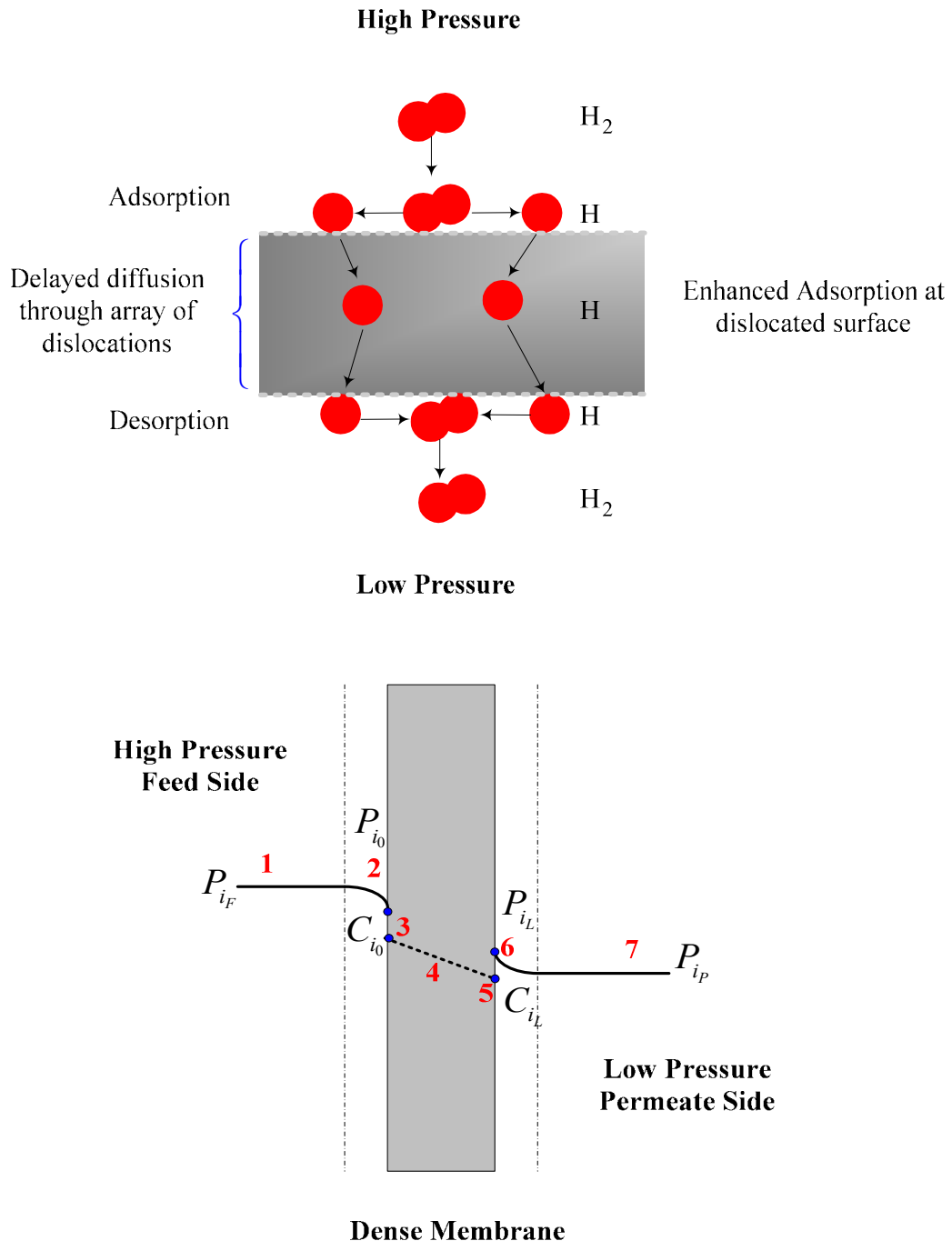

Figure 2.1. Hydrogen transport mechanism in dense Pd membrane [11]

Thus, it is very important to understand several aspects of membrane technology, namely: i) the metallurgical properties of palladium and its alloy metals, ii) the effect of alloy materials on permeability, iii) selection criteria of support material, iv) the interaction of support material components with H_2 perm-selective Pd and Pd alloy film, v) the effect of heat treatment on membrane film, vi) the role of external mass transfer resistance and different approaches to overcome this resistance, vii) the effect of grain size on the permeability, and viii) different fabrication approaches and their effect on the membrane characteristics and so on. The following sections give a brief discussion on these topics.

2.3 Membrane and Membrane Processes

The primary role of membrane is to act as a selective barrier. It permits passage to certain components and remains impermeable to other components, particles, molecules, or substances of a mixture; when exposed to the action of a driving force. According to Lakshminarayanaiah et al., membrane is defined as, "A phase that acts as barrier to prevent mass movement but allows restricted and/or regulated passage of one or more species through it" [14].

Membranes can be classified based on their application in separation processes. Depending on the driving force and physical sizes of separating species, membrane processes can be classified as: (a) Microfiltration (MF), (b) Ultrafiltration (UF), (c) Reverse Osmosis (RO), (d) Dialysis, (e) Electro-dialysis (ED), and (f) Pervaporation (PV). These membrane classifications are summarized in Table 2.2 in terms of applications and problems associated with membrane technologies [12].

Table 2.2. Current status of membrane technology [12]

Process	Problems			Comments
	Major	Minor	Mostly Solved	
Microfiltration	Reliability (fouling)	Cost	Selectivity	Better fouling controls could improve membrane lifetime significantly
Ultrafiltration	Reliability (fouling)	Cost	Selectivity	Fouling remains the principal operational problem. Current fouling control techniques are a substantial portion of process cost.
Reverse osmosis	Reliability	Selectivity	Cost	Incremental improvements in membrane and process design will gradually reduce costs.
Gas separation	Selectivity flux	Cost	Reliability	Membrane selectivity is the principal problem in many gas separation systems. Higher permeation rates would help to reduce costs.
Electro-dialysis	Fouling temperature stability	Cost	Selectivity Reliability	Process reliability and selectivity are adequate for current uses. Improvements could lead to cost reduction, especially in newer applications
Pervaporation	Selectivity Reliability	Cost	-	Membrane selectivity must be improved and systems developed that can reliably operate with organic solvent feeds before major new applications are commercialized

2.4 Organic and Inorganic Membranes

Synthetic membranes can be subdivided into organic (polymer or liquid) and inorganic (metal or ceramic) membranes. Although organic membranes (polymeric membranes) are widely used, inorganic membranes have certain advantages over their organic counterpart. Notably, inorganic membranes can operate in extreme operating conditions, such as, at high temperature, in a wide range of pH and at high pressure [13]. In most cases, structures of organic polymeric membranes deteriorate around 373 K. In contrast, the operating limit of inorganic metal membranes is close to metal's Tamman temperature (in most cases more than 773 K). They can be used at elevated temperatures and show stability at temperatures ranging from 773 to 1073 K. On the other hand, many ceramic membranes are usable over 1273 K. Inorganic membranes are also much more resistant to chemical attack, resistant to corrosive liquids and gases; even at elevated temperature compared to organic polymer membranes.

Another important issue in membrane applications is fouling or concentration polarization. Fouling or concentration polarization is generally the adsorption, accumulation of the solutes or rejected components on the membrane surface or in the pores of the substrate during separation process. For liquid separation, the issue of fouling is very crucial when considering a process operation. In gas separation, concentration polarization may be an important factor in some cases. According to Hsieh et al., some inorganic membranes, such as, microporous alumina and porous glass are more resistant to fouling. In contrast, some organic membranes undergo biological and microbial degradation in chemically harsh environment [13].

2.5 Structure of Inorganic Membranes

Membranes can be structurally classified in two categories: (a) dense membranes, and (b) porous membranes. Dense membranes are free of pores or voids. The transport mechanism through dense membranes solely depends upon the characteristics of material and its selective interactions with the species. The microstructures of porous membrane are shown in Figure 2.2 [12-14]. The membranes those have straight pores are referred as straight pores membranes. On the other hand, membranes those have interconnected pores with several tortuous paths are known as tortuous-pore membranes. If the membrane has a homogeneous structure and the same composition along the direction of membrane thickness is termed as a symmetric or isotropic membrane. If the membrane has a graded pore structures but made from same materials throughout the thickness, it is called asymmetric membrane. On the other hand, if the membrane has two or more thick layers made at different steps, the membrane is known as composite membrane. In a composite membrane, support layers are chosen to provide necessary mechanical support to separate layers.

There is another type of membrane termed as liquid membranes; those have potential applications, especially, in biotechnology and biomedical areas. In a liquid membrane, a liquid complexing agent is immobilized into a rigid porous structure and functions as separating medium. The liquid complexing agent occupies the pore structures of the support matrix and reacts with permeating components. Thus, separation is accomplished through the combination of permeating components with liquid complexing agent and diffusion (activation and transportation).

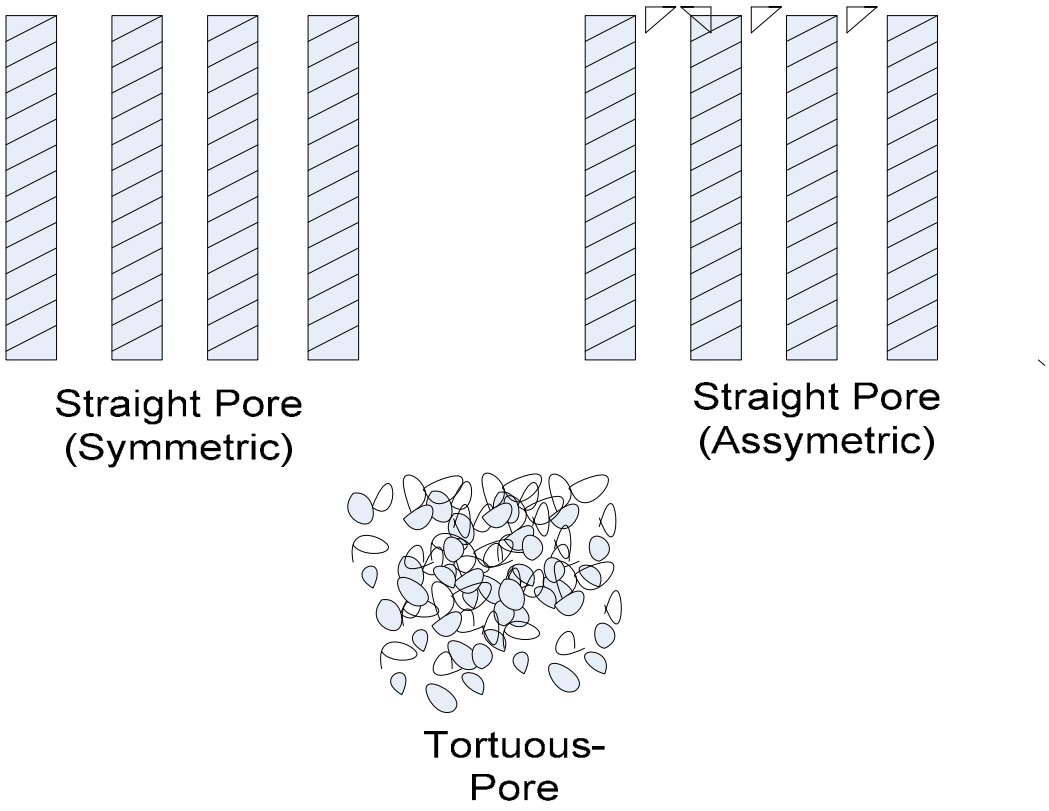

Figure 2.2. Schematic representation of various porous membranes [12-14]

2.6 Gas Separation in Membranes

Transport mechanism of gaseous mixtures through porous membrane can be described by six possible transport mechanisms: (a) Viscous flow, (b) Knudsen diffusion, (c) Surface diffusion, (d) Multi layer diffusion, (e) Capillary condensation, and (f) Molecular sieving shown in Figure 2.3 [12-15]. Viscous flow through the membrane is not effective for gas separations. Knudsen diffusion is based on the mean free path of the molecules. If the mean free path of the molecules increase or the pore diameter decreases, lighter molecules will move faster than heavier molecules, and thus results in separation. In practice, when the pore diameter is less than 5 to 10 nm under pressure, Knudsen diffusion becomes dominant transport mode. Surface diffusion becomes important, when the gas molecules are adsorbed on the surface in a significant amount. As the surface become covered by adsorbed molecules time to time, molecules diffuse through the bulk of the surface due to concentration gradients. This phenomenon is dominant when the surface area is very large. When the gas pressure increases continuously at temperature below the critical temperature, the surface coverage by the diffused gas can be larger than unity results multilayer diffusion. Capillary condensation occurs for some gases at relatively low temperature when gases become liquid in adjacent to the pore. If the other gases (non-condensed) cannot be dissolved in the condensed gases, separation occurs. Phase transition occurs during capillary condensation. Molecular sieving occurs when the pore sizes are even smaller than the size of any molecules present in the gases. Currently, some commercially available zeolites and carbon molecular sieves having narrow pore size are capable of separating gases having molecular diameter of about 0.02 nm [13].

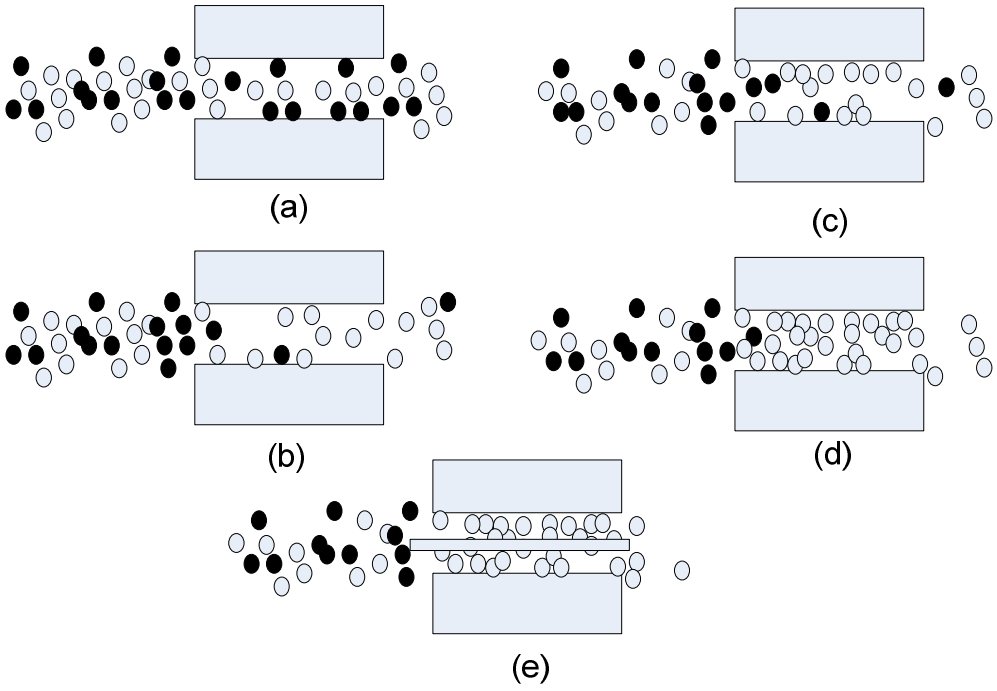

Figure 2.3. Gas transport mechanisms in membranes: (a) Viscous flow, (b) Knudsen flow, (c) Surface diffusion or multi layer diffusion, (d) Capillary condensation, and (e) Molecular sieving [12-15]

2.7 Metallurgical Properties of Palladium and its Alloy Metals

It is important to understand the metallurgy of metal/alloy-hydrogen system for the fabrication and successful application of Pd based membrane as a commercial separation unit. A good understanding of the metallurgy of metal/alloy-hydrogen system will lead us to know better about hydrogen diffusion technology. Bruning and Sieverts were the first to conduct the work to determine isotherms in the palladium-hydrogen system in 1933, Gillespie and Downs in 1939 and later Gillespie and Sievert in 1948 [26]. Sometime later, these data were then extended to include higher pressure and lower temperature. More recently, Shu et al., studied pressure-composition isotherm in 1991 [17]. A typical pressure-temperature and composition phase diagram of palladium-hydrogen system is shown in Figure 2.4 [27-28]. As shown in Figure 2.4, at temperature below 573 K and pressure below 20 atmospheres, increasing the hydrogen concentration led to the formation of β-palladium hydride phase which can co-exist with the α-phase. In comparison with the α-phase, the β-phase has a considerably expanded lattice. However, the α- to β-phase conversion does not affect the hydrogen content in two phases, only the relative proportion of two phases is affected. The lattice parameter in β-phase is 10% larger than the α-phase for hydrogen to palladium ratio of 0.5. Nucleation and growth of the β in α matrix therefore set up severe strains in the material resulting in distortion, dislocation multiplication and hardening. This can result in premature fracture of the diffusion membrane after undergoing only a few hydrogenation/dehydrogenation cycles [26]. One method to avoid the phase change in pure palladium is to ensure that, the diffusion membrane always operates in the single phase region shown in Figure 2.4.

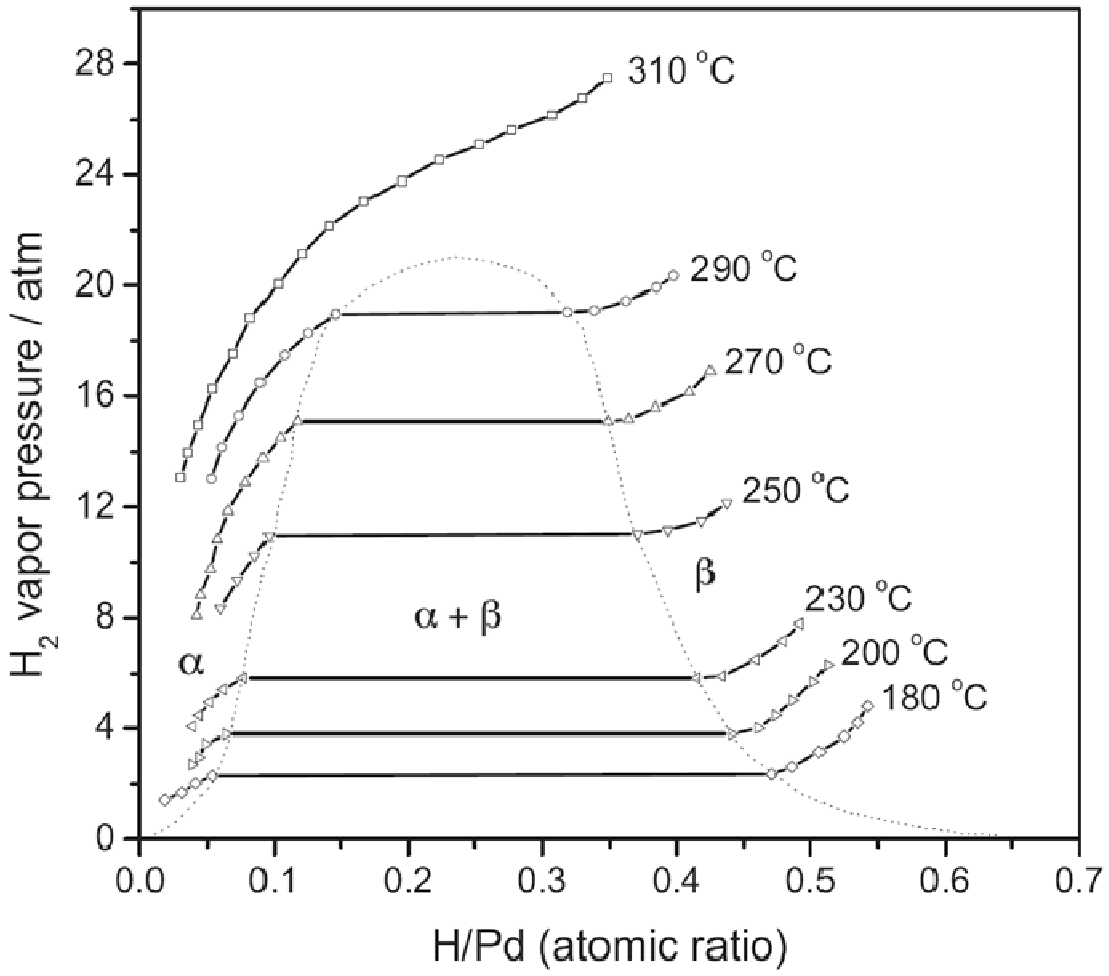

Figure 2.4. Phase diagram of palladium-hydrogen system [27-28]

This may be achieved by operating the membrane above 300 ^{o}C or 573 K in hydrogen atmosphere or by ensuring that cooling takes place only when it is in a dehydrogenated condition with the hydrogen completely removed from the system. However, this approach will really narrow down its application [26]. The other method is to change the metallurgy of the palladium membrane rather than changing the operational regulation. It is necessary to suppress the β to α- phase transition in order to avoid distortion. Adding a number of elements to palladium can suppress the transition sufficiently, which significantly reduces or eliminates distortion. These elements include transition metals of group VB (tantalum, vanadium and niobium), VIIIB (nickel, rhodium, ruthenium, iridium, platinum) and group IB (copper, silver and gold).

Success of palladium as a membrane is closely connected to the catalytic activity of the surface, allowing the ready adsorption and dissociation of hydrogen molecule. This factor is absent in group VB metals such as tantalum, vanadium and niobium [26]. In spite of having high hydrogen diffusivity and a pressure/concentration isotherm similar to palladium, these metals are not considered due to the lack of it's catalytic activity. Also, these base metals are generally considered to be unsuitable for use as diffusion membranes due to well-documented embrittlement that occurs during adsorption of hydrogen. Another disadvantage of group VB metals is the instant poisoning of the membrane caused by the formation of stable oxides. Alloying with group VIII metals are not of interest since they are generally poor in hydrogen permeability. Only group IB (Cu, Ag and Au) metals show significant encouragement in both suppression of β-phase to α-phase transition at higher temperature and in hydrogen

permeability. In addition, adding more than 20% of silver to palladium makes alloy dimensionally stable and does not distort during hydrogen cycling. Gold and copper are like silver, elements of group IB of the periodic table, and have therefore received a large amount of attention as alloying elements with palladium. They also show resistance to sulfur poisoning. Sometimes, alloys might have higher hydrogen diffusion rates than pure palladium, for example, 23% of Ag or 40% of Cu addition to palladium gives a considerable enhancement in hydrogen permeability [1, 18, 26, 29-31]. Therefore, a large number of palladium systems have been studied and described in the literatures; claiming alloys with one or more of these desirable features previously discussed are summarized in Table 2.3 [29]. Significant breakthrough in the hydrogen diffusion technology was achieved in late 1950s and early 1960s by Hunter and by Darling [26, 32-34]. They established substantial data on hydrogen diffusion through a wide range of palladium alloys, thus, allowing the selection of an optimum, high performance hydrogen diffusion alloy. Hydrogen permeability data for a series of palladium alloys (Pd-Ag, Pd-Cu, Pd-Au, Pd-Ni and Pd-Fe) are also shown in Figure 2.5 [26].

Table 2.3. Permeability of different Pd-alloy membranes at 623 K and 300 psig [29]

Permeability of Miscellaneous Palladium Alloys to Hydrogen at 623 K, 300 psig			
Material (weight percent)	**Permeability ($cm^3/cm^2/s$)**	**Remarks**	**References**
Palladium	1.43	-	-
80Pd-20 Ag 77Pd-23 Ag 70Pd-30Ag 48Pd-52Ag	2.46 2.48 1.46 0.13	Hydrogen output maximum at 20 to 25 percent Ag.	
95Pd-5Au 80Pd-20Au 60Pd-40Au 45Pd-55Au	1.52 1.37 0.60 0.13	Small increase in permeability at low Au contents. Alloys more resistant to sulfur poisoning.	[18]
90Pd-10Cu 70Pd-30Cu 60Pd-40Cu 55Pd-45Cu 45Pd-55Cu	0.69 0.12 1.52 0.25 0.01	Sharp maximum in output at 40 percent Cu, corresponding with ordered β-phase in Pd-Cu system.	
99.5Pd-0.5B	1.35	Interstitial boron tends to block lattice sites	[18]
90Pd-10Ni 95Pd-5Ru	0.27 0.47	Low permeabilities for Fe, Ni, Ru, Pd and Rh additions.	[18]
65Pd-30Ag-5Pt 68Pd-30Au-2Ru	- -	Examples of wide range of complex alloys claimed in literature	
85Pd-13Ag-2Ni 70Pd-20Ag-10Rh	- -		
73Pd-24Ag-3Au Pd-20Ag-5Au-1.26Ru	- -		
68Pd-25Ag-5Au-2Ru Pd-10Ag-1Au +0.1 each of Ru, Al,Pt.	- -		
92.3Pd-7.7 Ce 87.3Pd-12.7 Ce	2.24 1.27	The higher Ce alloy is prone to poisoning by oxidation.	
93.4Pd-6.6Y 90Pd-10Y	4.99 5.38	Estimated from 200 psi results by the √P (Sievert's Law) relationship.	

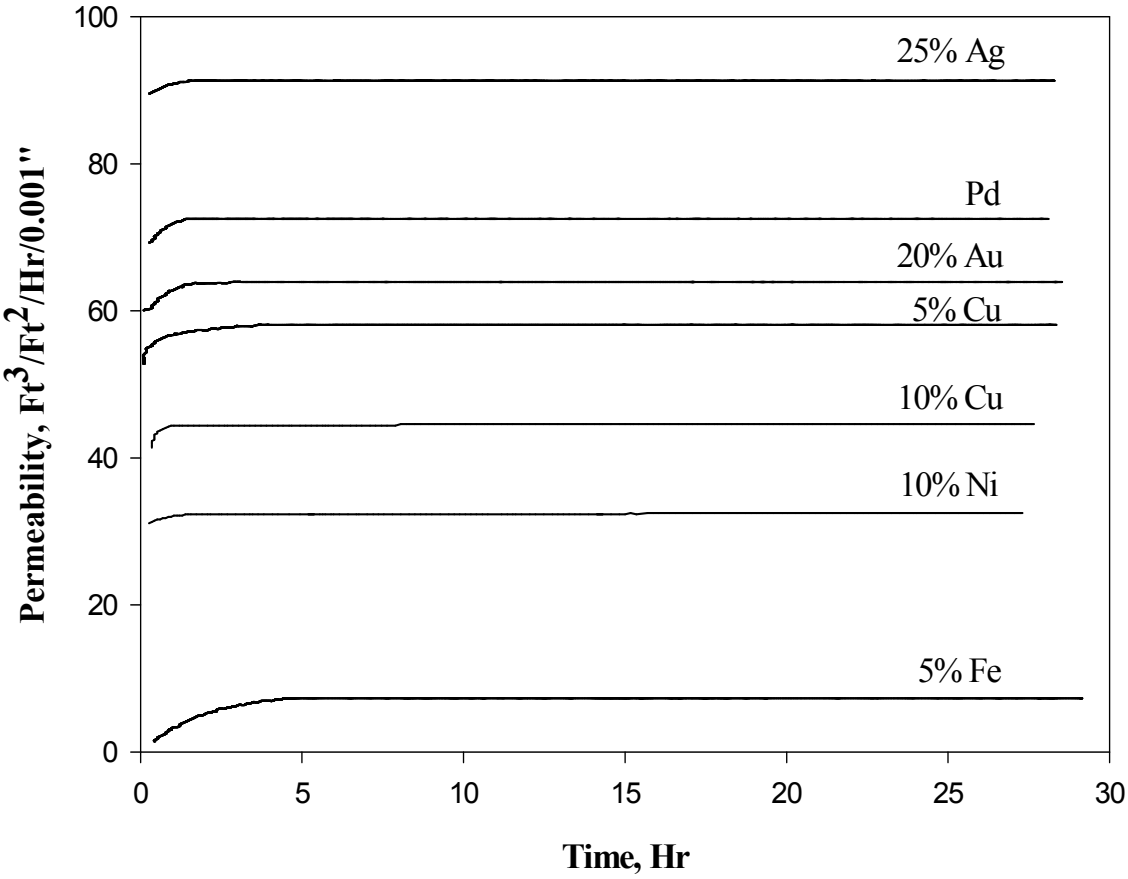

Figure 2.5. Rate of diffusion of hydrogen in palladium and number of palladium binary alloys (T = 813 K and P = 50 psi) [26]

2.8 Phase Diagram of Palladium and its Alloy Metals

Pd and other elements of group IB (Ag, Cu and Au) in the periodic table are generally used for membrane fabrication since they have high hydrogen diffusivity and are relatively resistant to oxidation. When adsorbed poisons are not present on the membrane surface, the rate-limiting step in membrane applications is often hydrogen diffusion through the bulk metal. Diffusion through the crystalline lattice is determined by the atomic structure and the chemical nature of the material used in membranes [1]. Therefore, it is important to understand the phase diagram of palladium and its alloying materials used for membrane fabrication. An understanding of phase diagrams will allow us to find the limit for annealing temperature for alloys after fabrication of membranes. This will provide a clear pathway for post fabrication treatment of membranes. For palladium alloy membrane, such as, palladium-copper membrane, two different systems need to be addressed: Pd/PSS binary system and Pd/Cu/PSS ternary system.

2.8.1 Pd/PSS Binary System

The binary phase diagram of the Pd/Fe system is shown in Figure 2.6 [35]. The main features of the phase diagram of the Pd/Fe system are characterized by the phase separation in the Fe rich region (> 90 wt % of Fe) due to the size mismatch among αFe, δFe and γFe phases and the appearance of the two ordered phases, namely FePd and $FePd_3$, in the Pd rich region (> 62 wt % of Pd) [31]. The Pd/Fe binary phase diagram also shows a continuous region of solid solution with f.c.c. phase structure existing over the entire composition range at high temperature (> 973 K). However, the f.c.c. phase is still stable at lower temperature above 90 wt % of Pd.

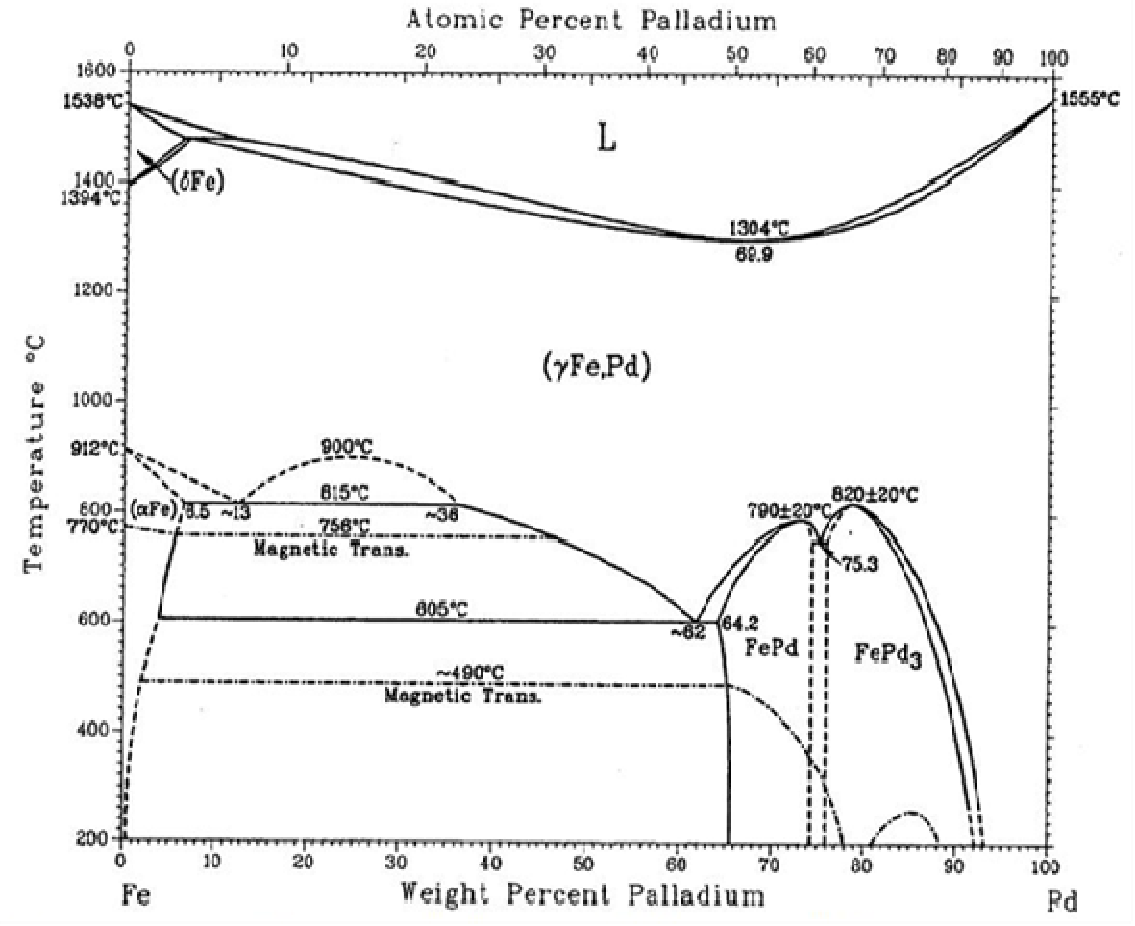

Figure 2.6. Phase diagram of palladium/porous stainless steel (PSS) system [35]

2.8.2 Pd/Cu/PSS Ternary System

Palladium membranes can be made less prone to hydrogen embrittlement, better resistant to poisoning by sulfur and deterioration by H_2S, which is the most common impurity present in synthesis gas along with H_2 by alloying with copper. Alloying Pd with Cu decreases the critical temperature of H_2 embittlement as a result; the potential for H_2 embrittlement is reduced at lower temperature. Alloying 40% of Cu with pure Pd to fabricate Pd-Cu membrane results in permeability of hydrogen to be 1.1 times higher than the pure Pd membrane [18]. The permeability of hydrogen is significantly lower when the Cu content is above or below 40% shown in Figure 2.7 [36].

The $Pd_{60}Cu_{40}$ alloy system does not undergo any phase transformation even at room temperature with lower permeability and higher resistance to sulfur. At temperature higher than 673 K, this particular alloy undergoes from ordered b.c.c. structure (β-phase) of high permeability to disordered f.c.c. structure (α-phase) of low permeability. Since Pd-Cu alloy membrane shows higher resistant to S-poisoning due to the presence of H_2S and S-containing compounds, a balance is required for utilizing Pd-Cu alloy membrane in terms of resistance to sulfur poisoning and its low permeability characteristics over the temperature ranges [36]. However, Pd-Cu alloy is structurally different from other alloys, such as, Pd-Ag, which forms a disordered face centered cubic (f.c.c.) structure at all composition. In contrast, Pd-Cu alloy can be present either as disordered f.c.c. structure (α-phase) or ordered b.c.c. structure (β-phase) at temperatures below 873 K, as illustrated in Figure 2.8 [37]. It is clear from Figure 2.8 that annealing temperature for a given alloy composition has a significant effect on the alloy phase.

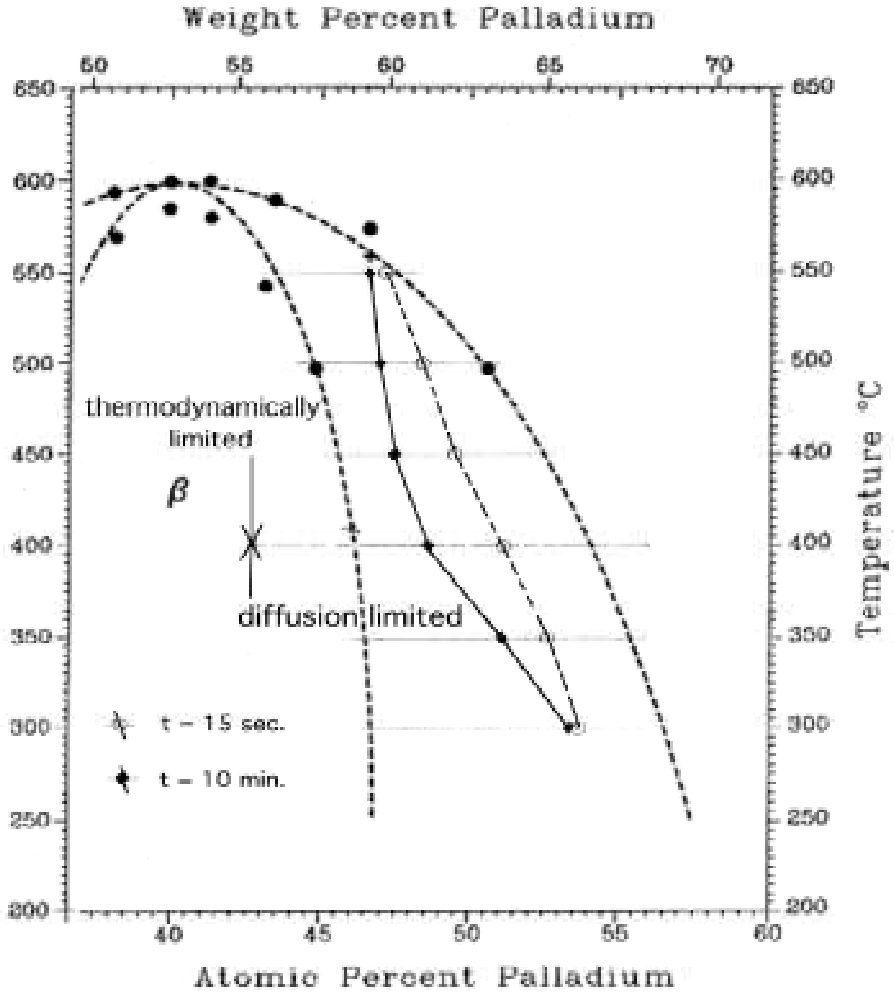

Figure 2.7. Pd/Cu-H phase diagram [36]

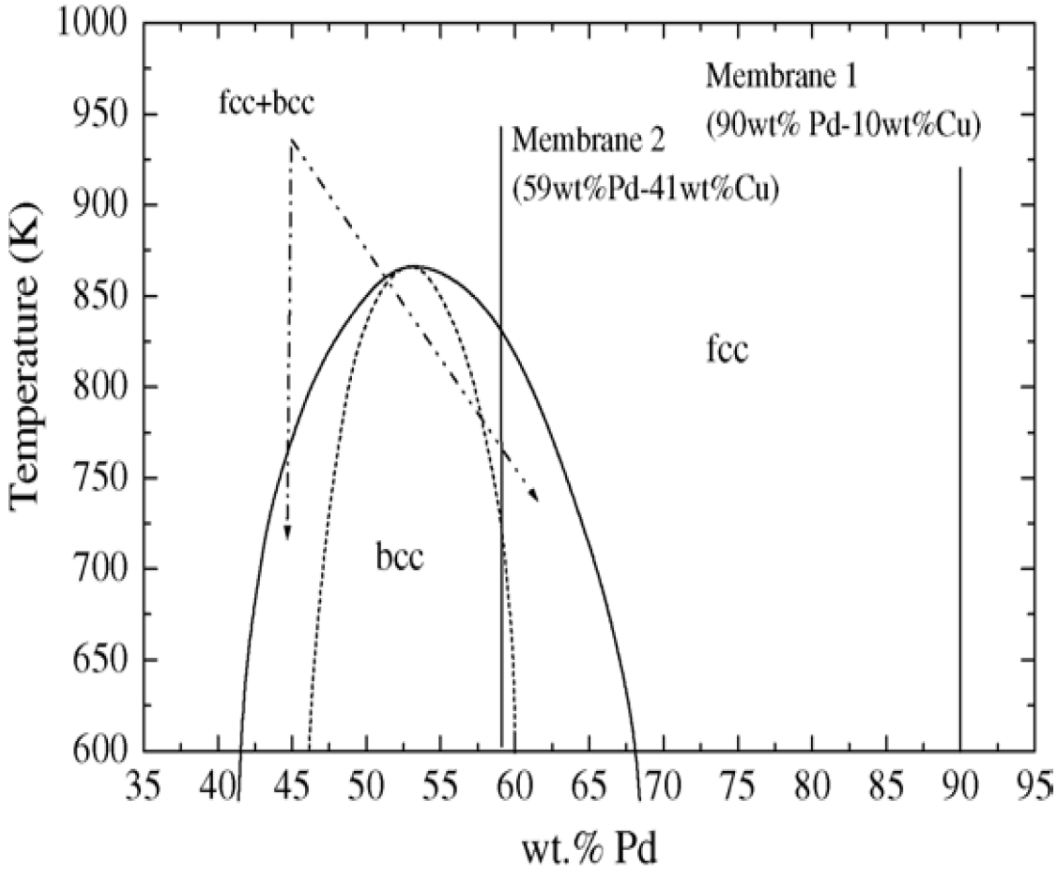

Figure 2.8. Pd-Cu alloy phase diagram of two different Pd-Cu membranes with different metal composition [37]

Pd-Cu alloy membranes also have generated much research attention, because not only they do not exhibit hydrogen embrittlement even at room temperature but also they are more resistant to H_2S poisoning than pure Pd membranes; when the Cu composition of the membrane is in the f.c.c. region of the Pd-Cu phase diagram shown in Figure 2.9 [38]. One of the disadvantages of f.c.c. structured Pd-Cu membranes is their low permeance in comparison to Pd and other Pd alloy membranes due to the decreased solubility of H_2 in Pd-Cu alloy membranes. Addition of only 10 and 30 wt % of Cu to Pd decreased the permeance of Pd-Cu membranes by 35% and 85% respectively at 623 K. An even larger decrease was observed at 813 K with the permeance decreasing by 20% and 40% at concentrations of merely 5 and 10 wt % of Cu respectively [38]. The relative permeability of Pd-Cu alloy membranes as a function of Cu content is also overlaid in the phase diagram in Figure 2.9.

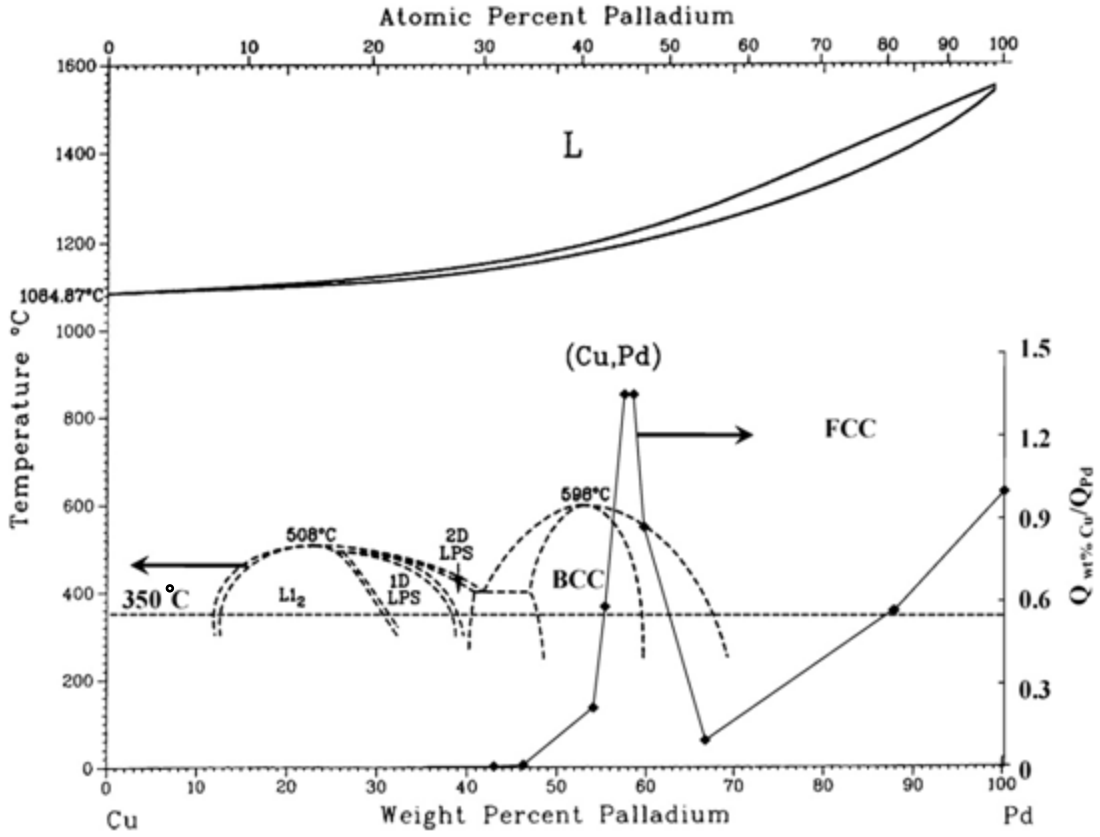

Figure 2.9. Pd-Cu phase diagram overlaid with the relative permeability of Pd-Cu membranes to Pd membranes as a function of Cu content at 623 K [38]

2.9 Selection of Membrane Support Materials

In general, palladium based composite membranes are composed of a thin palladium film for separation and a substrate for its mechanical support. It's not only the mechanical property but there are few other selection criteria for selection of the desired support material. The first ever fabricated Pd membrane was a free standing palladium foil. But the thickness of free standing Pd foil membrane resulted in a low hydrogen flux and a high investment. Also exposure of the palladium foil in the H_2 environment resulted in severe distortion. In order to overcome these disadvantages, an economical route was chosen by using palladium based films on top of a substrate as a composite membrane. This approach significantly improved the hydrogen flux and reduced the investment level. The choice of support materials is an important issue in fabricating palladium-alloy composite membranes. The ideal support materials shall have the following features, but not limited to:

- Support material should be chemically inert in reaction with palladium at any operating temperature and pressure.
- It should not allow any crystal migration from the substrate to film or film to substrate.
- The pore size and pore size-distribution of the support should be very fine and narrow, respectively. Significant interconnections between the pores are very desirable.
- There should not be any blind pores in the support. Pore size and pore morphology should not damage the top surface smoothness.

Different types of support materials were used in fabricating composite Pd membrane. Ceramic (Al_2O_3, silica, zeolites and TiO_2), porous iron (hastelloy, inconel, stainless steel), porous nickel and porous silver were widely used for support materials. Most of the metallic supports led to inter-metallic diffusion above 573 K. Ceramic or vycor glass did not show any migration at all. In case of porous stainless steel, inter-metallic migration of Fe, Cr and Ni into the membrane film affects H_2-permeability and membrane quality. Many researchers attempted to develop inter-metallic diffusion barrier in between metal support and Pd-film to avoid metal migrations from substrate to the deposited film. The use of TiN (titanium nitride) as a diffusion barrier in Pd-Ni alloy membrane was also reported in the literature [10, 39-41]. TiN (titanium nitride) has a high melting point (3223 K), and it provides thermally stable intermetallic diffusion barrier, which enhances hydrogen permeability and selectivity in a nonoxidative atmosphere. Gryaznov et al., concluded that tungsten, magnesia or zirconia of less than 1 μm thick layer would be better as an inter-metallic diffusion barrier as they have relatively higher melting point [42]. Nam & Lee reported fabrication of Pd-Cu alloy membrane with a thin silica layer as an inter-metallic diffusion barrier between palladium alloy layer and substrate to improve the structural stability of the composite membrane [39]. In their work, nickel powder was used to improve the surface smoothness.

Pore size of the microporous metallic support plays a significant role in the quality of the final Pd/Pd-alloy film deposited by electroless plating process. Maximum pore size in a support material is characterized by pore diameters. Support materials are graded by pore size, such as 0.1 μm, 0.2 μm, 0.5 μm or so. Mercury Porosimetry can be

used to determine the pore size distribution in support materials. Theoretically, it has been shown that for a defect-free stable film, the Pd-film thickness should be at least three times larger than pore diameter of the surface [43]. For support materials, very fine pore size and narrow pore size-distribution with significant interconnections of the pores are desirable. The support material has to be chemically inert in reaction with palladium and other membrane materials at any time under any pressure and temperature. As a result, the synthesis of Pd and Pd/alloy deposits on porous sintered metal supports are widely used. This makes micro-porous stainless steel (MPSS) as promising support materials for Pd and Pd/alloy based membrane application. MPSSs are also favorable support materials because of their various advantages, such as, good mechanical strength, less fragility, resistant to cracking, ease of operation at high temperature and pressure, ease of module fabrication, and maintenance. In addition, similar thermal expansion coefficients among the membrane fabrication metals provide better mechanical properties for Pd and Pd/alloy membranes. Metal properties of film and PSS support are summarized in Table 2.4 [11].

Table 2.4. Physical properties of palladium, silver, copper, stainless steel and its constituent elements [11]

Material Properties for Membrane materials and Porous Stainless Steel (PSS) as Membrane Support				
Material	**Thermal Expansion Coefficient, K^{-1}**	**Tamman Temperature, ^{o}C**	**Lattice Parameter, Å**	**Density, gm/cc**
Iron, Fe	$1.2x10^{-5}$	632	2.87	7.874
Nickel, Ni	$1.3x10^{-5}$	590	3.52	8.903
Chromium, Cr	$2.335x10^{-5}$	817	2.88	7.190
SS 316L	$1.73x10^{-5}$	550 - 560	3.59	8.000
Palladium, Pd	$1.2x10^{-5}$	640	3.89	12.023
Silver, Ag	$1.95x10^{-5}$	345	4.08	10.500
Copper, Cu	$1.7x10^{-5}$	405	3.6	8.960

2.10 Electroless Deposition of Palladium and its Alloy Metals

There are several membrane preparation techniques those have been employed in fabricating Pd based composite membranes. These methods include chemical vapor deposition, sputtering coating, electrochemical plating and electroless plating. Among these methods, electroless plating (EP) is a widely used process because of some important advantages over the other processes. Membrane synthesis via the EP produces uniform deposition of metals on substrate surfaces with complex geometries and large surface areas. Electroless plating has added other advantages, such as, good hardness of the deposited film, good adhesion to the substrate and ease to scale-up. Additionally, it requires simple equipment and low investment.

Electroless plating is a controlled autocatalytic deposition of a continuous film on a catalytic interface by the reaction of a metal salt and a chemical reducing agent [44]. Electrochemically, an electroless deposition reaction is considered as the combined result of two independent electrode reactions, such as, a cathodic partial reaction (i.e. metal ion reduction) and an anodic partial reaction (i.e. oxidation of reducent). The electrons required for the reduction of metal ions are supplied by the reducing agent. A typical bath chemistry for the electroless plating of Pd consists of a metal ion source ($PdCl_2$, $Pd(NH_3)_4Cl_2$, $Pd(NH_3)(NO_3)_2$, $Pd(NH_3)_4Br_2$), a complexing agent (ethylene-di-amine tetra-acetic acid (EDTA), ethylene-di-amine (EDA), ammonium hydroxide (NH_4OH)), a reducing agent (NH_2NH_2, $NaH_2PO_2.H_2O$, tri-methyl-amine-borane), stabilizer (ammonium hydroxide, NH_4OH) and an accelerator. The metal source for the electroless plating of Cu includes $CuSO_4$ salt.

The reaction steps involved in Palladium and Copper deposition in electroless plating baths are:

Palladium Bath Reactions:

$$2Pd(NH_3)_4^{2+} + 4e^- \rightarrow 2Pd^o + 8NH_3$$
$$H_2NNH_2 + 4OH^- \rightarrow N_2 + 4H_2O + 4e^-$$

Overall Reaction:

$$2Pd(NH_3)_4Cl_2 + H_2NNH_2 + 4NH_4OH \rightarrow 2Pd^o + N_2 + 8NH_3 + 4NH_4Cl + 4H_2O$$

Copper Bath Reactions:

$$Cu(NH_3)_6^{2+} + 2e^- \rightarrow Cu^o + 6NH_3$$
$$2HCHO + 4OH^- \rightarrow 2HCOO^- + 2H_2O + H_2 + 2e^-$$

Overall Reaction:

$$Cu(NH_3)_6SO_4 + 2HCHO + 4NaOH \rightarrow Cu^o + 6NH_3 + 2HCOONa + Na_2SO_4 + 2H_2O + H_2$$

$NaH_2PO_2.H_2O$ based plating baths with EDA as the complexing agents have been frequently used. But microstructures of the deposited films were significantly altered with the formation of cracks due to the evolving of hydrogen and ammonia gases during bath reactions [44]. For this reason, hydrazine based electroless plating bath is very attractive. Rhoda was the first to develop this type of bath using $Pd(NH_3)_4Cl_2$ [45]. Rhoda observed a linear increase in the plating rate of palladium within the temperature range of 313 to 353 K, a spontaneous precipitation of the bath above 343 K in the absence of stabilizer EDTA salt and a rapid decrease in the plating rate over time, which was due to the catalytic decomposition of hydrazine by palladium. Currently hydrazine based electroless plating process is well established and employed in the fabrication of dense hydrogen selective Pd and Pd-alloy composite membranes on various substrate support, such as, porous glass, ceramics and porous sintered metals.

2.11 Different Approaches to Enhance Electroless Deposition Technique of Palladium and its Alloy Metals

For the economic viability of the membrane technology, some specific requirements, such as, high hydrogen permeation rates, high selectivity, long-term thermal and chemical stability and defect free (pinhole and cracks) film has to be achieved. The synthesis procedures for achieving these requirements, as well as, their reproducibility were a long deadlock. However, finding a single synthesis procedure that will optimize the membrane properties, as well as, the durability, it is of utter importance to understand the solution chemistry, reaction mechanism of the electroless deposition, influence of the processing parameters on the properties of the deposited layer and the ways and means for reducing mass transfer resistances. Thus, the effects of temperature, initial metal ion concentration and initial reducing agent concentration on electroless plating rates of Pd and other metal deposited on porous sintered metal were thoroughly studied [4].

Now, it is well established that the plating rate and conversion are heavily dependent on the initial concentration of metal ion and reducing agents. Apart from the metal ion and the reducing agents, there are sufficient evidences about the effect of temperature on the plating technique. However, the plating rate and the efficiency differ from metal to metal; for example, the deposition rate of Cu is faster than that of Pd and Ag, as well as, in the efficiency. Interestingly, most of the previous investigators ignored the mass transfer limitations. Ma et al., observed the external mass transfer has a pronounced effect on the deposition kinetics [43, 46-47]. They found that the electroless plating of Pd was strongly affected by the external mass transfer in the absence of bath

agitation. The external mass transfer limitations for Pd deposition have been minimized at or above an agitation rate of 400 rpm. The result was a maximum conversion of the plating reaction at 333 K, which dramatically shortened the plating time. The plating also yielded a uniform morphology. Ayturk et al., applied agitation through internal rotation in EP solution bath as an external driving force, which improved reaction rate, as well as, grain size [4]. Their experiments demonstrated that plating efficiency can be as high as 90%, if the rotation rate is set at 500 rpm during the electroless deposition process.

Applying osmotic pressure during deposition made it possible to deposit Pd-nuclei into the deeper pores so that most of the pores become covered by Pd thin film [39, 43, 45, 48]. Souleimanova et al., suggested that the increase of osmotic pressure results in the decrease in Pd-grain size during the electroless plating process [49]. They also showed that agglomeration of Pd-grains increased with osmotic pressure. However, other approaches were also studied for reducing the mass transfer resistances, which were different from external forces (agitation, rotation, applying vacuum, and osmotic pressure).

A very simple approach of using surfactant by Chen et al., were studied to see the effects of adding surfactants in the acidic hypophosphite plating baths on the properties of the resulting electroless nickel-phosphorus (Ni-P) deposits on brass substrates [50]. They reported, addition of suitable amounts of surfactants can increase the deposition rate up to 25% and reduce the formation of pores on the surface of Ni-P alloys, as well as, enhance the corrosion resistance of the deposits. Their study attempted to establish a quantitative and qualitative relationship between the effect of surfactants and the surface

properties of the Ni-P plating layer obtained, as well as, the corrosion resistance of the resulting Ni-P deposits. They reported that the effect of surfactant was governed by the structure of the surfactant, the dosage of surfactant in the electroless nickel-phosphorus (Ni-P) bath, and the interaction of surfactant with other constituents of the plating solution. The rationale behind their study lies in the following two aspects: first, surfactant molecules affect the deposition rate of the Ni-P alloy because of their influence on the availability of the reductive hydrogen atoms adsorbed on the plating frontier; second, the identity of the surfactant plays a role in shaping the surface morphology, as well as, the porous structure of the deposit due to various interfacial behaviors. They assessed the effect of adding nine different surfactants at optimal concentration in the electroless Ni-P deposition bath. During the electroless plating process, the release of N_2 from bath reactions got adsorbed by the support surface, and eventually creates micro-porosity in the deposited film. In contrast, they also reported that addition of an excessive amount of nonionic surfactants in the plating baths will in general yield the Ni-P deposits with an inferior surface quality and slowing down the deposition rate. Conversely, they also mentioned that surface properties of the Ni-P deposits were less influenced by the concentration effect of ionic surfactants initially present in the plating baths.

Although Chen et al., used the concept of using surfactant in electroless plating of Ni-P, no one has reported the use of surfactant in Pd or Cu bath in electroless plating. Based on the notion of easy removal of N_2 and NH_3 gas molecules to the surrounding liquid aided by the surfactant, we have devised a new surfactant induced electroless plating (SIEP) technique for depositing dense, pinhole free and durable Pd film [16].

2.12 Surfactant Induced Electroless Plating (SIEP)

In conventional Electroless plating process, the resulting Pd-film is formed by columnar grain growth and there is little control on the grain size distribution for the deposited film [51]. The grain size distribution is an important parameter for the uniformity of the deposited film, as well as, for making it free of pinholes. The microstructure of deposited film has a pivotal role on hydrogen permeability. According to Kirchhiem et al., the diffusivity of hydrogen in nano-crystalline Pd was lower than that of single crystal at low hydrogen concentrations [52]. The diffusivity of hydrogen is significantly higher in nanocrystalline Pd than its single crystal counterpart at higher hydrogen concentration. According to Gleiter et al., nanocrystalline palladium has almost 10 times higher diffusivity than conventional polycrystalline Pd [53]. In small nanocrystalline metal, at least 20 to 50% of its atom located in the grain boundaries and act as a network for faster diffusion. Therefore, it is critically important to obtain control over microstructure and grain size distribution of Pd or Pd/alloy film during metal deposition over substrate material. The control on grain size distribution on metal film will eventually make the membrane fabrication reproducible, reliable and yield a desired membrane, which will have thin film, no pinholes, has high selectivity for H_2, and will be thermally stable in any process condition. The SIEP is a process that is capable of controlling the grain size distribution. The charge and concentration of surfactant can be used to tailor the Pd grain size and subsequent agglomeration. Islam et al., used a balance between micelles concentration and retention time as a control to facilitate uniform nucleation and agglomeration of Pd-grains in dense Pd film fabrication [54].

The presence of surfactant helps continuous removal of the evolved gases (NH_3, N_2 etc.) from the substrate's top layer. The interaction of surfactant with solid-liquid and solid-gas interface during grain coarsening helps to remove gas bubbles making almost entire substrate surface available for deposition. It was also noticeable that the surfactant took part in the reduction reaction enhancing the plating process. As a result, the equilibrium shifts to the right and increases the rate of reduction of Pd^o. Another advantage of this process is that an extremely dense thin film can be prepared. The concentration of the surfactant was chosen as a function of critical micelle concentration (CMC) [54]. It appears that during electro-crystallization, the driving force between newly formed crystallite and original coarse grains depends on the relative size and crystalline configuration of newly formed crystallite. The crystallites on the other hand, are affected by the localized over potential, presence of active nucleating particles, texture of MPSS surface and operating conditions. The size of the newly formed grain is smaller when the concentration of surface active agents is relatively higher. This suggests that active polar group of surfactant inherently participated in deposition process and effectively began the process of grain nucleation and agglomeration in electro-crystallization.

Pure Pd membranes with different grain size distribution were fabricated using different concentration of surfactant, and control over deposited Pd film microstructure was attained. Since the use of the surfactant can control the film microstructure in the Pd membrane, this suggests that the same might be applicable for Pd-Cu alloy membrane. It is known that Pd membrane also suffered from cracking and there was a gradual

reduction in hydrogen permeability over long exposure at high temperature due to the intermetallic diffusion of the support materials. In contrast, Pd-Cu alloy membranes can withstand cracking and sulfur poisoning virtually, in the wide range of operating temperature in processes where sulfur rich synthesis gas is used. One of the disadvantages of Pd-Cu membranes is their low permeance in comparison to Pd and other Pd alloys due to the decreased solubility of H_2 in Pd-Cu alloys. In previous works, our group was able to fabricate defect free, thin film Pd and Pd-Ag alloy membranes by using surfactant in electroless plating baths [11-12]. To prepare a stable, defect free Pd-Cu alloy membrane with a longer lifetime having optimum throughput of hydrogen and superior selectivity, it is of great interest to apply the same surfactant induced electroless plating (SIEP) technology to fabricate Pd-Cu alloy membranes. So far, there has been no report of using surfactant in electroless plating bath to fabricate Pd-Cu alloy membranes.

CHAPTER 3
Materials and Methods

Micro porous stainless steel (MPSS) disc from Mott Metallurgical Corporation (Farmington, CT) was used as support for membrane fabrication. Specifications of the 316L SS discs are 1 inch in diameter and 0.062 inch in thickness with an average pore size of 0.2 μm. The average pore size of the substrate was taken from the manufacturer's product information. Before using these substrates in sensitization and activation processes, cleaning was done in three steps. First, the top surface was brushed with a metal brush then cleaned with an alkaline cleaning solution (prepared in the laboratory) for 40 to 60 minutes at 333 K in an ultrasonic bath followed by a thorough cleaning with de-ionized water until the pH of the surface became 7. The composition of the cleaning solution is given in Table 3.1. Finally, the support was dipped into an isopropanol (Fisher Scientific) solution for 10 minutes, and dried for 2 hours at 393 K.

The sensitization and activation solutions were prepared using reagent grade $SnCl_2$ (Sigma-Aldrich, 98%) and $PdCl_2$ (Sigma-Aldrich, 99.9%) in hydrochloric acid. The composition of the sensitization and activation solutions is given in Table 3.2. In Table 3.3 the composition and the operating conditions of the Pd and Cu electroless plating baths used in this study are given. The activation procedure consisted of dipping the substrate in the sensitizing solution, then in activation solution. Duration of each step was 4 to 5 minutes. The substrate was rinsed with deionized water between sensitization and activation steps. After dipping the substrate in activation solution, the activation

Table 3.1. Chemical composition of cleaning solution

Name of Chemicals	Supplier	Composition
$Na_3PO_4.12H_2O$ (ACS Reagent grade, 99.4%)	Alfa Aesar	45 g/L
Na_2CO_3 (ACS Grade, ≥ 99.5%)	Alfa Aesar	65 g/L
NaOH (ACS Grade, 97%)	Alfa Aesar	45 g/L
Industrial Detergent (Liqui-Nox^R)	Alconox	5 mL/L

Table 3.2. Chemical composition of sensitization and activation solutions

Name of Chemicals	Supplier	Sensitization Solution	Activation Solution
$SnCl_2.2H_2O$ (ACS Reagent grade, 98%)	Sigma-Aldrich	1 g/L	-
$PdCl_2$ (ACS Reagent grade, 99.9%)	Alfa Aesar	-	0.1 g/L
HCl (ACS Reagent grade, 37%)	Sigma-Aldrich	1 mL/L	1 mL/L
Temperature		20 ^oC	20 ^oC
Time		4-6 minutes	4-6 minutes
pH		4-5	4-5

Table 3.3. Chemical composition of Pd-bath and Cu-bath solutions

Name of Chemicals	Supplier	Pd-bath	Cu-bath
Pd $(NH_3)_4Cl_2.H_2O$ (≥ 99.99%)	Sigma-Aldrich	4 gm/L	-
$CuSO_4.5H_2O$ (ACS grade, 98.0-102.0%)	Alfa Aesar	-	1.22 gm/L
Na_2EDTA (≥ 99%)	Acros Organics	40.1 gm/L	10.05 gm/L
NH_4OH (ACS grade, 29.17%)	Fisher Scientific	198 mL/L	-
NaOH (ACS grade, 97%)	Alfa Aesar	-	10 gm/L
NH_2-NH_2 (1.0 M)	Sigma-Aldrich	5.6 mM	-
DTAB (~ 99%)	Sigma-Aldrich	4 CMC	4 CMC
Formaldehyde (ACS, 37% in aq. sol^n)	Alfa Aesar	-	280µL
2, 2'- Bipyridine (> 99%)	Alfa Aesar	-	2.5g/L
Time		1 Hour	20 Minutes
Temperature		60 ^oC	60 ^oC
pH		10-11	12-13

cycle ended with rinsing the activated substrate with 0.01 M HCl solution in order to prevent hydrolysis of Pd^{2+}. The sensitization and activation cycles were repeated 6 to 10 times until a perfectly activated (a uniform dark brown color) surface was prepared. Typically, a uniform activated surface over the substrate was achieved after 6 cycles of sensitization and activation.

Pd and Cu were deposited sequentially on the activated MPSS surface by surfactant induced electroless plating (SIEP) process. The sequential deposition was carried out in an electroless plating bath at a constant temperature of 333 K. For preparing the Pd and Cu electroless plating baths, sodium salts of EDTA and analytical grade ammonium hydroxide were obtained from Acros Organic and Fisher Scientific, respectively. ACS grade copper (II) sulfate pentahydrate (98.0-102.0%) was supplied by Alfa Aesar. Hydrazine (1.0 M) and tetra-amine palladium chloride were obtained from Sigma-Aldrich. Cationic surfactant DTAB (dodecyl tri-methyl ammonium bromide, MW 308.35) was also obtained from Sigma-Aldrich. DTAB concentration was controlled as a function of critical micelle concentration (CMC). The 4 CMC concentration of the DTAB was used for both Pd and Cu baths as it was used in fabricating Pd and Pd-Ag alloy membranes in our previous works [11-12, 54].

In the plating process, Pd was deposited followed by Cu deposition. The amount of copper deposition was controlled based on the deposition rate of Pd and Cu. To maintain the Pd to Cu metal ratio 60 to 40 in the deposited film, the deposition time for Pd bath was set to 60 minutes. As Cu deposits faster than Pd, the deposition time for Cu bath was fixed to 20 minutes. The thickness and composition of the films were calculated

using the gravimetric method after each Pd or Cu layer was deposited. The plating process was continued until the surface was deactivated. When the surface of deposition got deactivated, 5 to 6 cycles of sensitization and activation process were repeated to reactivate the surface. After each cycle of Pd and Cu deposition, helium leak test was carried out and the He flux was recorded. Completion of the fabrication of membrane was determined, when the helium flux through the membrane was found zero at pressure of 140 KPa. The helium leak test for each fabricated membrane was tested in our laboratory experimental setup shown in Figure 3.1 [11-12].

The microstructure of the fabricated Pd-Cu membranes was analyzed using scanning electron microscopy (SEM), energy dispersive spectroscopy (EDS), X-ray diffraction (XRD) and atomic force microscopy (AFM) techniques. The grain sizes were determined using point-to-point measurements from representative SEM images. The statistical distributions of deposited metal grains were estimated considering a minimum 500 number of grains in a constant cross-section area. For Pd-Cu alloy membranes He gas tightness, H_2 permeability, H_2/N_2 selectivity and long term thermal stability studies were carried out in our in-house diffusivity measurement setup shown in Figure 3.1 [11-12]. After the permeability studies, the membranes were cut into pieces to analyze the cross-section across the thickness of the Pd-Cu alloy film. The cross sections were studied in terms of metal diffusivity from Pd-Cu film to substrate, as well as, from substrate to film using EDS mapping and line scanning at multiple location across each cross-section.

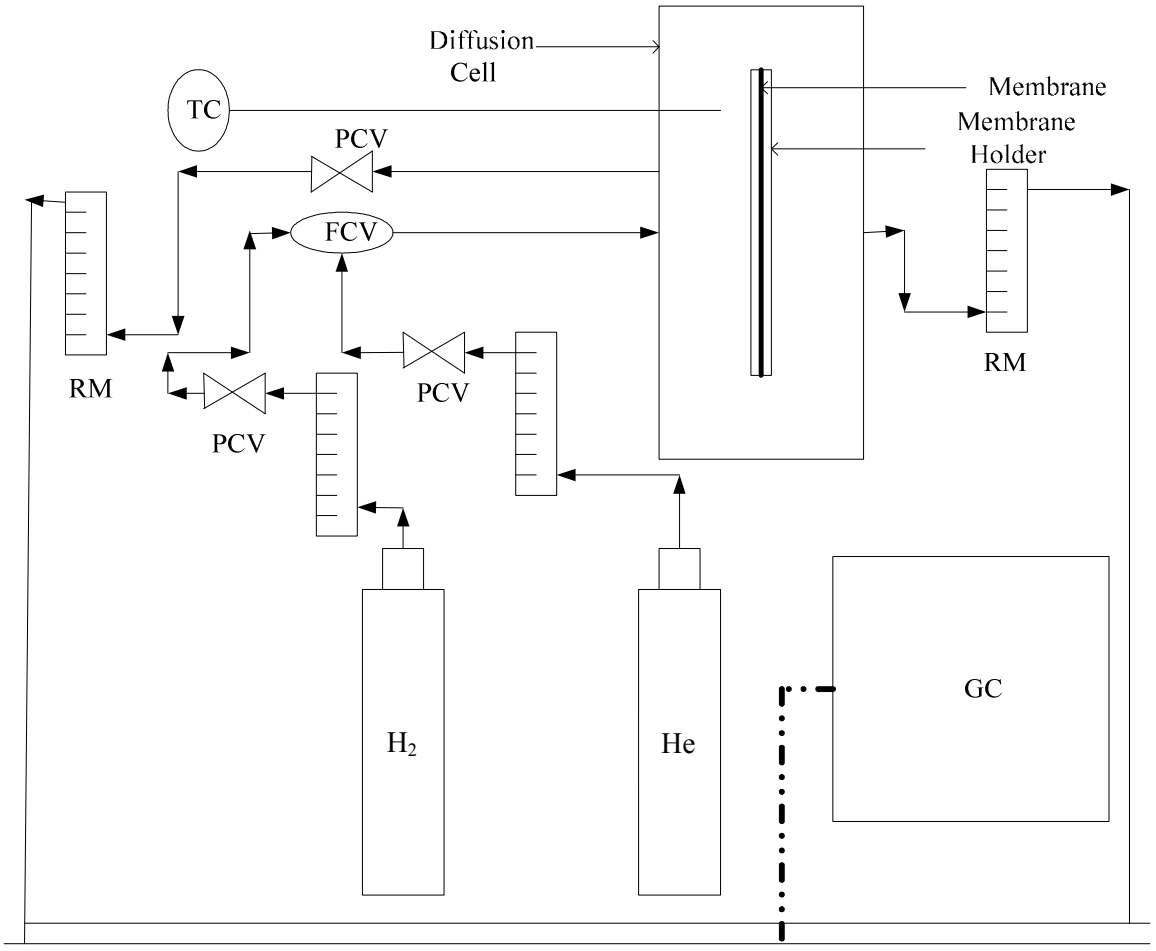

Figure 3.1. Experimental set up for gas permeation through membrane at high temperature (FCV - flow control valve, TC - thermocouple (K -type), GC -gas chromatograph, PCV - pressure control valve, RM - rotameter or mass flow meter) [11-12]

CHAPTER 4

Results and Discussion

Membrane fabrication with agglomerated film microstructure largely depends upon the fabrication process. The fabrication process also plays an important role in microstructure integrity and stability of the film. For higher hydrogen throughput a uniform, thin, and dense agglomerated film is required. The newly devised surfactant induced electroless plating (SIEP) process provides the desired control over the film microstructure. Using SIEP process, the particle size distribution can be controlled, which helps to make a robust membrane of microstructure having desired grain agglomeration. This was demonstrated by our research group previously [11-12, 16, 54]. A brief introduction of the SIEP process is presented below.

The SIEP process is basically a modification of conventional electroless plating (CEP) process. The same set of anodic and cathodic reactions for deposition of Pd and Cu is applicable in the SIEP process. The use of a surfactant in the SIEP process enhances the plating by reducing the external mass transfer resistances. In CEP process, evolution of N_2, and NH_3 gas bubbles adhered to the substrate surface are making the space unavailable for deposition. This produces a porous (pinholes) film microstructure having unrecognizable grain agglomeration. The use of surfactant facilitated to eliminate the mass transfer resistance by helping adhered gas bubbles come out from the surface. The interaction of surfactant with the solid-liquid and gas-liquid interfaces controls the grain size distribution. This enables fabricating a dense and thin film with very rare or no defects. Additionally, SIEP process enabled us to have the desired particle size

distribution and grain agglomeration, which enhanced H_2 permeability [16]. In this work, Pd-Cu membrane was fabricated by both conventional electroless plating (CEP) and surfactant induced electroless plating (SIEP) Process. The purpose of fabricating two Pd-Cu membranes by CEP was to compare the performance of Pd-Cu membrane fabricated by SIEP. The SIEP process used to fabricate Pd-Cu membranes is an extension of our previous works, assuming that the surfactant will behave in the same way in Cu bath as it did in Pd and Ag Baths [11-12]. Basically, the scope of SIEP process was evaluated in fabricating Pd-Cu alloy membranes in this work. Throughout this work, surfactant DTAB (dodecyl tri-methyl ammonium bromide), was chosen at a concentration of 4 CMC, which was appropriate to form very tiny and repetitive grain sizes of deposited metals on the surface during deposition according to our previous studies [16, 54].

The structure, grain size distribution, grain agglomeration and metal composition in the film were characterized by SEM (Hitachi S3200 a Variable Pressure Scanning Electron Microscope), XRD (Bruker AXS D8 DISCOVER), and AFM (JOEL SPM 4200D) analysis. The film characteristics were also evaluated from the cross-section of film after annealing. The microstructures of Pd-Cu membrane films were characterized in terms of elemental analysis, particle size distribution and surface morphology. In subsequent sections, the effect of intermediate heat treatment on the film microstructure and the film stability is presented. The H_2 transport behavior, H_2/N_2 selectivity and activation energy of permeance of Pd-Cu membranes fabricated by SIEP and CEP are discussed in the penultimate section. Finally, long term thermal stability of Pd-Cu membrane fabricated by SIEP method as a function of H_2 flux is discussed.

4.1 Microstructure Analysis of Different Pd-Cu Membranes Fabricated by SIEP and CEP Methods

4.1.1 Helium Gas-tightness and Thickness Analysis of Different Pd-Cu Membranes

Microstructure of Pd based membranes depends on a number of factors, such as, substrate surface roughness, pore dimension, fabrication technique and bath parameters. The use of different reducing agent in different concentration also manipulated the reaction kinetics, hence affected the surface microstructure and grain size distribution to some extent. For this work, we kept all these parameters (bath composition, bath parameters, surfactant and its concentration) constant in order to elucidate the effect of SIEP process on the microstructure of the Pd-Cu films. The substrate we used was from Mott metallurgical corporation and it was assumed to have the same roughness for all the substrates. For dimensions, we used the manufacturer's provided information of pore size of 2 μm and diameter 1 inch with thickness of 0.062 inch. In Figure 4.1 microstructure of bare substrate is shown.

Table 4.1 summarizes the attributes of Pd-Cu membranes fabricated by both CEP and SIEP processes with a surfactant (DTAB) concentration of 4 CMC [16, 54]. Table 4.1 presents data on plating time, film thickness, metal composition, H_2 flux and selectivity. At the bottom part of Table 4.1, shows similar data for Pd membrane fabricated by both SIEP and CEP processes for comparison. The film thickness of Pd-Cu membrane was calculated using gravimetric method and SEM analysis for SIEP membranes; however, only using gravimetric method for CEP membranes. As expected, for all these Pd-Cu SIEP membranes the calculated thicknesses by these two methods are very comparable. From Table 4.1, it is evident that Pd-Cu membranes fabricated by SIEP

process are thinner compared to Pd-Cu membranes fabricated by CEP process. The average thickness of Pd-Cu film fabricated by SIEP process is 15.38 μm, whereas, that of Pd-Cu film fabricated by CEP process is 19.68 μm. In our previous study, we found that the film thickness of pure Pd membrane fabricated by SIEP process was 8.5 μm and the average film thickness of Pd-Ag membrane fabricated by SIEP process was 13 μm [11-12]. From the Table 4.1, it is also clear that Pd-Cu films are considerably thicker than that of Pd film which is consistent with the deposition mechanism of copper. Cu is difficult to deposit on a freshly activated substrate surface. It is a common procedure to deposit Pd first; then, Cu is deposited on top of Pd particle layer. It is also well known that electroless plating is an autocatalytic reaction, which means both Pd and Cu deposition are accelerated in the presence of Pd and Cu particles in baths. Hence, during Pd-Cu membrane fabrication by SIEP method using sequential deposition technique, Cu was deposited on the top surface of Pd film. However, when Pd was deposited on Cu film, it washed away the Cu film. This mechanism of deposition led us to do an intermediate heat treatment of the membrane before Pd film was deposited on Cu film. The heat treatment was conducted for one hour in presence of pure H_2 flow at 10 psi pressure in diffusion cell set up in our laboratory shown in Figure 3.1 of chapter 3. This eventually resulted in better Pd film deposition above Cu film; however, it took longer time to fabricate Pd-Cu alloy membrane compared to pure Pd membrane. While pure Pd membrane took only 10 hours of deposition time to complete the fabrication, Pd-Cu alloy membrane took 30 hours of deposition time on an average to complete fabrication process. This suggests that it requires higher number of deposition cycles of Pd and Cu to ensure Pd-Cu membrane

leak proof during He leak test study and ready to use for H_2 separation from other gas mixtures. Consequently, Pd-Cu membranes formed thicker films over the substrate than the pure Pd membrane did. The results presented in the Table 4.1 indicate that thinner Pd-Cu membranes can be fabricated in shorter time in presence of surfactant DTAB compared to Pd-Cu membranes fabricated without presence of surfactant in plating baths.

The results associated with the gas-tightness of membranes shown in Figure 4.2 confirmed the effects of surfactant in fabricating dense and thin membranes. The fabrication of Pd-Cu membrane was assumed to be complete when the pure helium flow through the membrane at 20 psi and 298 K was zero. In Figure 4.2, helium gas-tightness results are presented for two Pd-Cu membranes (S2 and S3) fabricated by SIEP method and two Pd-Cu membranes (C1 and C2) fabricated by CEP method. For indicating the end of fabrication process and assessing gas-tightness, helium (atomic radius = 0.98 Å) was chosen as it being the smaller molecule compared to hydrogen (atomic radius = 1.58 Å), and specifically helium is inert. To achieve zero helium gas-tightness as an indication of ending of membrane fabrication, it is evident from Figure 4.2 that Pd-Cu membranes prepared by CEP method require thicker deposition of film over substrate than Pd-Cu membranes prepared by SIEP method.

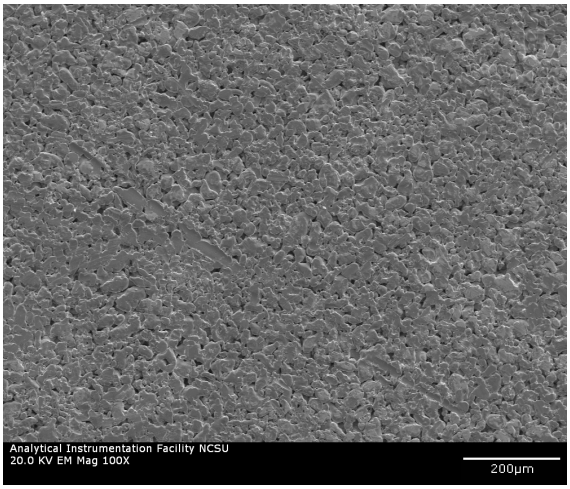

Magnification 100x

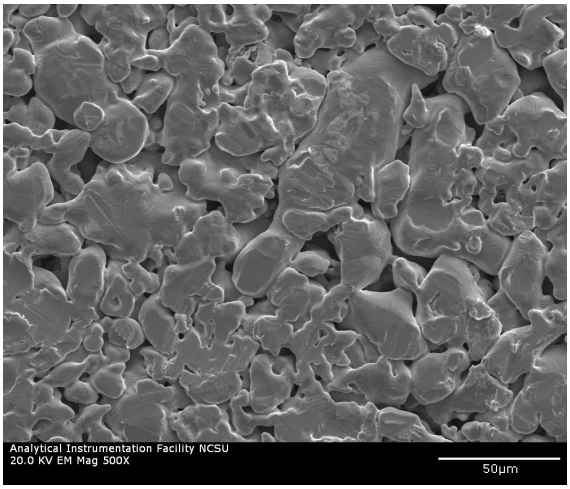

Magnification 500x

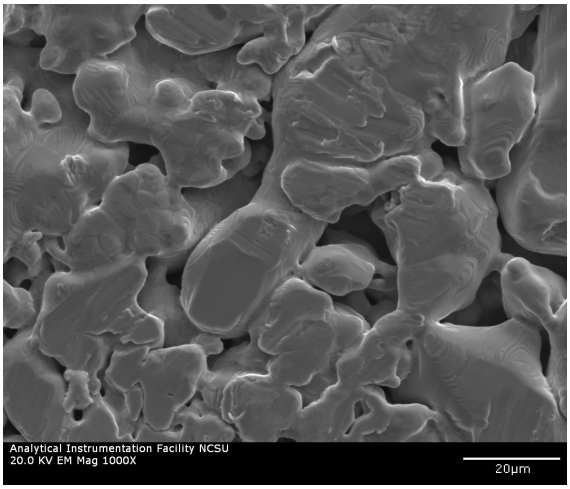

Magnification 1000x (location-1)

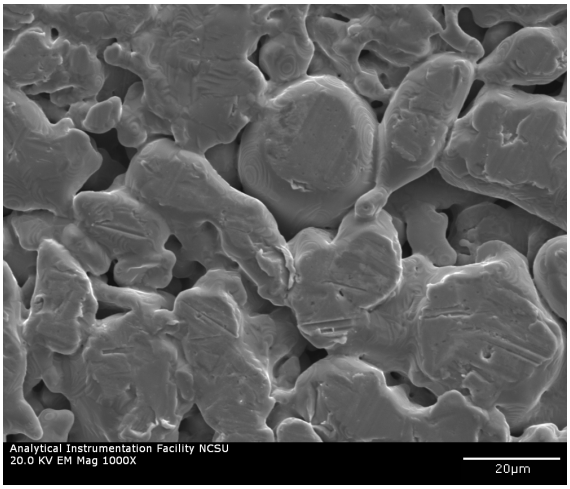

Magnification 1000x (location-2)

Figure 4.1. SEM images of the top surface of bare 316L micro-porous stainless steel (MPSS) substrate

Table 4.1. Summary of Pd and Pd-Cu membranes attributes fabricated by SIEP and CEP methods

Membrane Sample	Deposition Time (hr)	Film Thickness (μm)		Film Composition (% of Cu)	H_2 Flux at 723K (mol/m^2-s)		Selectivity at 723K (H_2 Flux/N_2 Flux)	
		Gravimetric Analysis	SEM Analysis		20 psig	100 psig	20 psig	100 psig
S1 Pd-Cu	26.8	15.6	-	-	-	-	-	-
S2 Pd-Cu	33.8	16.73	-	35.8	0.145	0.54	123	49
S3 Pd-Cu	31.4	14.5	13.34	44.69	0.156	0.55	110	43
S4 Pd-Cu	27.8	14.7	13.61	25.8	-	-	-	-
C1 Pd-Cu [a]	34.3	19.18	-	36.7[c]	0.094	0.43	19	7.42
C2 Pd-Cu [a]	35.7	20.17	-	33.4[c]	0.097	0.44	17	8
Pd 4CMC[b]	10	8.5	8.5	-	-	-	-	-
Pd 0CMC[b]	28	28.5	27.5	-	-	-	-	-

a. Membranes Fabricated by CEP

b. Data from previous work [12]

c. By Gravimetric analysis

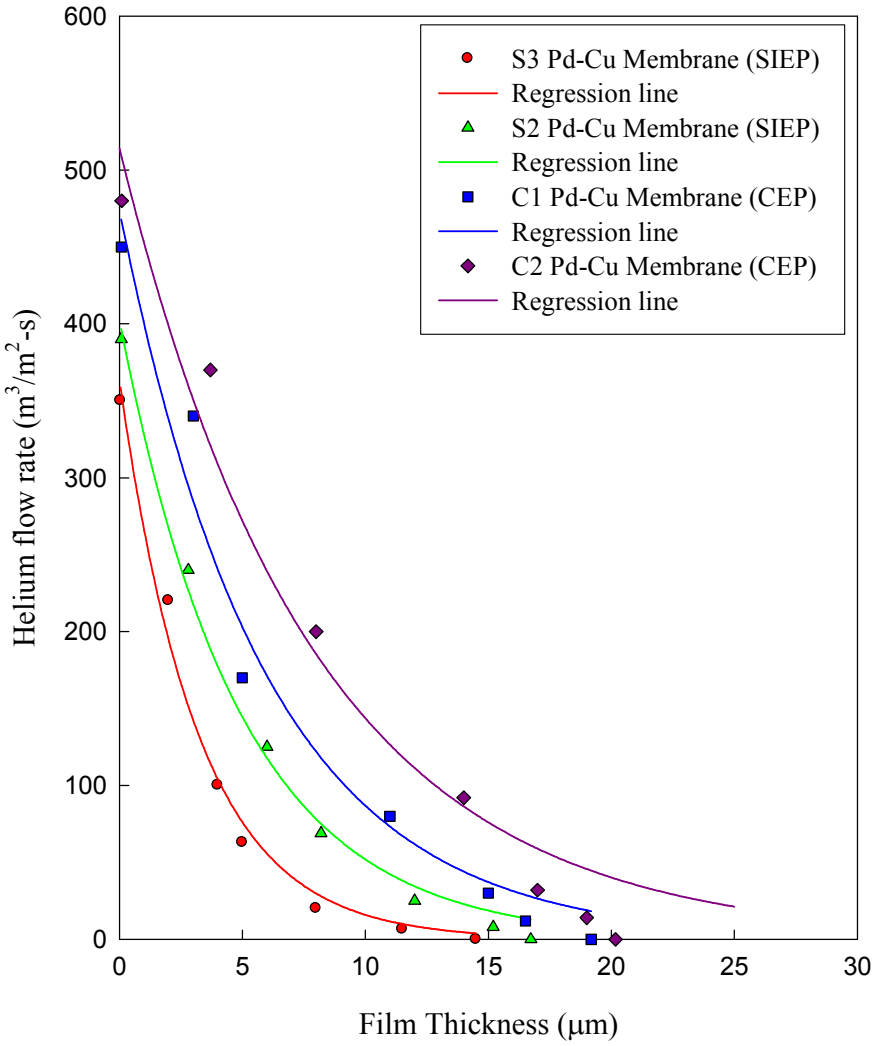

Figure 4.2. Helium gas-tightness as a function of membrane thickness for Pd-Cu membranes fabricated using surfactant and without surfactant

4.1.2. Microstructure Analysis of Pd-Cu Membranes

A comparison of SEM images of both Pd and Pd-Cu membranes fabricated by CEP and SIEP processes is presented in Figure 4.3 to better understand the microstructure of Pd-Cu membranes. It helps to explain the effect of surfactant on the microstructure of the deposited Pd-Cu film on activated surface. The SEM images of all three membranes are presented at magnification of 5K and 10K at electron beam energy of 30 kV. In Figure 4.3, SEM images of Pd membranes are demonstrated to compare the effect of alloying of Pd with Cu in Pd-Cu membrane. In Figures 4.3 (a) and (b), Pd films fabricated in absence of DTAB, clearly show the non-diffused grains and the grain boundaries. These non diffused grains and grain boundaries are actually responsible for intra or inter granular porosity of the deposited film. From the SEM images of Figures 4.3 (c) & (d) and (e) & (f), it is clear that, the Pd film fabricated using DTAB at 4 CMC level has finer grains, and the diffusion of grain boundaries resulted in an uniform, smooth and continuous surface. The Pd-Cu film also shows finer grain size, as well as, agglomeration of the grains. However, the apparent uniformity of the agglomeration for Pd-Cu film is not as high as Pd film alone. As long as the surface roughness is concerned, the Pd membrane is much more uniform and smoother than Pd-Cu membranes.

The differences between fabrication process of Pd and Pd-Cu membranes can explain the differences in surface morphology. Pd and Cu are deposited on an activated surface by an autocatalytic SIEP process. Cu particles are deposited on the top of Pd layer in a sequential deposition process. But Pd is not deposited over Cu layer; so intermediate heat treatment is required to prepare the surface for deposition of Pd over Cu layer for the

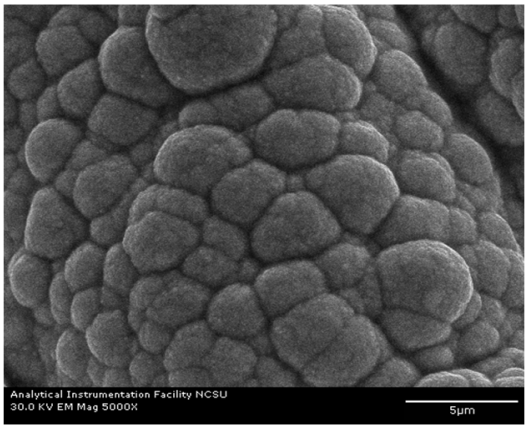

(a) Pd at 5K (CEP)

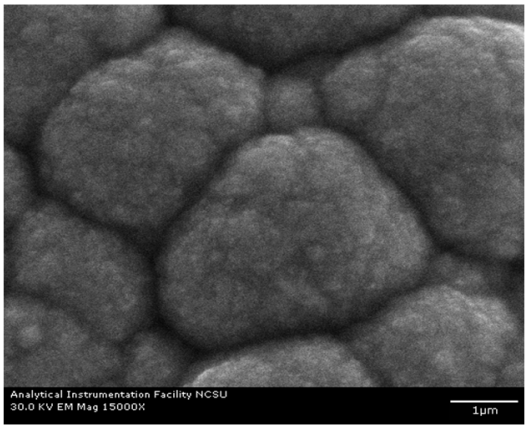

(b) Pd at 10K (CEP)

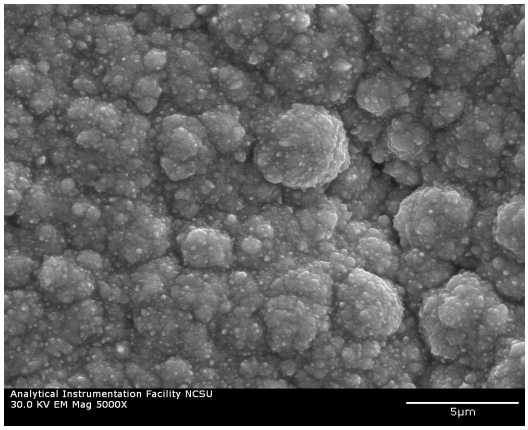

(c) Pd at 5K (SIEP)

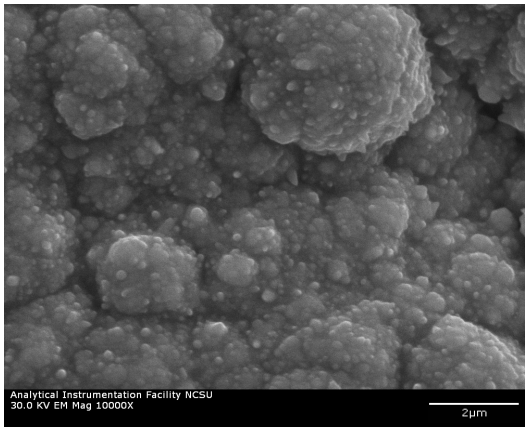

(d) Pd at 10K (SIEP)

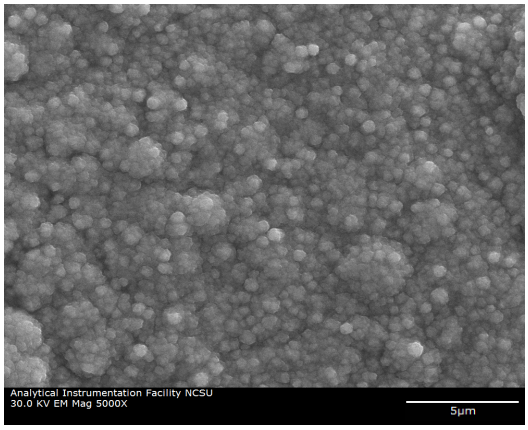

(e) Pd-Cu at 5K (SIEP)

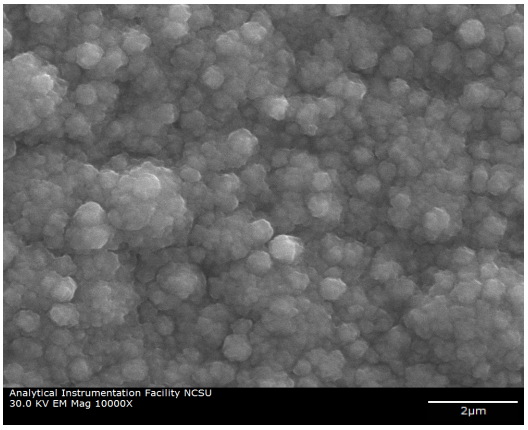

(f) Pd-Cu at 5K (SIEP)

Figure 4.3. SEM images of surfactant activated Pd and Pd-Cu deposition showing agglomerated grain throughout the surface at different magnification

fabrication of Pd-Cu membranes. This difference in fabrication technique and different particle sizes of Pd and Cu made the film surface rough. To investigate the particle size, surface roughness and grain boundary diffusion, the SEM images were taken in different agglomerated sites with different magnification of 5K, 10K, 20K and 50K, which are shown in Figure 4.4. The energy of the electron beam was chosen as 15 kV to take the SEM images. From Figure 4.4, we can infer grossly that two different particle sizes are dominating grain size and subsequent grain agglomeration. Higher magnification SEM images (20 K and 50 K) at lower electron beam energy of 15 kV in Figures 4.4 (c) & (d) show the presence of two different particles having two different mean grain sizes. As we gradually move to the higher magnification images it is clear that there is exactly similar grain boundary diffusion just beneath the top particle layer. For fabrication of Pd-Cu membrane, we followed the sequential SIEP process that ended with Cu deposition. This makes Cu to deposit on the crest of the hills where Pd particles were previously deposited, as well as, in the furrow of the hills where Pd particles were not deposited. Sequential electroless deposition for Pd-Cu membrane also required heat treatment, before applying Pd deposition on top of Cu film in intermediate stages of deposition. Heat treatment was carried on for one hour in presence of pure H_2 flow at 10 psi pressure. The purpose of heat treatment was to prepare the film surface to deposit Pd on Cu film. For Pd-Cu film, it has continuous grain boundaries diffused into one another just below the rough top layer with different particle sizes, which ended up with an apparent increase in film roughness. This is the combined effect of heat treatment and interaction of Pd and Cu particles during surfactant induced sequential electroless deposition.

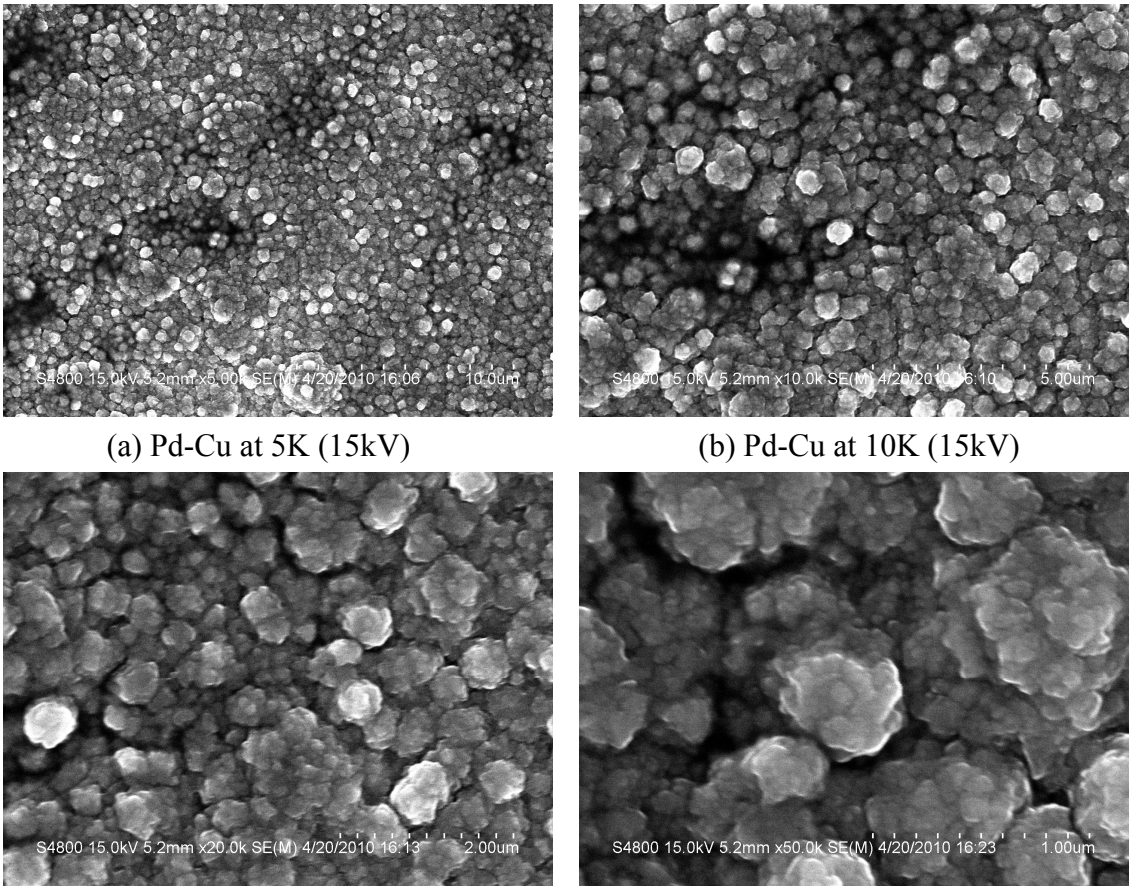

(a) Pd-Cu at 5K (15kV)

(b) Pd-Cu at 10K (15kV)

(c) Pd-Cu at 20K (15kV)

(d) Pd-Cu at 50K (15kV)

Figure 4.4. SEM images of Pd-Cu membrane film top surface fabricated by SIEP process showing smooth and uniform grain agglomeration

Figure 4.5 shows the grain size distribution of Pd and Cu in Pd-Cu membranes fabricated by SIEP method. The particle size distribution of Pd and Cu shows two sharp peaks at 0.65 μm and 1.01425 μm. The existence of two peaks in Figure 4.5 indicates the presence of two different metals (Pd and Cu) from two different sequential electroless deposition during fabrication of Pd-Cu membrane. The first peak in Figure 4.5 is for Cu and the second one is for Pd, as the size of Cu (atomic radius = 128 pm) is small compared to the size of Pd (atomic radius = 137 pm). Both peaks indicate the presence of two different mean size particles, which is consistent with SEM images showed in Figure 4.4. In a sequential deposition cycle of Pd and Cu, the cycle ends with Cu deposition. To control the metal composition of Cu in Pd-Cu membrane during deposition in baths, it is required to maintain the amount of Pd and Cu in a deposition cycle. Therefore, after careful study of gravimetric deposition of both Pd and Cu metals, the deposition cycle for Pd was set for an hour, where as that for Cu was set only for twenty minutes; to maintain the gravimetric metal composition of Pd and Cu. The targeted value for metal composition in film was 40% of Cu. H_2 permeability of Pd-Cu membrane passed through a maximum, when film had around 40% of Cu; and notably, reducing membrane cost (relative to pure Pd), and it showed increased resistance to H_2S poisoning [55]. Both Pd and Cu have to be deposited before the surface got deactivated, which actually left some nucleation sites unused. Hence, the Pd and Cu particles did not get enough particles aggregation into the grain to grow to its normal dimension. Average particle size of Pd grain is 2 μm for pure Pd membrane [11]. From Figure 4.5, it is evident that the mean dimension of the particles is lower for Pd-Cu membrane than that for pure Pd membrane.

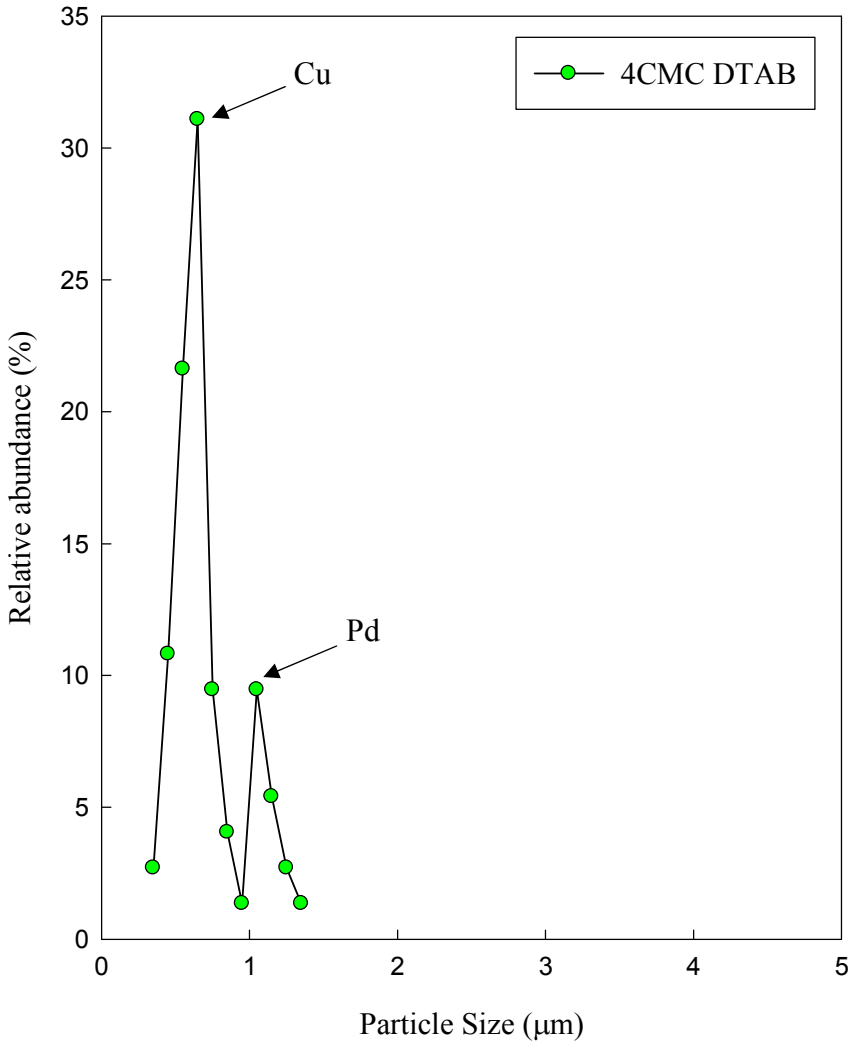

Figure 4.5. Cu and Pd grain size distribution observed in Pd-Cu membrane fabricated by SIEP method with 4 CMC of DTAB surfactant

Figure 4.5 shows the suface microstructure in terms of grain agglomeration and particle size distribution. Now, it is important to illustrate the SEM images of the top surface morphology of Pd-Cu membranes taken at different electron beam energy. Figure 4.6 shows the SEM images of Pd-Cu membrane fabricated by SIEP method. From Figure 4.6 it is clear that, as we move to higher electron beam energy the more we loose the minute details of surface morphology. On the other hand, moving to lower energy leads to loss of the organization of grains and diffusion of grain boundaries. To comprehend the surface morphology and the particle size distriubution, it is necessary to capture SEM images with different magnifications and with different electron beam energy to get the finest image of the film top surface. From Figure 4.6 (f), it is clear that at 20 kV and 5K magnification gives the best image of surface morphology and grain size for Pd-Cu membrane fabricated by SIEP method.

In Figure 4.7, the SEM images of Pd-Cu membranes fabricated by CEP and SIEP processes are shown. Figures 4.7 (a), (b), (c) and (d) show the SEM images of Pd-Cu membrane fabricated by CEP process. Figures 4.7 (a) and (b) are without intermediate heat treatment and Figures 4.7 (c) and (d) are with intermediate heat treatment for Pd-Cu membrane fabricated by CEP process. But the grain agglomeration and size of particles are much bigger in size and shape compared to those of Pd-Cu membranes fabricated by SIEP process, which is clear in Figures 4.7 (e) and (f). Therefore, comparing the SEM images of Pd-Cu membranes fabricated by CEP and SIEP processes, it is fair to mention that SIEP process gives more control on grain size and repeatable microstructure during fabrication of Pd-Cu membranes compared to CEP process.

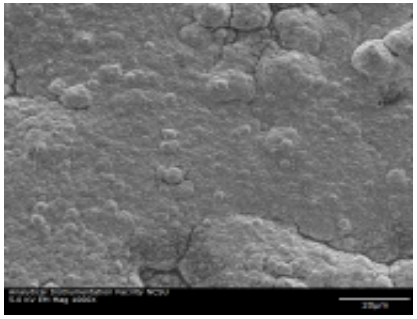

(a) Pd-Cu at 1K (5kV)

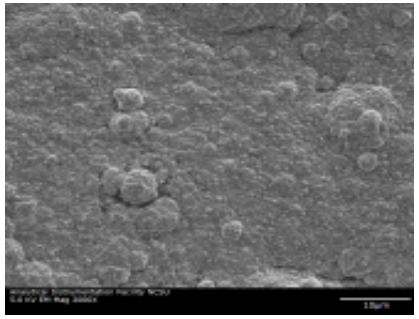

(b) Pd-Cu at 2K (5kV)

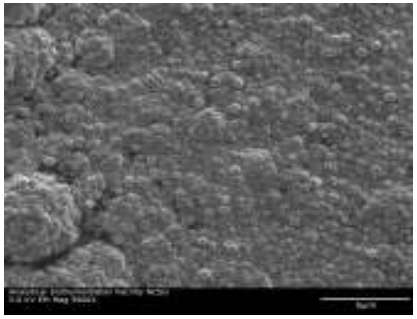

(c) Pd-Cu at 5K (5kV)

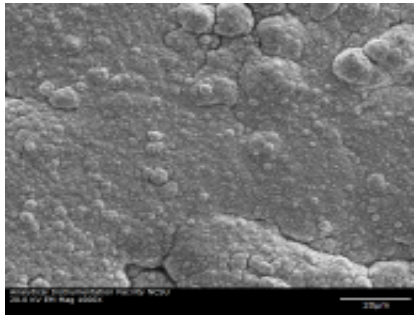

(d) Pd-Cu at 1K (20kV)

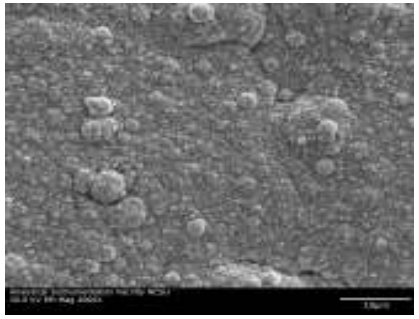

(e) Pd-Cu at 2K (20kV)

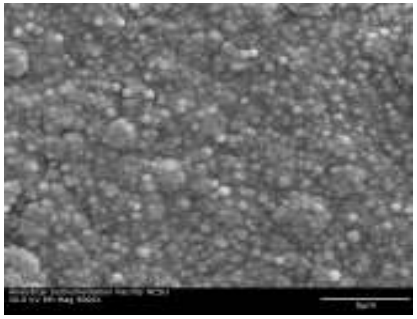

(f) Pd-Cu at 5K (20kV)

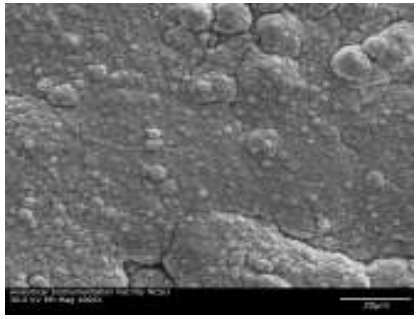

(g) Pd-Cu at 1K (30kV)

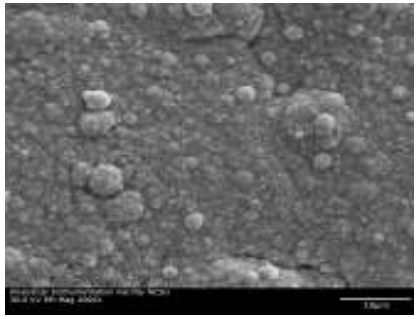

(h) Pd-Cu at 2K (30kV)

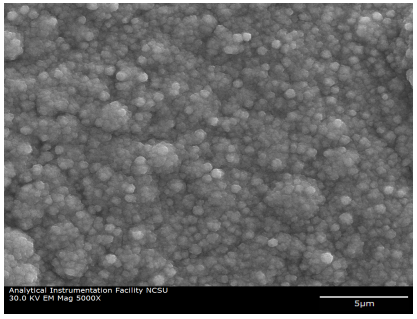

(i) Pd-Cu at 5K (30kV)

Figure 4.6. SEM images of Pd-Cu membrane top surface at different resolution showing grain agglomeration fabricated by SIEP method

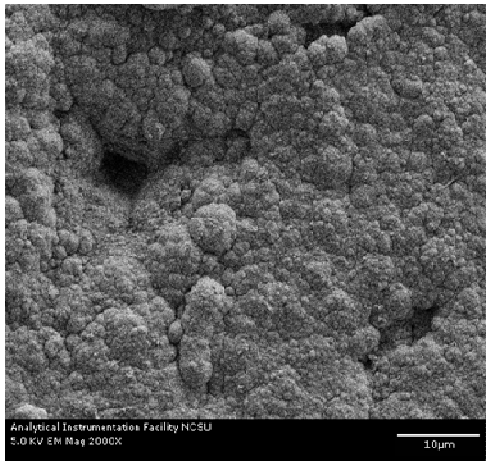

(a) Pd-Cu at 2K (CEP) WHT

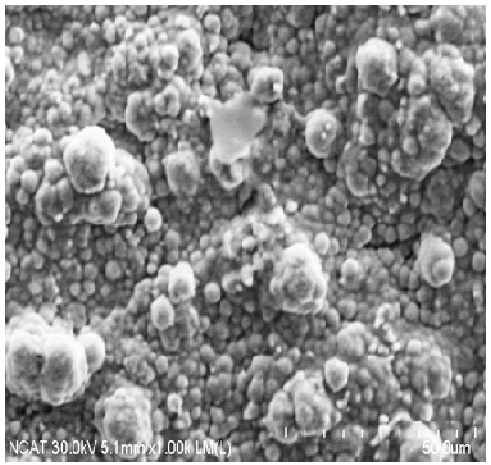

(c) Pd-Cu at 1K (CEP) HT

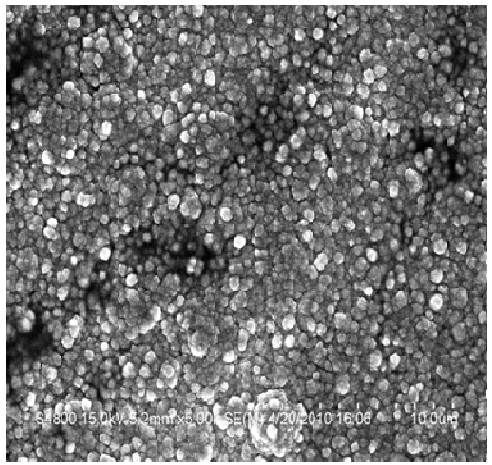

(e) Pd-Cu at 5K (SIEP) WHT

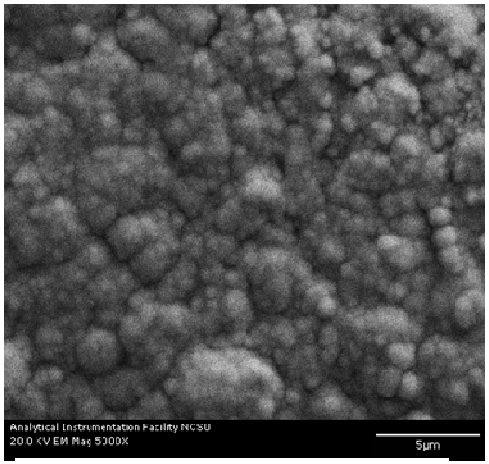

(b) Pd-Cu at 5K (CEP) WHT

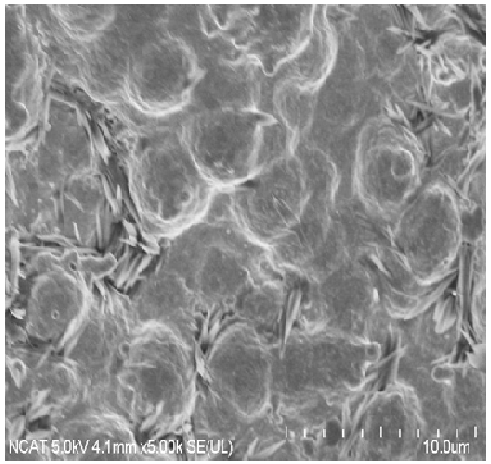

(d) Pd-Cu at 5K (CEP) HT

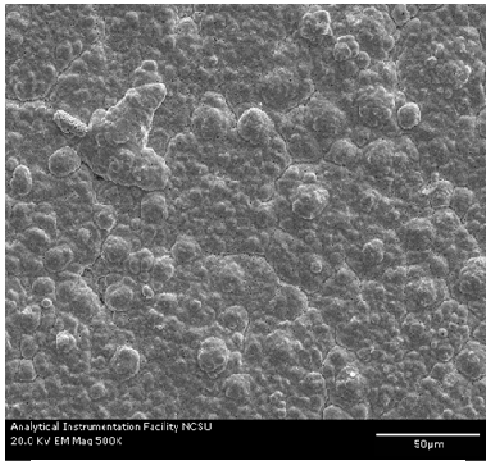

(f) Pd-Cu at 0.5K (SIEP) HT

Figure 4.7. SEM images of top surface of Pd-Cu membranes fabricated by CEP and SIEP methods at different resolution as shown by grain agglomeration

Surfactant DTAB is hydrophobic in nature and the molecules are aligned around gas-liquid interfaces and form various cylindrical and spherical cage like structures. Surfatant DTAB also tends to form meta-stable cylindrical and spherical structures in the solid-liquid interfaces that helps to form finer grains and subsequent coarsening of the grains, which were elucidated over a hydrophobic glass surface shown in Figure 4.8. Figure 4.8 shows that surfatant DTAB forms regular cage like structures at regular interval throughout the surface. These cage like structures support the idea of forming meta-stable structures in the solid-liquid interfaces by surfactant DTAB [16, 54]. Further, Figure 4.8 suggests that the use of DTAB surfactant in electroless plating baths supports the formation of thin layers of film as well.

To comprehend the film surface roughness in different locations of the film it is essential to study the film topographic structures. The surface topography of Pd-Cu membranes fabricated by SIEP and CEP methods was examined with AFM analysis and presented in Figure 4.9, Figure 4.10 and Figure 4.11. In Figure 4.9, the AFM image before heat treatment of Pd-Cu membrane fabricated by SIEP process is shown, where we see the presence of cage like structures comparable to Figure 4.8. However, the grains are diffused to one another due to presence of both Pd and Cu molecules. The average roughness of the top surface is 1.122 μm. In Figure 4.10, the AFM image with heat treatment of Pd-Cu membrane fabricated by SIEP process is shown, where we see more deeper cage like structures compared to Figure 4.9. The average roughness is 1.250 μm, which is slightly high compared to that in Figure 4.9. Heat treatment causes the top surface to be resturcutured and reshaped; hence, resulting slight increase in roughness.

Finally, the AFM image of Pd-Cu membrane fabricated by conventional electroles plating (CEP) process is shown in Figure 4.11. The AFM image is taken before the membrane was heat treated. The AFM image in Figure 4.11 is less sharp, the surface roughness is high and the grain agglomerations are not uniform throughout the top surface of the Pd-Cu membrane fabricated by the CEP process. It is also not apparent from Figure 4.11, the presence of cage like uniform structures of Pd-Cu films, which ultimately causes to form a thick film of metals above the substrate. The average roughness of the top surface is 2.275 μm, which is almost double compared to that of membrane fabricated by SIEP process, shown in Figure 4.9. Therefore, the AFM images also confirmed that the Pd-Cu membranes fabricated by SIEP process have less top surface roughness and more uniform grain structures compared to Pd-Cu membranes fabricated by CEP process. The presence of cage like structures in Pd-Cu membranes fabricated by SIEP process, which is shown in Figure 4.9, supported the formation of uniform and thin Pd-Cu film over the MPSS substrate and resulted in better membrane performance and thermal stablity, which will be discussed later in this chapter.

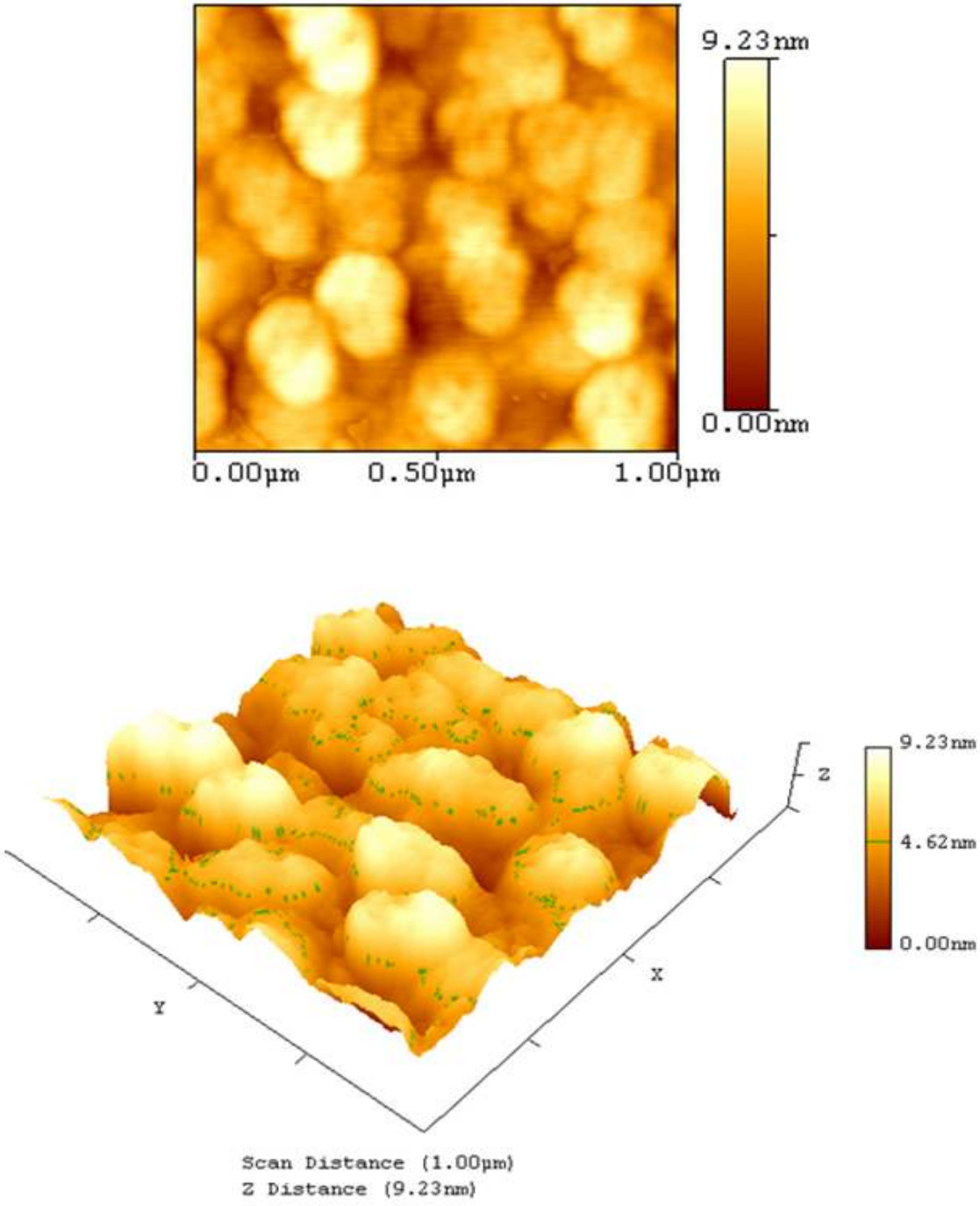

Figure 4.8. AFM images of Pd solid surface aggregation onto typical hydrophobic glass surface using DTAB

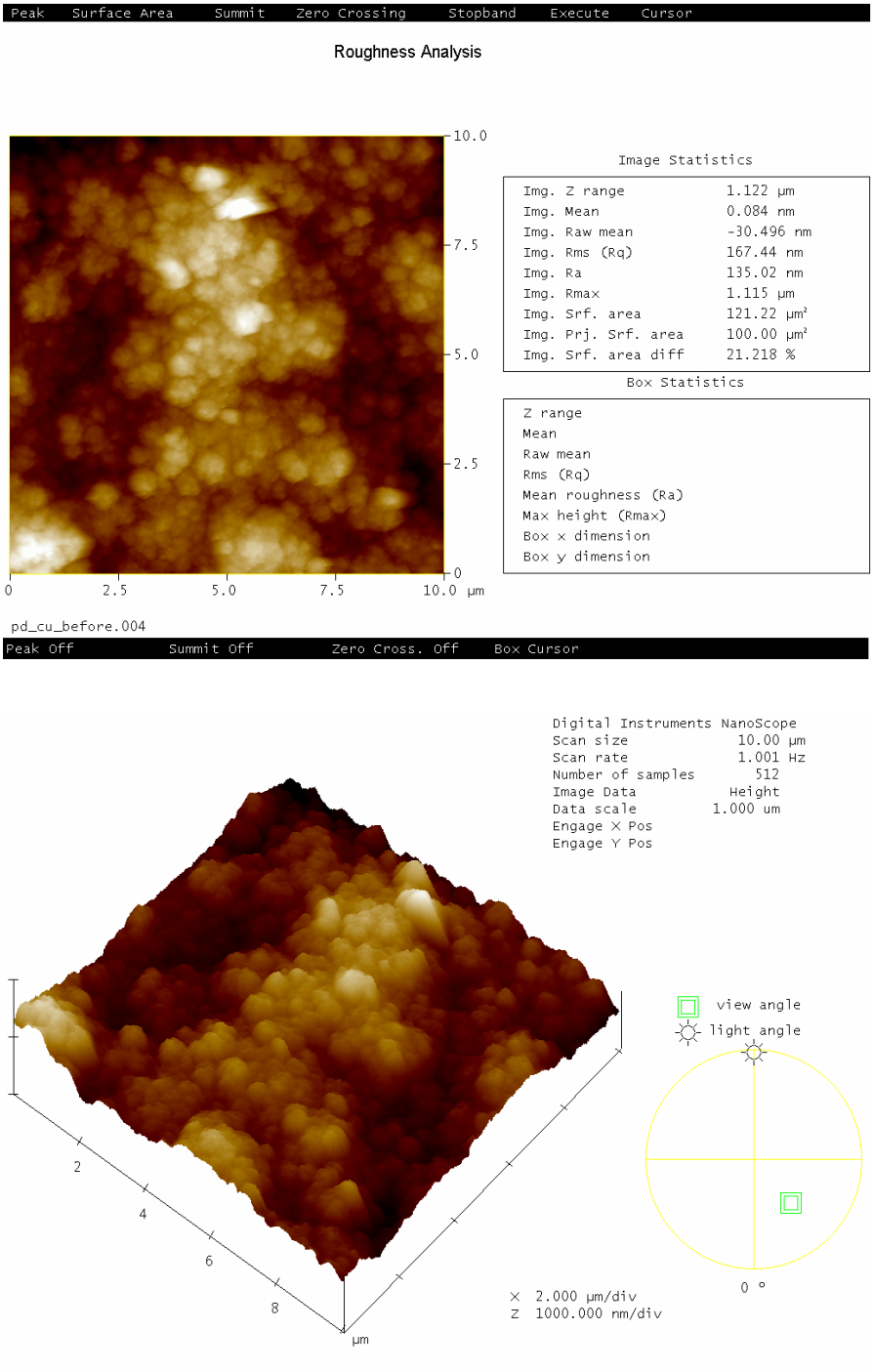

Figure 4.9. AFM images of solid Pd-Cu surface aggregation onto typical MPSS surface using DTAB

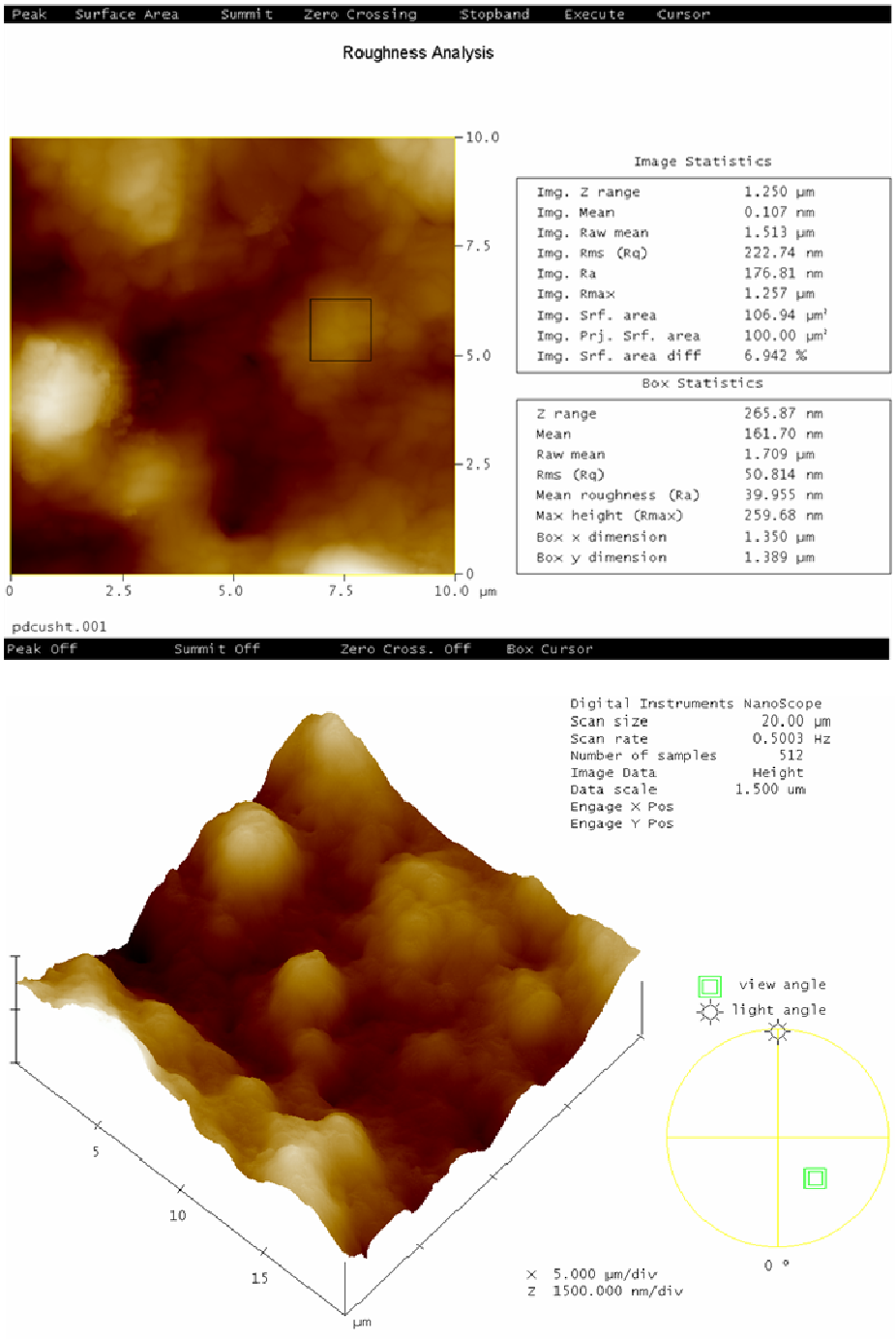

Figure 4.10. AFM images of solid Pd-Cu surface aggregation onto typical MPSS surface using DTAB after heat treatment

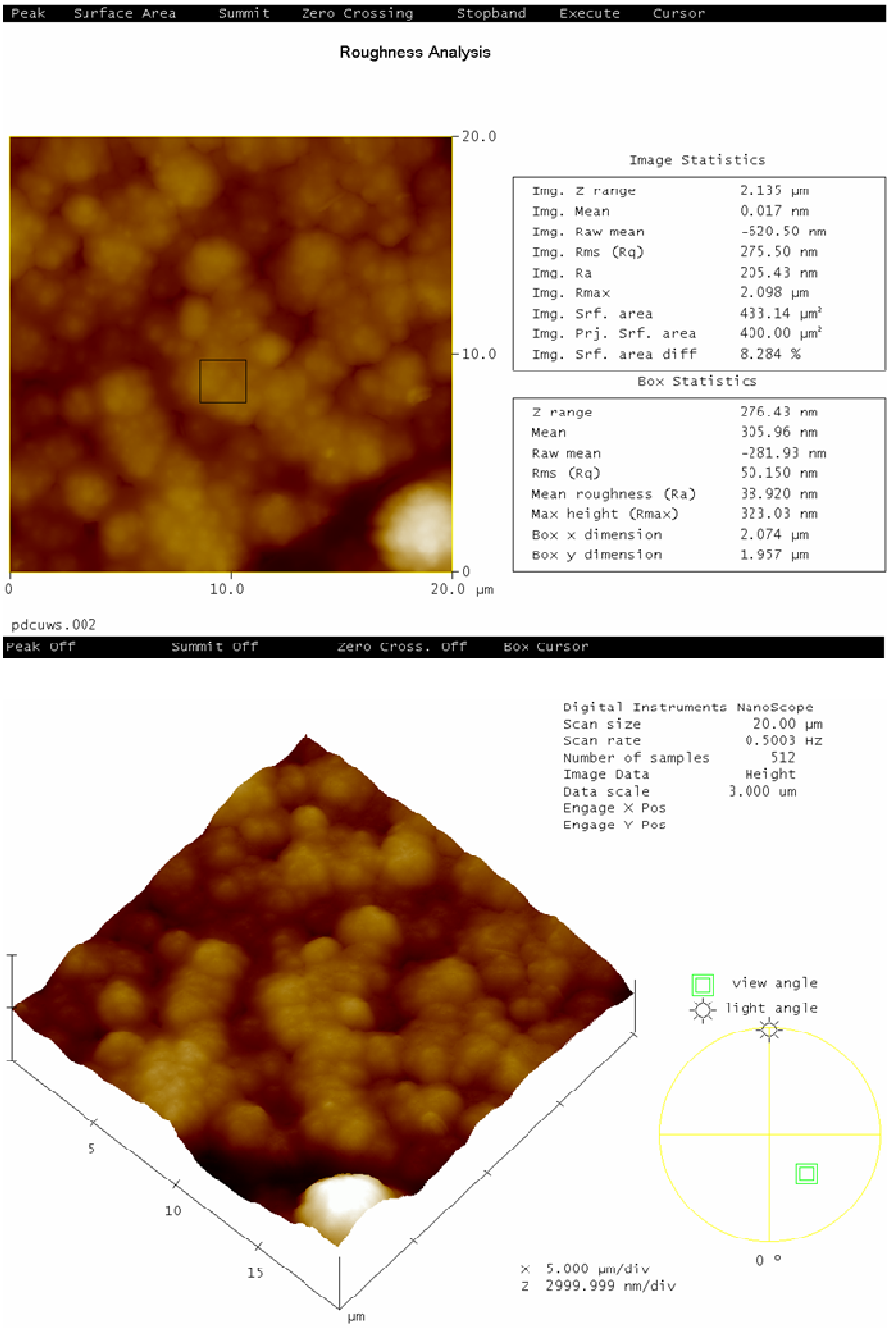

Figure 4.11. AFM images of solid Pd-Cu surface aggregation onto typical MPSS surface without using DTAB

Surface elemental analysis of Pd-Cu membranes fabricated by SIEP process was carried out by X-ray diffraction (XRD) and energy dispersive spectroscopy (EDS). Typical XRD patterns after fabrication of Pd-Cu membranes are shown in Figure 4.12. From the XRD patterns in Figure 4.12, the reflection peaks of Pd and Cu in the Pd-Cu film (f.c.c. phase) were found at [111], [200], [220] and [311] planes. Table 4.2 lists the 2θ and d-spacing values corresponding to the four major reflection peaks at [111], [200], [220] and [311] planes for pure Pd and Pd-Cu film for comparison. The 2θ values suggest all the characteristics peaks of Pd are in the same position for both Pd and Pd-Cu films and also presence of different lattice bravais confirmed formation of polycrystalline structure throughout the film. No reflection peak was observed during XRD characterization for Fe, Cr, Ni and Mn/Mo metals.

The typical EDS pattern of Pd-Cu film fabricated using surfactant is presented in Figure 4.13. EDS pattern shows two distinct peaks for Pd and Cu. Quantitative EDS elemental analysis of Pd-Cu film showed 44.69% of Cu deposition, which is mentioned in Figure 4.13. The targeted value for metal composition was 40% of Cu, as H_2 permeability of Pd-Cu membrane passed through a maximum when film had around 40% of Cu and resulted more stable membrane compared to pure Pd membrane [55]. Hence, we were able to deposit more Cu compared to our target value. This will ultimately reduce the fabrication cost of membrane. EDS measurements were done at approximately 20 kV X-ray energy emissions with 500x magnification of the membrane surface. Absence of other metal peaks in EDS pattern in Figure 4.13 also implied that use of surfactant in the plating baths did not introduce any kind of impurities in membrane film.

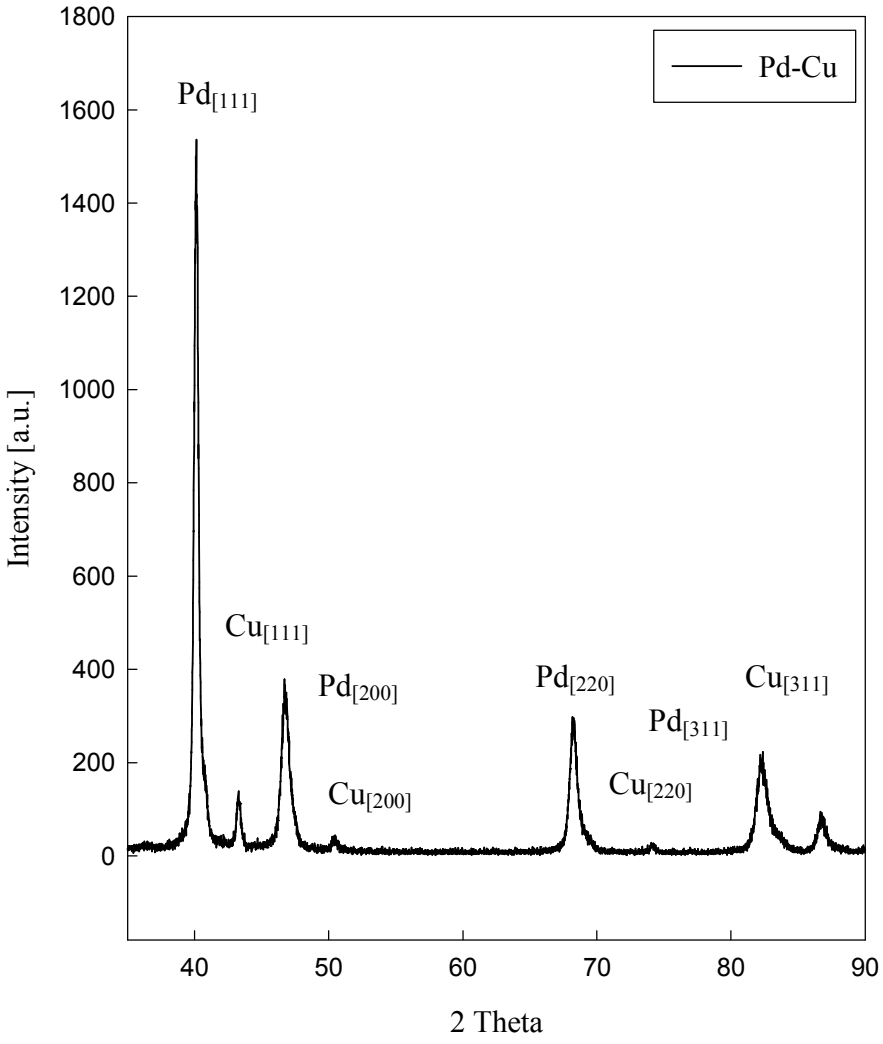

Figure 4.12. Typical XRD pattern of Pd-Cu membrane fabricated by SIEP method showing polycrystalline Pd and Cu deposition

Table 4.2. Comparison of high angle XRD reflection peaks of Pd and Pd-Cu film fabricated by SIEP method

	Bravais lattice	Pd-film		Pd-Cu-film		
		Pd (Pre annealed)	Pd (Post annealed)	Pd (Pre annealed)	Cu (Pre annealed)	Pd-Cu (Post annealed)
2-theta	111	40.214	40.109	40.145	43.316	40.366
	200	46.776	46.652	46.695	50.448	46.956
	220	68.303	68.107	68.176	74.125	68.585
	311	82.338	82.086	82.173	89.936	82.702
d-spacing	111	2.2407	2.2463	2.24439	2.0871	2.2326
	200	1.9405	1.9454	1.94370	1.8075	1.9335
	220	1.3721	1.3756	1.37440	1.2781	1.3671
	311	1.1701	1.1731	1.17210	1.0899	1.1659
Lattice parameter, a		3.881	3.8908	3.8874	3.6150	3.867
Lattice structure		f.c.c.	f.c.c.	f.c.c.	f.c.c.	f.c.c.

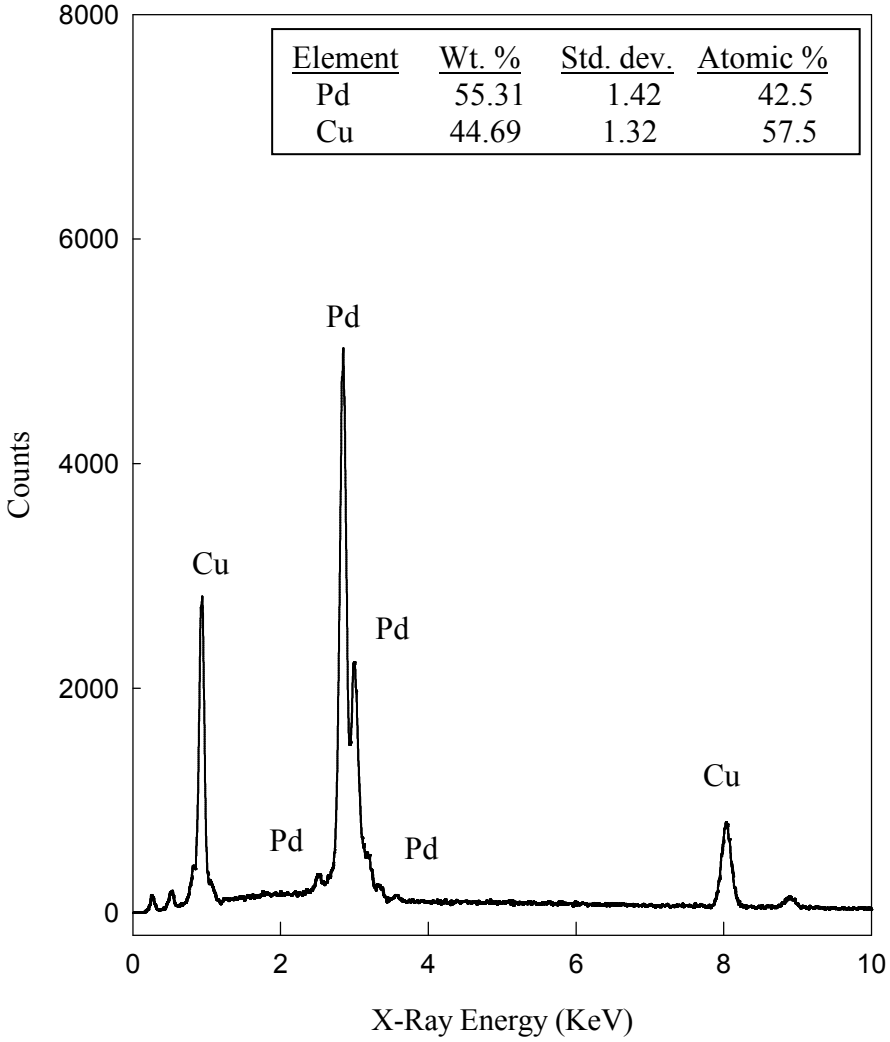

Figure 4.13. Typical EDS spectrum of Pd-Cu membrane shows the presence of polycrystalline deposition of Pd and Cu particles

4.2 Heat Treatment on Pd-Cu Membranes

After fabrication, Pd-Cu membranes were heat treated in a gas tight diffusion cell shown in Figure 3.1 of chapter 3. The membrane was heat treated for 18 hours at 773 K under H_2 environment at 1 atmospheric pressure. Actually, formation of alloy by Pd and Cu metals was almost completed after 10 hours; however, to be certain of this, we did the heat treatment for 18 hours. The temperature (773 K) was chosen based on Tamman temperatures of Pd, Cu and substrate metal constituents, which are shown previously in Table 2.4 of chapter 2. The Tamman temperature is generally half of the melting temperature of a metal and is considered as the point at which sintering begins to start in ceramics materials. It also indicates at which temperature the phase transition (from α-phase to β-phase) of a metal will take place. From Table 2.4 of chapter 2, the Tamman temperature for Pd and Cu are 913 K and 678 K, respectively. For MPSS substrate, it is 823 K to 833 K (Fe-905 K, Cr-1090 K and Ni-863 K). To minimize the effect of Fe and other support metal diffusion into the Pd-Cu film a temperature of 773 K was chosen, which is in between the Tamman temperatures of Cu and MPSS substrate. This annealing temperature eventually gave us Pd-Cu alloy metal film, which was almost free from substrate constituent metals. The heat treatment of Pd-Cu membrane gave us the opportunity to study the change in microstructures of deposited Pd-Cu film and alloy formation, which had a bare minimum influence of Fe, Cr and Ni. After complete alloy formation by Pd and Cu in the film, membranes were cut into pieces for further study of the effect of heat treatment on the Pd-Cu film cross-section. In this section, the diffusion patterns of Pd, Cu and substrate constituent metals are presented in detail.

4.2.1 Effect of Heat Treatment on Microstructures

In Figure 4.14, the effect of heat treatment is evident as the metal grains are diffused into one another making uniform alloy between Pd and Cu. The XRD analysis confirmed the alloy formation. The XRD reflection patterns for Pd-Cu membranes after 18 hours of heat treatment are shown in Figure 4.14. In Figure 4.14, three XRD patterns (a) before annealing (b) after 10 hours of annealing and (c) after 18 hours of annealing are shown for Pd-Cu membranes. The XRD patterns taken after 10 hours of annealing indicated that alloying of Pd-Cu layer was almost complete; however, annealing was continued for 18 hours to make sure that no change of peaks took place over time. It is clear from Figures 4.14 (b) and (C) that the characteristics peaks of Cu at [111], [200] and [220] planes shifted towards those characteristics peaks of Pd at [111], [200] and [220] planes. This shifting of peaks indicated the coexistence of pure Pd and pure Cu phases in the deposition layers [55-57]. Actually, Pd and Cu in the film formed interstitial alloys. Interstitial alloy formation occurs when the atoms of one component are smaller than the other, and the smaller atoms fit into the spaces (interstices) between the larger atoms. Annealing in the same condition for a total of 18 hours, a single phase f.c.c. lattice of Pd-Cu alloy was observed at the characteristics planes shown in Figure 4.14 (c). However, the reflection peaks for single phase f.c.c. of Pd-Cu alloy was found between pure Pd and Cu peaks at 2θ values of 40.366, 46.956 and 68.585 for [111], [200] and [220] planes. During 18 hours of annealing, we did not observe alloy formation between Pd and Cu at [311] plane. Allowing more time could result alloy formation at [311] planes. However, additional annealing was accomplished during H_2 permeation testing.

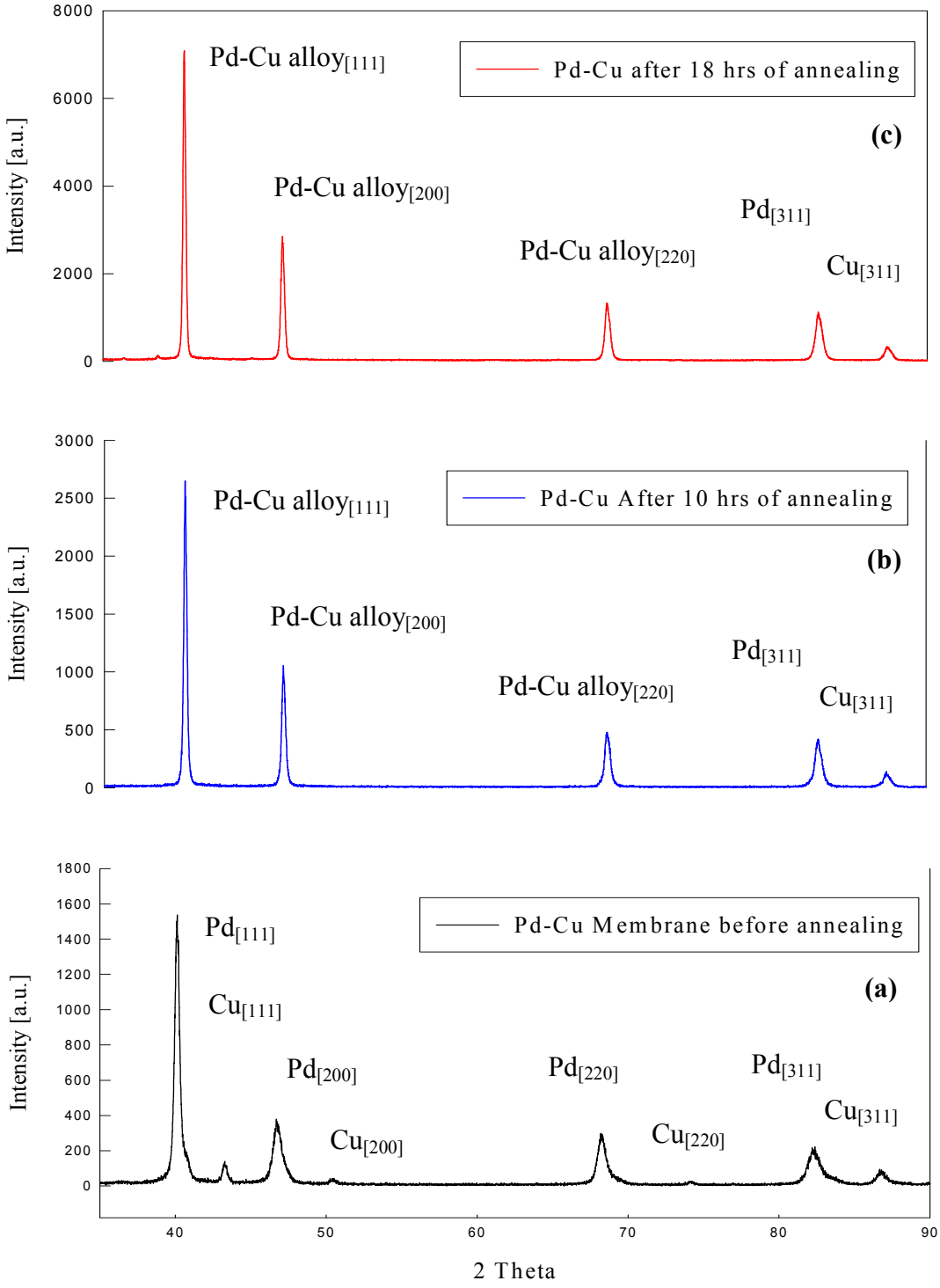

Figure 4.14. Effect of heat treatment on XRD pattern of Pd-Cu membrane fabricated by SIEP method

Using Brag's law, the lattice parameter was calculated and found 3.867 Å for Pd-Cu alloy, which was 3.6150 Å for pure f.c.c. lattice of Cu. Evidently this is an indication that the observed increase in the Cu cluster size was associated with the lattice expansion of the Cu metal. These results are in qualitative agreement with literature, which indicates an annealing temperature of 773 K or above is required to get a homogeneous alloy of Pd and Cu [55].

Figure 4.15 portrays a representative surface morphology of Pd-Cu membranes fabricated by SIEP process after annealing. Figure 4.15 (a) shows SEM images of the surface before annealing and Figure 4.15 (b) shows SEM image of the surface after annealing. Both, Figures 4.15 (a) and (b) were captured at 20 kV and 1K magnification. It is recognizable from the images that the smaller grains agglomerate to form larger grains with recognizable boundaries. In Pd-Cu membrane there were only Pd and Cu particles in the film and diffusion of Fe from substrate into film was carefully prevented during heat treatment by choosing annealing temperature remote enough from the melting temperature of Fe. The diffusion of metal is dependent on the temperature of the environment. Melting point of Cu is 1357 K and that of Fe is 1811 K, so annealing temperature of 773 K is close to the melting temperature of Cu. This suggests that diffusion of Cu will take place first. Annealing temperature also helped to orient Pd and Cu particles to form large clusters between them. As a result, great extent of grain agglomeration was achieved after heat treatment. Throughout the surface, dimension of agglomerated grains increased by 2 to 5 times after heat treatment. During heat treatment, Cu particles diffused into Pd layers forming homogeneous alloys of large clusters.

Figure 4.16 shows the enlarged SEM images of Pd-Cu film showing formation of tiny pinholes after heat treatment on microstructure. Figure 4.16 (a) was captured at 30 kV & 2K magnification and Figure 4.16 (b) was captured at 20 kV & 5K magnification. In both images of Figure 4.16, it is clear that tiny holes are created, which are 130 to 400 nm in size for Pd-Cu membranes. Figures 4.16 (a) and (b) also depict the pinholes created on the top surface and interstitial space may form during the sequential deposition and drying steps. Apart from interstitial spaces, a very low amount of oxidation of the metal might occur during 2 hours of drying step at 423 K at the time of fabrication process. After preparing the Pd-Cu membranes, heat treatment under H_2 environment for continuous 18 hours at 773 K might drive oxygen and other impurities away from the film layers. The metals from the top surface were used up occupying inter granular spaces. Reorientation of the crystals also occurred during this time. While cooling started after the heat treatment, recrystallization occurred and diffusion ceased. As a result, these tiny holes are believed to be created on the top surface of Pd-Cu membrane after heat treatment. Figure 4.17 presents the pre- and post annealing SEM images of Pd-Cu film top surface microstructure for comparison. For Pd-Cu film microstructure, a uniform grain agglomeration was observed as well. The low energy SEM images in Figure 4.17 illustrate the surface morphology of the agglomerated grains, showing uniform dissemination of the grain boundaries. On the other hand, SEM images of higher magnification in Figure 4.17 show increase in the grain size. Heat treatment produced nano pinholes only on the top surfaces, which are shown in different magnification in the insets of Figures 4.17 (b), (d), (f), (h), (j) and (l).

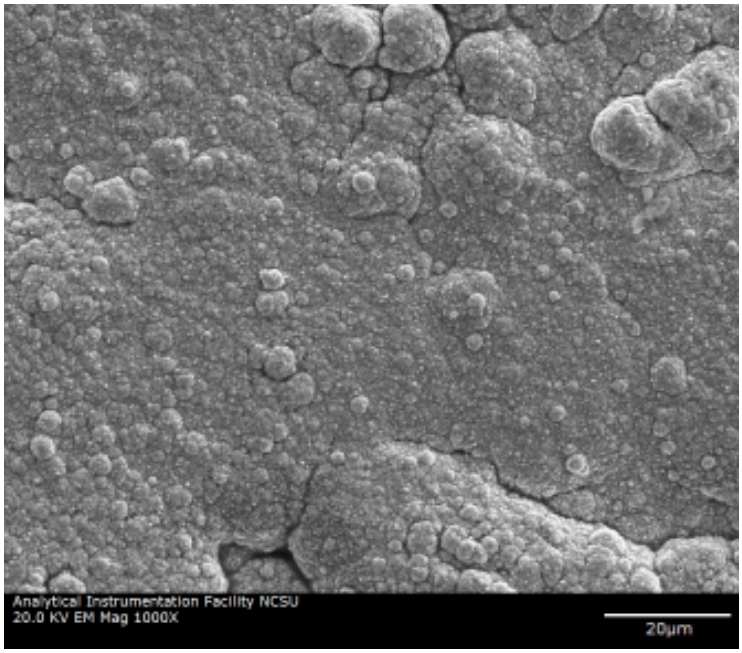

(a) Pd-Cu membrane at 1K (before annealing)

(b) Pd-Cu membrane at 1K (after annealing)

Figure 4.15. SEM images at 20 kV showing the effect of heat treatment on Pd-Cu microstructure fabricated by SIEP method

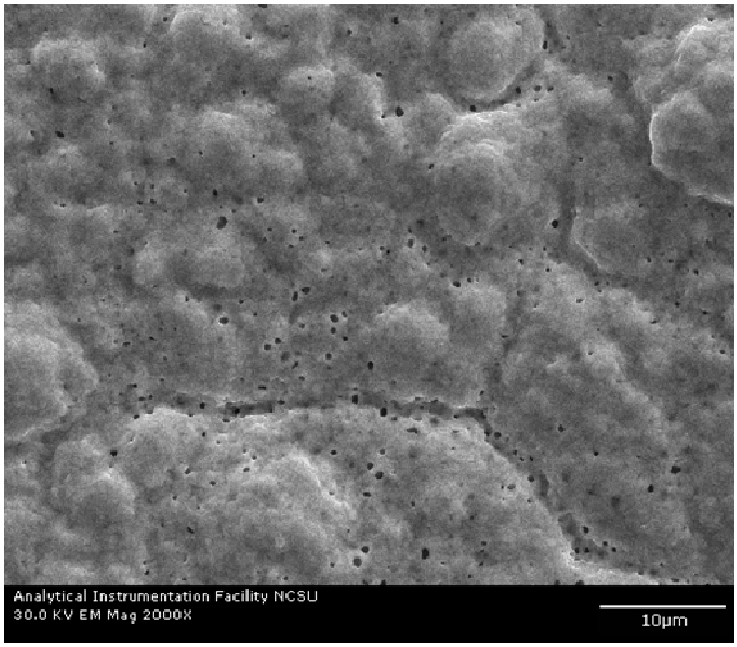

(a) Pd-Cu membrane at 2K (after annealing)

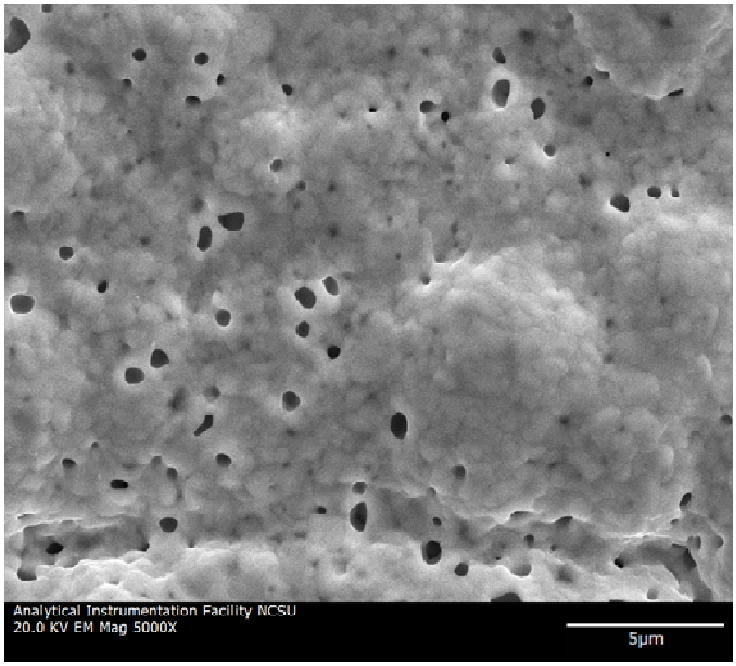

(b) Pd-Cu membrane at 5K (after annealing)

Figure 4.16. Enlarged SEM images (at 30 kV and 20 kV) of Pd-Cu film showing formation of tiny pinholes after heat treatment on microstructure

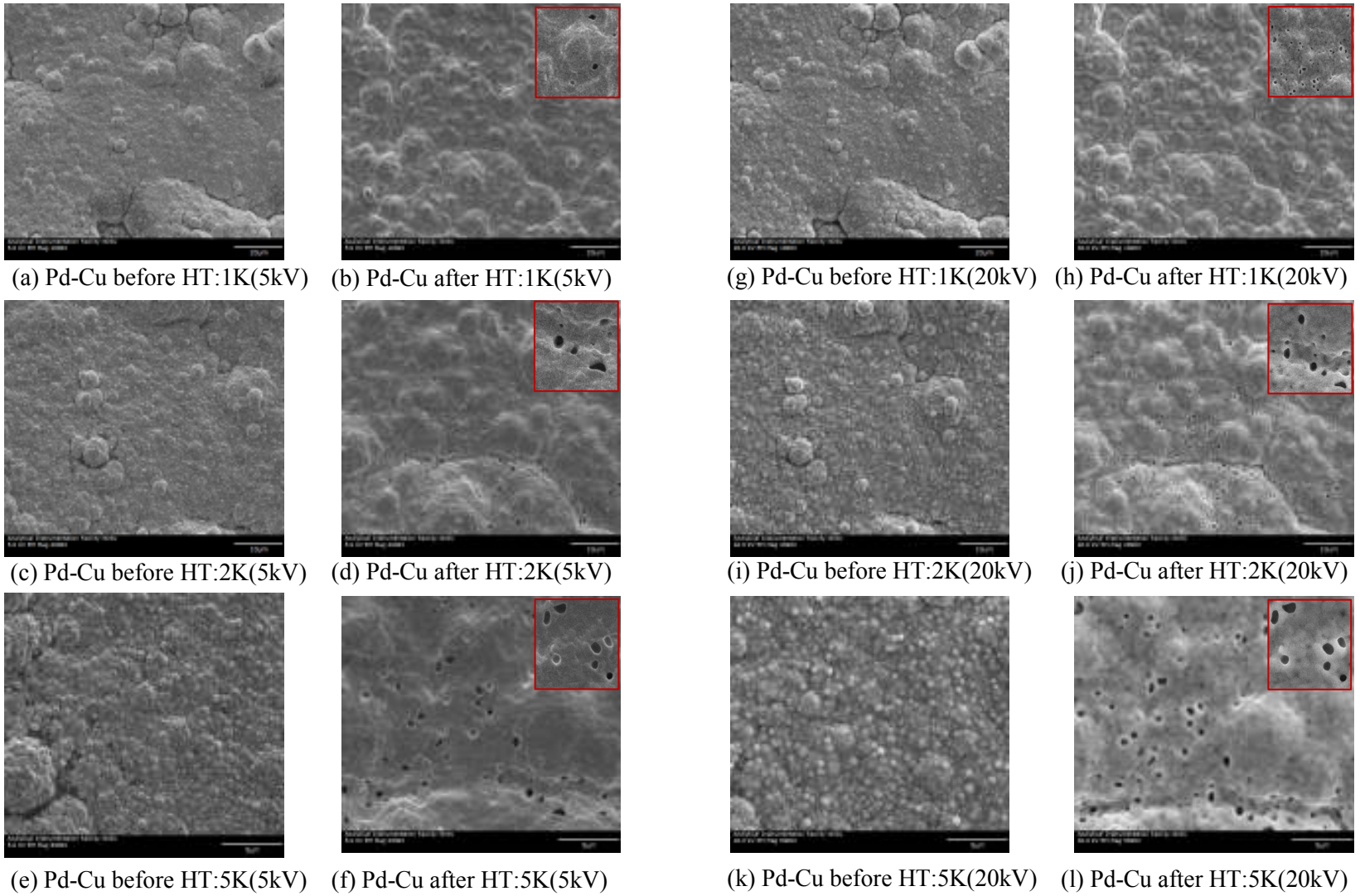

(a) Pd-Cu before HT:1K(5kV) (b) Pd-Cu after HT:1K(5kV) (g) Pd-Cu before HT:1K(20kV) (h) Pd-Cu after HT:1K(20kV)

(c) Pd-Cu before HT:2K(5kV) (d) Pd-Cu after HT:2K(5kV) (i) Pd-Cu before HT:2K(20kV) (j) Pd-Cu after HT:2K(20kV)

(e) Pd-Cu before HT:5K(5kV) (f) Pd-Cu after HT:5K(5kV) (k) Pd-Cu before HT:5K(20kV) (l) Pd-Cu after HT:5K(20kV)

Figure 4.17. Effect of heat treatment on the microstructure of Pd-Cu membrane (enlarged images in the inset)

4.2.2 Studies of Pd-Cu Membrane Cross-section

It is important to determine the propagation of nano-holes created after heat treatment. Metal distributions, as well as, diffusion of metals inside the substrate and inside the film are important issues for membrane fabrication and to its performance. A series of SEM images were captured to conclude about nano-holes propagation and metal diffusion inside substrate. Conventional secondary electrode (SE) images are not sufficient enough for investigating film cross-section, while it is recommended to take back scattered electrode (BSE) images to study membrane film cross-section. Figure 4.18 shows typical back scattered electrode (BSE) SEM images of Pd and Pd-Cu films at different magnification taken at 20 kV electron beam energy. As films are made of alloy of different metals, back scattered electrode responses gave brighter images with minute details. Film cross-sections were investigated thoroughly along the radius and found all substrate pores were plugged. A deep penetration of metals inside pores was also observed. Figures 4.18 (a) and (b) reveal that thinner Pd film requires, making membrane gas-tight than Pd-Cu film, which also comply with the results in Table 4.1. A few small dots were found on top of film cross-section, those were nothing but pinholes created during heat treatment. These pinholes were found few nanometers inside from top surface of films; however, its distribution extended more in Pd-Cu membrane. Importantly, none of these dots were found near the film and substrate interphase, which means that those little pinholes did not make any channels from the top surface to the substrate pores. These results are consistent with permeability data discussed later in this chapter. A total picture of Pd and Pd-Cu films microstructure is presented in Figure 4.19.

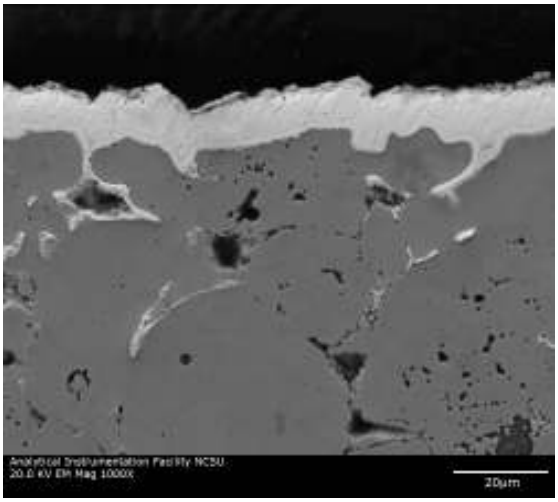

a) Pd film at 1K

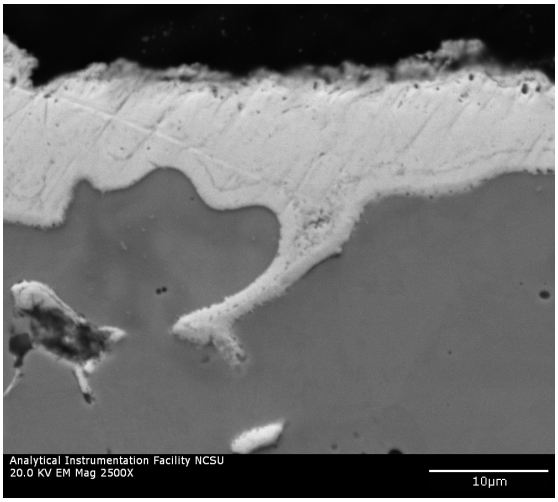

b) Pd film at 2.5K

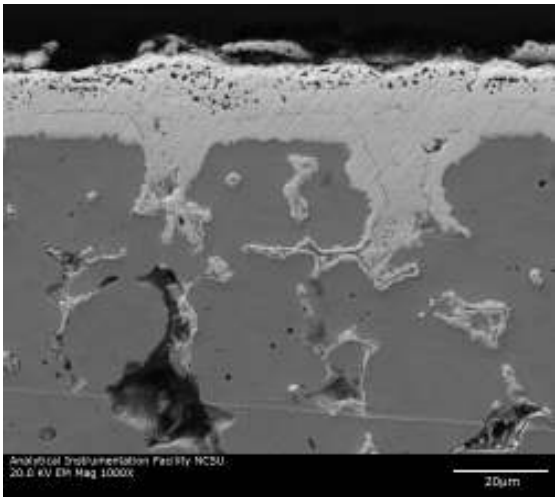

c) Pd-Cu film at 1K

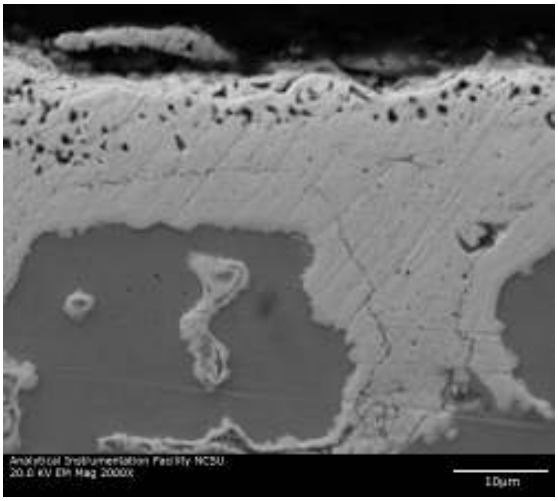

d) Pd-Cu film at 2K

Figure 4.18. Typical back scattered electrode (BSE) SEM images of Pd and Pd-Cu films cross-section after heat treatment

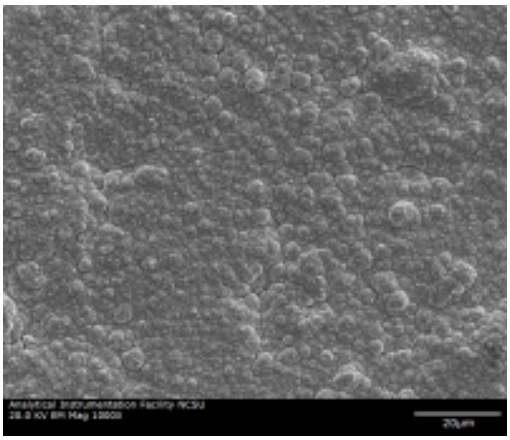

(a) Pd before annealing at 1K

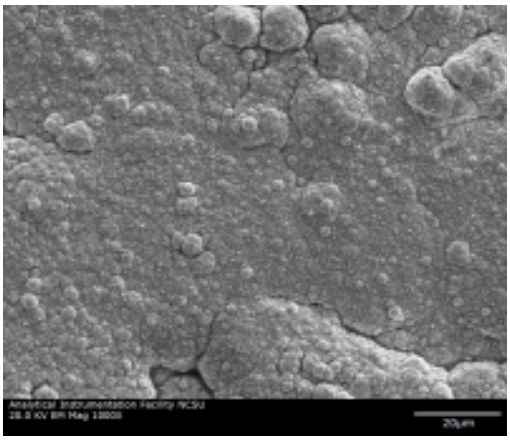

(d) Pd-Cu before annealing at 1K

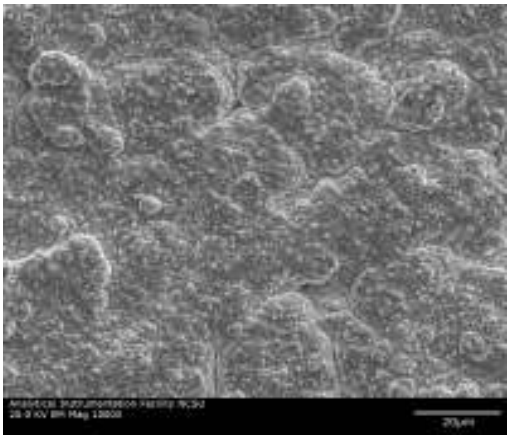

(b) Pd after annealing at 1K

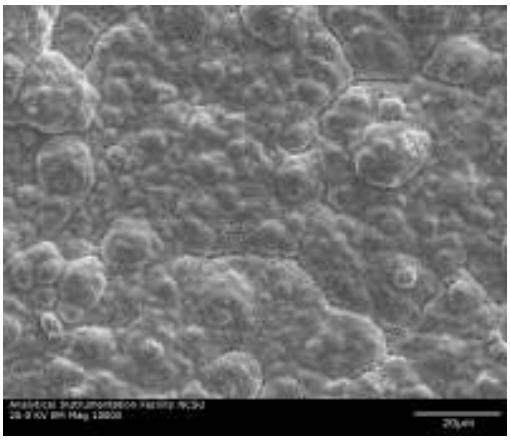

(e) Pd-Cu after annealing at 1K

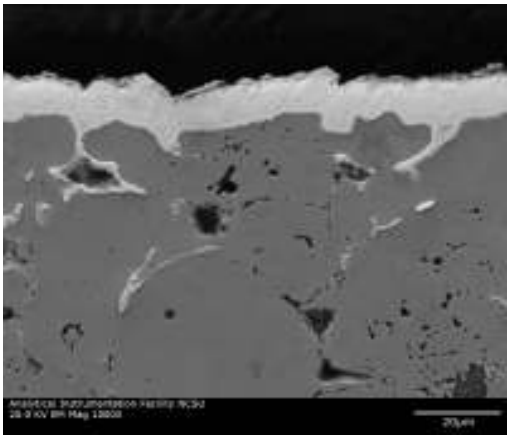

(c) Pd cross-section at 1K

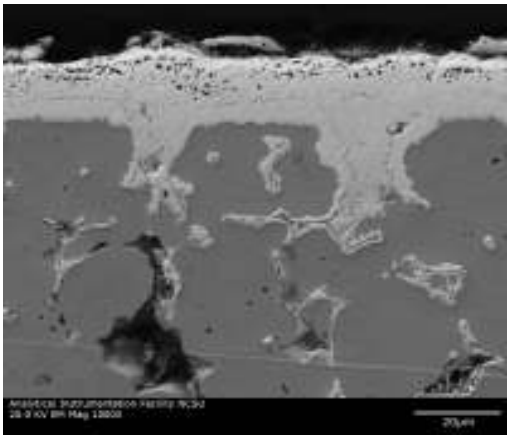

(f) Pd-Cu cross-section at 1K

Figure 4.19. Typical top surface morphology and cross-section views of Pd & Pd-Cu membrane at 20 kV fabricated by SIEP method

A detail study was carried out on a single pore of each film from pore mouth to the very deep inside of pores to examine metal deposition. The pores in MPSS substrate are interconnected and tortuous in nature. For Pd-Cu film, metals have been investigated in pores at a distance of 25 μm inside from top of the film. In Pd-Cu membrane, Pd was deposited first and Pd particles are supposed to deposit inside the pore walls. With the progress of deposition layers, pore opening shrinks and eventually plugged. Due to the annealing and diffusion of metals, Cu was found dispersed throughout the film. EDS elemental analysis was carried out at four different points starting from the pore mouth to deep inside of the substrate. The points of EDS analysis locations are shown in Figure 4.20. Figure 4.20 suggests that we are able to plug all the pores presents deep inside of substrate. Elemental analysis of these pores are then plotted as a function of metal composition shown in Figure 4.21, which describes as the points move inside the film, Cu content decreases.

A series of line scanning was carried out to study the cross-section of Pd-Cu film at different locations. Figure 4.22 shows the EDS line scanning of Pd-Cu film. From Figure 4.22, as EDS approaches the interphase from outside towards substrate, Pd and Cu peaks jump to their maximum and Fe, Cr and Ni peaks drop sharply. After crossing the film Fe, Cr and Ni peaks rise again. This suggests that the film consists of only of Pd and Cu metals. To know the relative amounts of each metal in the Pd-Cu film, EDS elemental analysis was studied for the substrate. The composition of substrate was Fe 68.73%, Cr 16.38%, Ni 11.38%, Mo 2.52% and 0.79% of other traces. Based on X-ray counts of line scanning, amount of Cu in the film was 24.99% after heat treatment.

In Figure 4.22, a repeated rise and fall of the X-ray counts were observed representing the sequential deposition. The oscillation of X-ray counts was prominent for Cu, as the Cu content is low in each deposition cycle. Being the minor constituent, Ni has the background effect and oscillates more, which was confirmed by EDS mapping. A similar result was observed for Pd as well. However, sharp rise of peaks for Fe, Cr and Ni (sharp trough for Pd and Cu) in the middle of the Pd-Cu alloy film were observed. Actually, these were the response from fine SS particles doped in the film during metal polishing while preparing the sample for EDS mapping. During sample preparation, membrane pieces were mounted in the resin and then the resin was dried up. The top part of the sample was polished with polishing metals to expose the membrane's cross-section from the resin. As Pd-Cu alloy film is soft, so some SS particles from the substrate might get separated and doped into the film.

The EDS mapping was carried out for Pd-Cu membrane cross-section to examine metal deposition and diffusion of metals inside substrate presented in Figure 4.23. For pure Pd, the mapping forms the exact film and pore shapes shown in Figure 4.23. Very minute amount of Fe, Cr and Ni diffusion inside the film were observed. As the Tamman temperature of Cu is lower than that of Pd (Pd_{Tamman} = 913 K and Cu_{Tamman} = 678 K), annealing at 773 K for 18 hours under H_2 environment resulted in relatively higher diffusion of Cu inside substrate. A baseline for noise was always found in EDS analysis. This noise became dominant in case of minor constituent of the sample, which is evident in Ni mapping. Hence, presence of Fe and Cr in the Pd-Cu alloy layer from EDS mapping can be ignored in the film. Post treatment XRD analysis also confirmed this result.

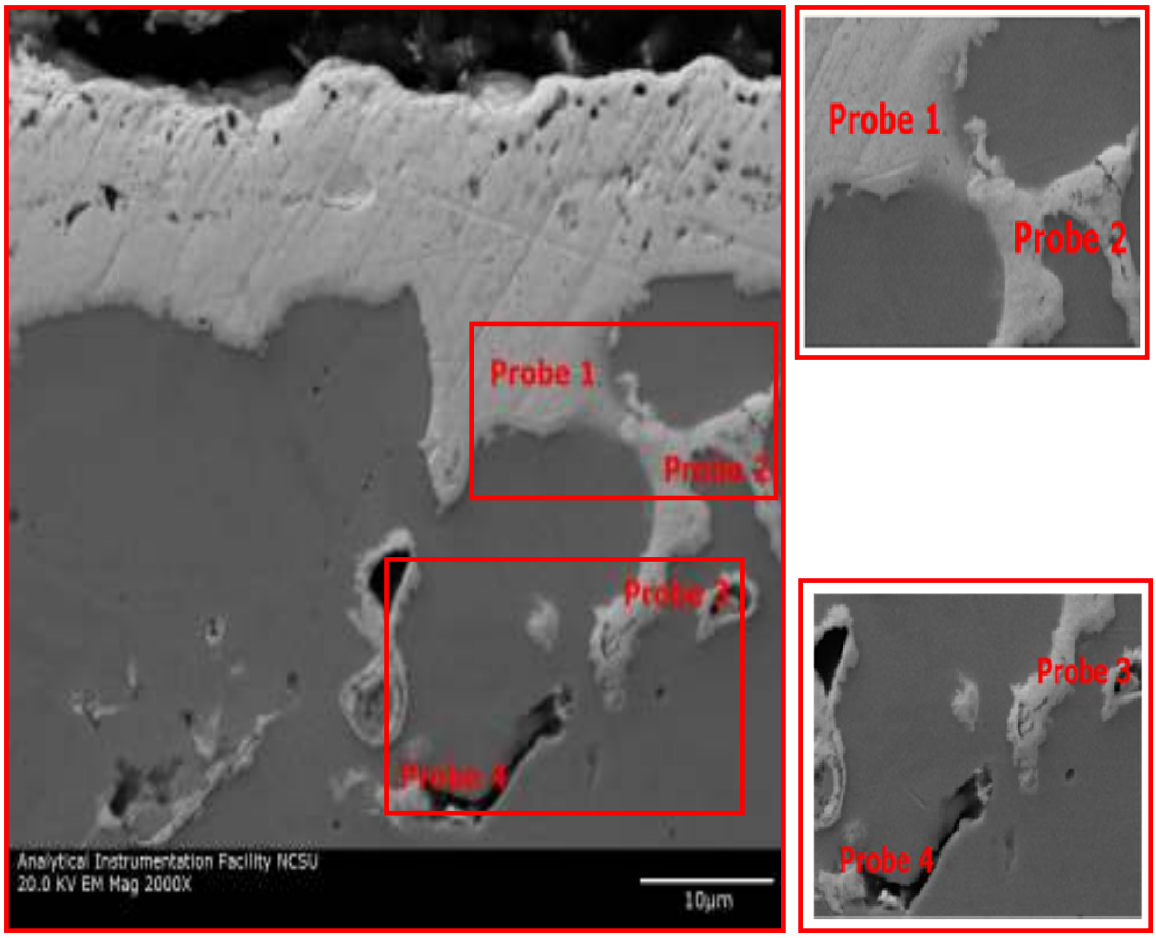

Figure 4.20. SEM images of Pd-Cu film from Pd-Cu membrane cross-section: showing the locations of EDS for metal deposition behavior analysis in the pores during the deposition

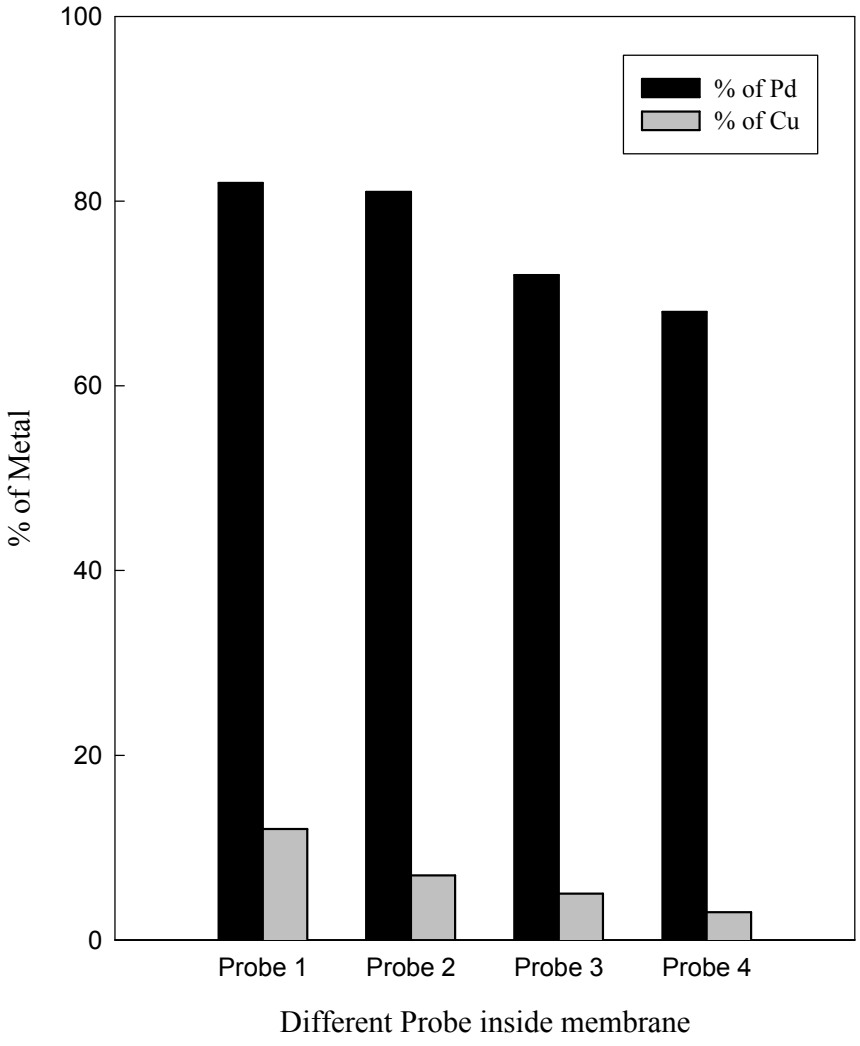

Figure 4.21. Metal (Pd and Cu) distribution during deposition in the pores starting from the pore mouth to the very deep inside (From Probe 1→Probe 4)

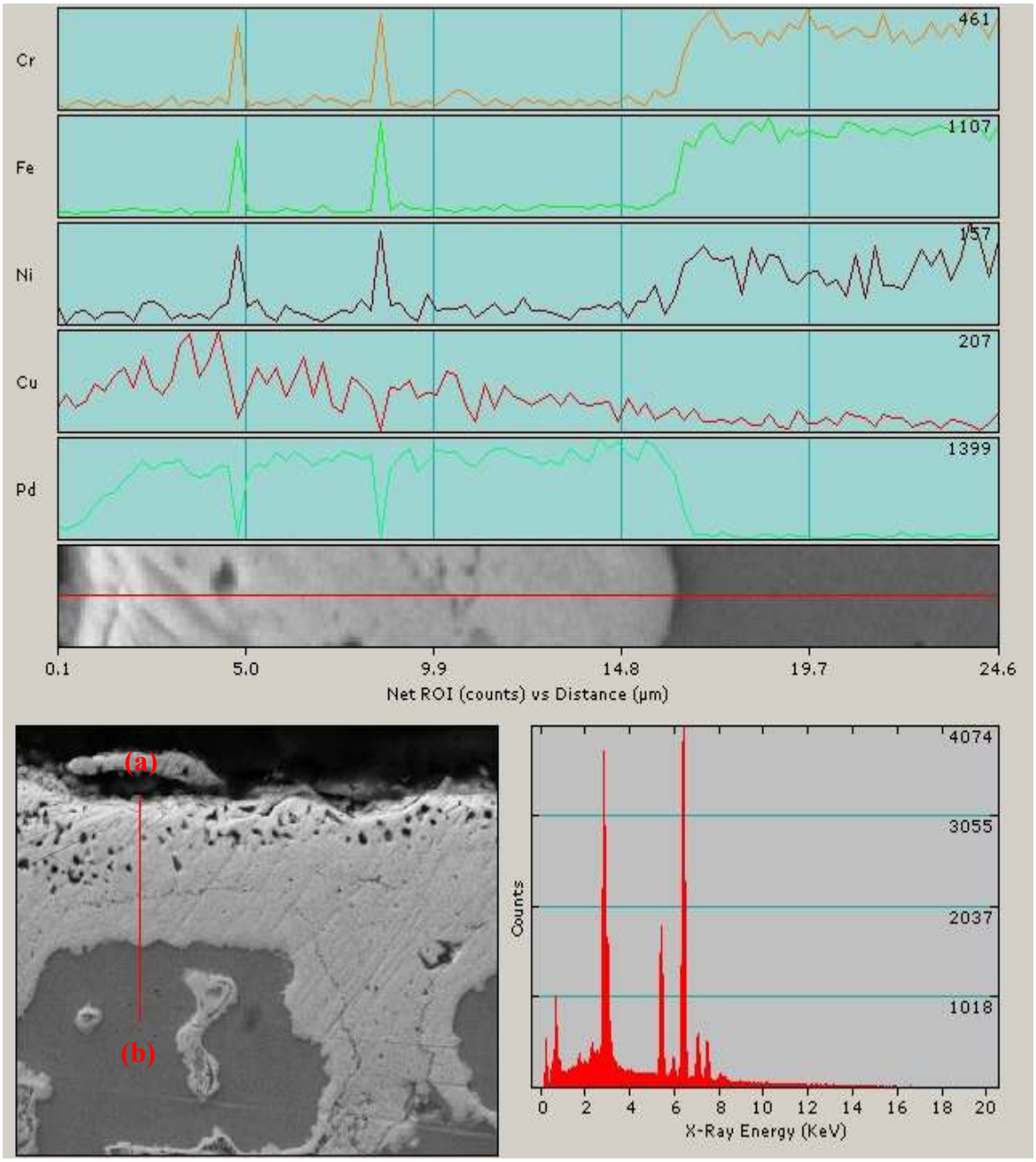

Figure 4.22. EDS line scanning of Pd-Cu film cross section (Scanning length 25 µm, scanning direction from (a) → (b))

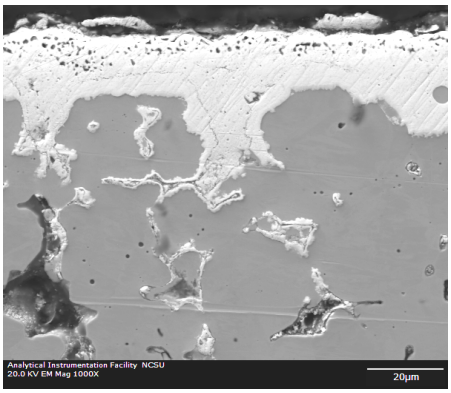

Cross section for EDS mapping

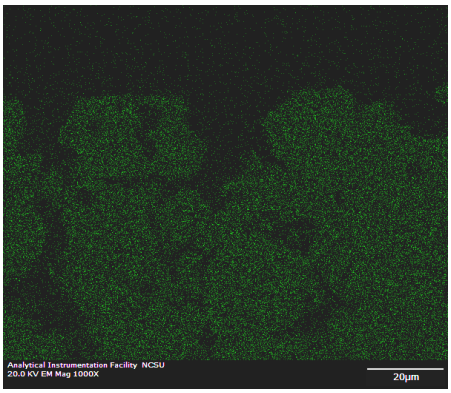

Fe-mapping

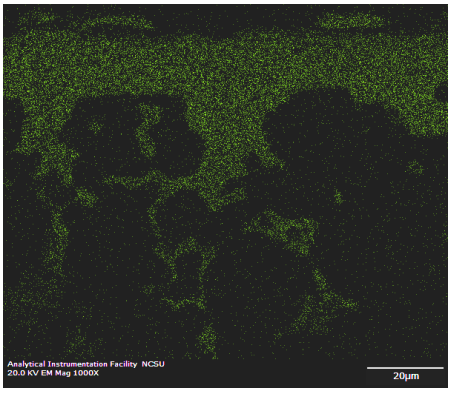

Pd-mapping

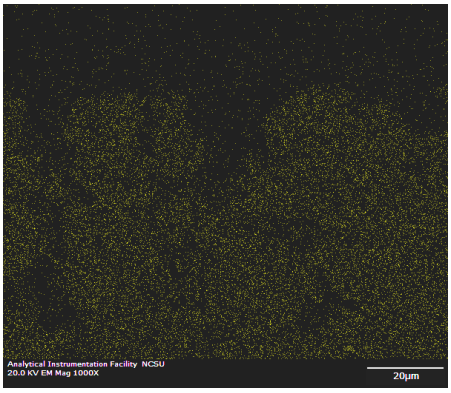

Cr-mapping

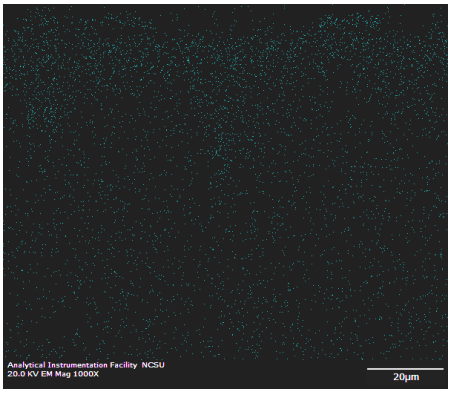

Cu-mapping

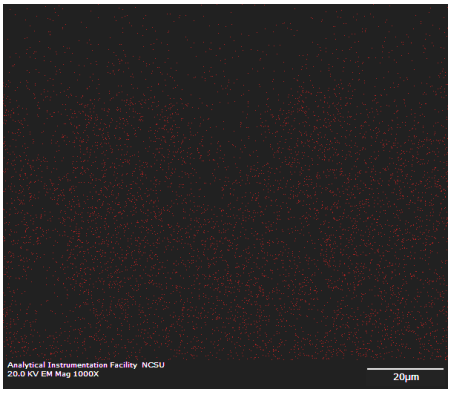

Ni-mapping

Figure 4.23. EDS mapping of Fe, Cr, Ni, Pd and Cu metals in Pd-Cu membrane fabricated by SIEP method showing the metal distribution in the Pd-Cu film and substrate

4.3 Permeability Studies of Pd-Cu Membranes

From this whole study, we found that DTAB at 4 CMC was the most effective surfactant in SIEP that enabled us to deposit integrated, defect-free Pd-Cu film on MPSS substrate. We tested Pd-Cu membranes fabricated by SIEP and CEP processes for helium gas-tightness and for hydrogen perm-selectivity in our permeability measurement set-up shown in Figure 3.1 of chapter 3. The film thickness of two different Pd-Cu membranes fabricated by SIEP process, were found to be 16.73 μm (S2) and 14.5 μm (S3), respectively. On the other hand, the film thickness of two different Pd-Cu membranes fabricated by CEP process were found to be 19.18 μm (C1) and 20.17 μm (C2), as determined by weight gain method.

For reasonably thick membranes (≥10 μm), it is generally assumed that the rate-controlling step is the diffusion of hydrogen atom through the bulk of the metal films [58]. The transport of hydrogen through dense Pd-film is a complex multistep process, which involves: (1) reversible dissociative chemisorptions of molecular hydrogen on the membrane surface; (2) reversible dissolution of atomic hydrogen in the bulk layers of the metal; (3) diffusion of atomic hydrogen through the bulk metal; and (4) association of hydrogen into hydrogen molecule. The hydrogen flux through dense Pd-film can be expressed in the form of Fick's first law as follows:

$$N_H = \frac{Q_H}{t}\left(P_H^n - p_H^n\right) \tag{4.1}$$

where, Q_H is the hydrogen permeability (a product of solubility and diffusivity), t is the membrane thickness or film thickness, and P_H and p_H are the partial pressures of

hydrogen on the high and low pressure sides, respectively. The exponent n is a parameter, whose value depends on the limiting transport mechanism. If H_2 surface reactions at the permeance side limit the flux then n= 0. If diffusion through the membrane limits the flux n = 0.5 and if gas phase resistance or surface reactions at the retentate side are limiting the flux, n becomes unity [5]. When diffusion through the bulk metal is the rate limiting step and hydrogen atoms form an ideal solution in the metal, n is equal to 0.5, and then Equation 4.1 becomes the Sievert's law, which states that the amount of a diatomic gas dissolved in metal is proportional to the square root of its pressure. We tested the Pd-Cu MPSS membrane for hydrogen flux in a temperature range of 523 K to 823 K to evaluate the transport mechanism. The hydrogen permeability measurements were carried out in our permeation measurement set-up using pure hydrogen shown in Figure 3.1 of chapter 3. The measured data as a function of pressure difference $\left(P_H^n - p_H^n\right)$ at 523 K, 623 K, 723 K and 823 K are presented in Figures 4.24, 4.25, 4.26 and 4.27. Figures 4.24 and 4.25 are for flux data of membranes (S2 and S3) fabricated by SIEP method and Figures 4.26 and 4.27 are for flux data of membranes (C1 and C2) fabricated by CEP method. The lines drawn in the Figures 4.24, 4.25, 4.26 and 4.27 are non-linear least-square fit; with power index, n = 0.85 (S2) & 0.83 (S3) for Pd-Cu MPSS membranes fabricated by SIEP method, and with power index, n = 0.94 (C1) & 0.93 (C2) for Pd-Cu MPSS membranes fabricated by CEP method. The value of power index (n) higher than 0.5 (commonly ranging between 0.5 and 1), is usually explained by the effect of surface phenomena that influence permeation. In some cases, the deviation is also observed for thick membranes for which the diffusion through the membrane controls almost

completely the permeation process [59]. In fact, hydrogen permeability of the membrane is closely related to the overlayer film thickness [60].The lower value of power index (n) of the membranes fabricated by SIEP method suggests that these membranes offer hydrogen atoms more diffusion through bulk metals compared to the membranes fabricated by CEP method. The flux data shown in Figures 4.24, 4.25, 4.26 and 4.27 show that with increasing temperature, hydrogen flux increases for a given trans-membrane pressure difference. Further, hydrogen flux increases with increased pressure drop across the membrane. A value of n greater than 0.5 may results, when surface processes influence the permeation rate [61]. The hydrogen diffusivity may become dependent on concentration of dissolved hydrogen and that may contribute to n values greater than 0.5 [62]. Leakage of hydrogen through defects in the metal film or membrane seals may also increase the value of n. Further, small resistance of the MPSS membrane support may also slightly increase the value of n. In fact, the increase of the driving force exponent (with respect to 0.5) can be due to the surface phenomena, as well as, porous support effects. Furthermore, the values of this exponent are estimated by means of a statistical-type analysis, usually a nonlinear regression, whose inevitable fitting errors represent another degree of uncertainty. For all these reasons, a deviation from the original Sievert's law (n = 0.5) may have different reasons and no unequivocal conclusion could be drawn [63]. However, the deviation in the observed flux data from idealized Sievert's law may be attributed to the factors just mentioned.

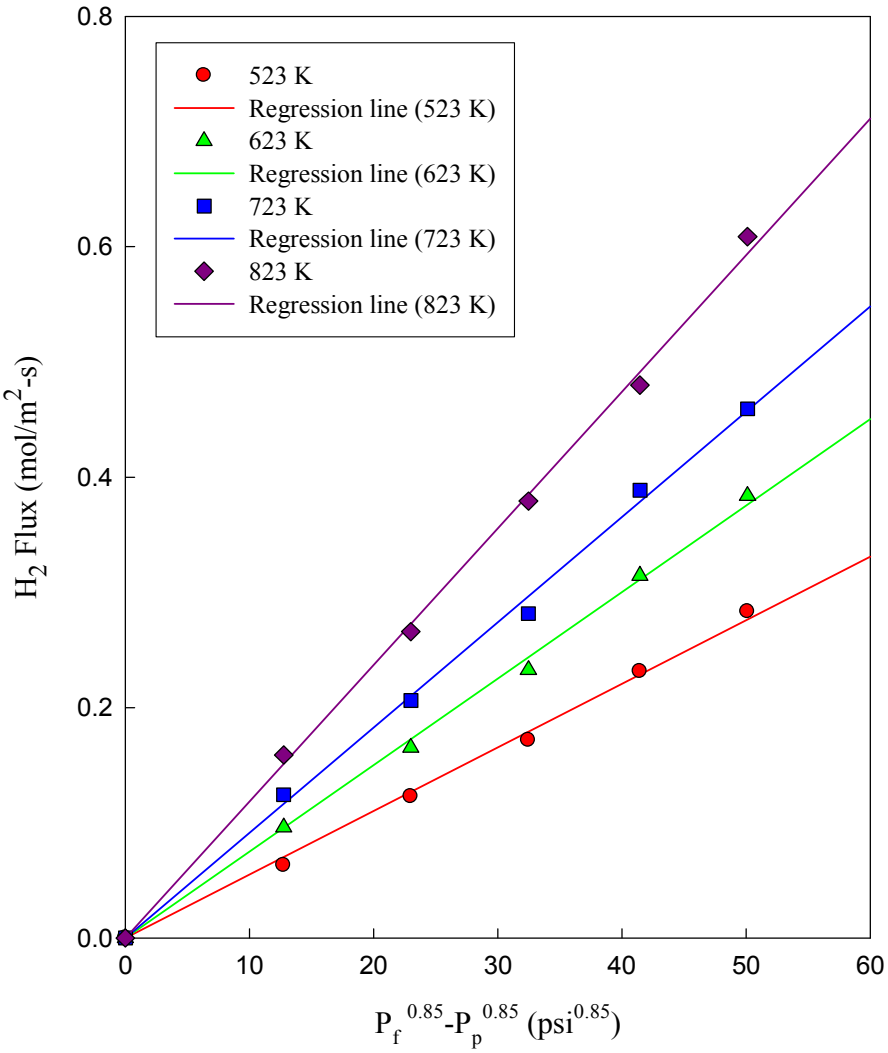

Figure 4.24. Hydrogen flux data of Pd-Cu membrane (S2) thickness of 16.73 µm at different temperatures fabricated by SIEP method

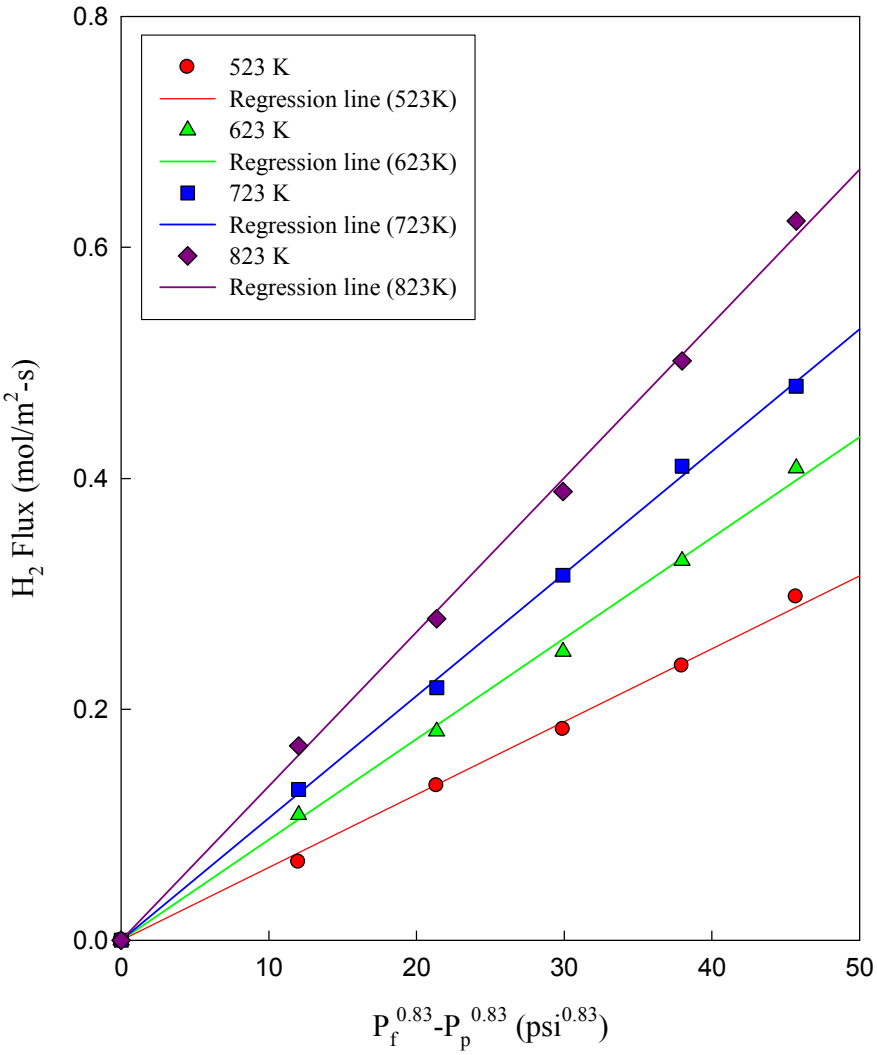

Figure 4.25. Hydrogen flux data of Pd-Cu membrane (S3) thickness of 14.5 µm at different temperatures fabricated by SIEP method

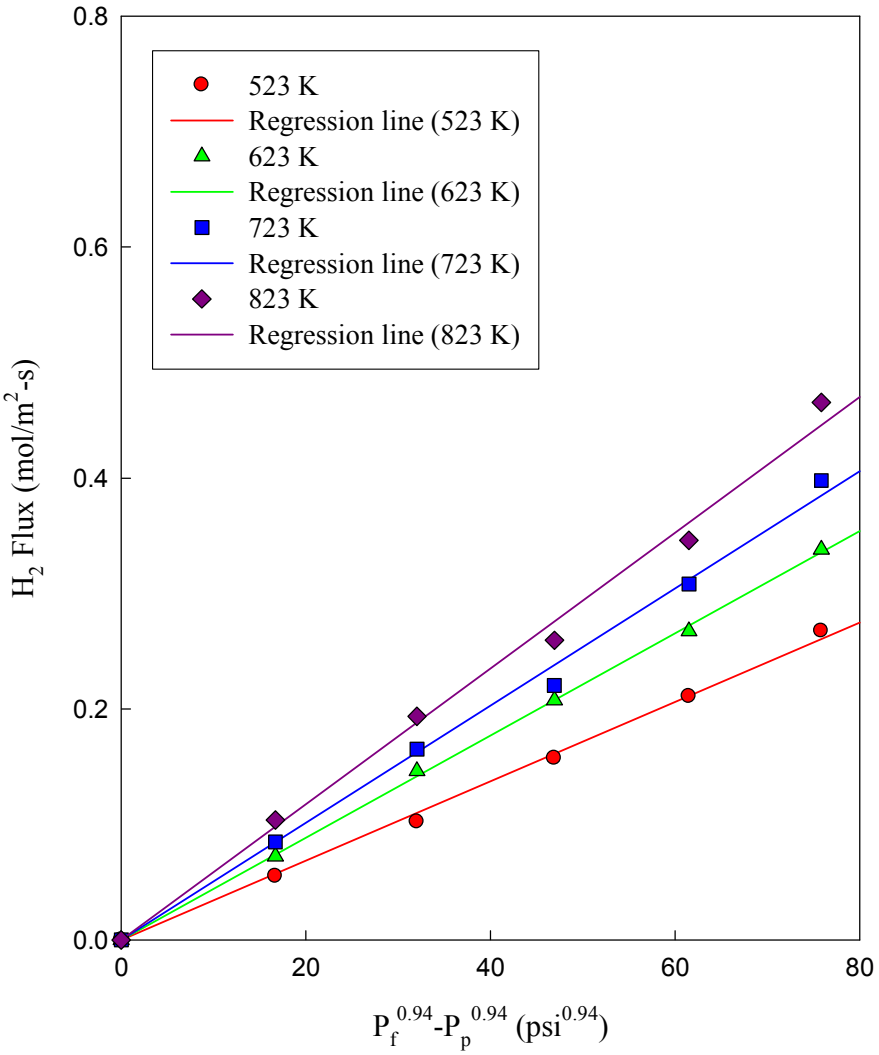

Figure 4.26. Hydrogen flux data of Pd-Cu membrane (C1) thickness of 19.18 µm at different temperatures fabricated by CEP method

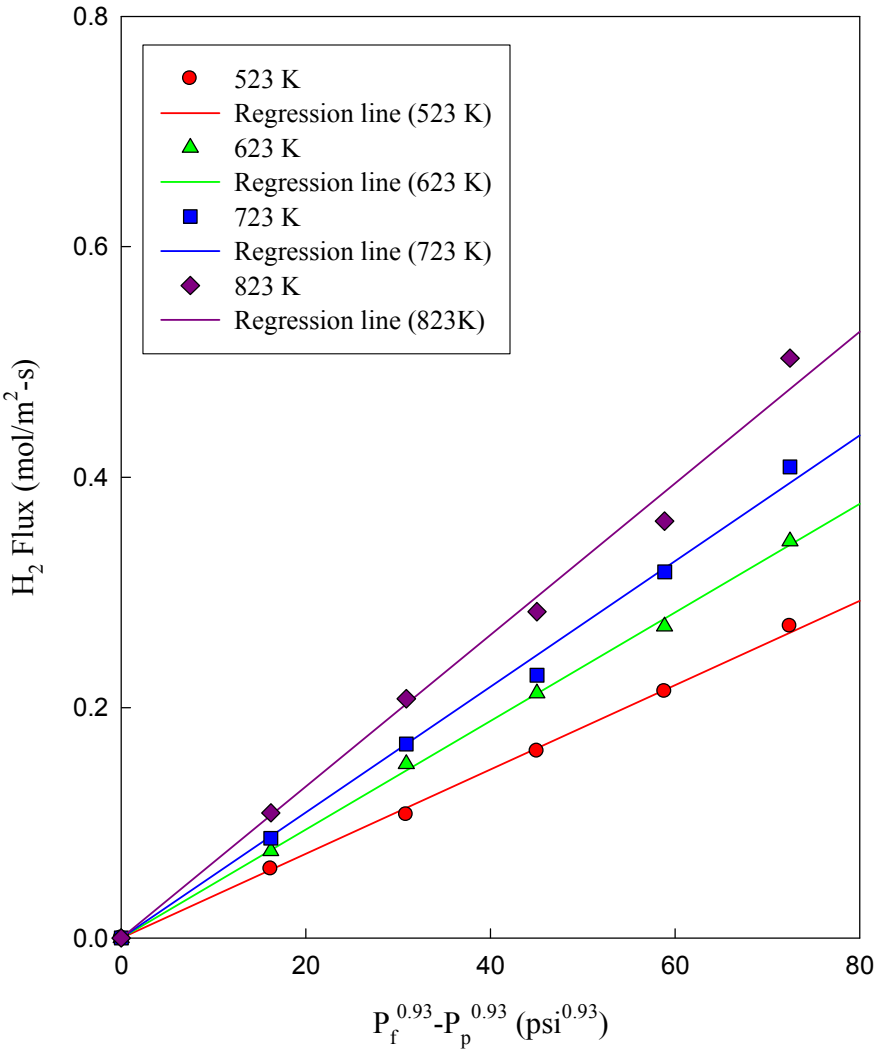

Figure 4.27. Hydrogen flux data of Pd-Cu membrane (C2) thickness of 20.17 µm at different temperatures fabricated by CEP method

The Hydrogen to nitrogen (H_2/N_2) selectivity was measured using our selectivity measurement set-up using pure hydrogen and pure nitrogen shown in Figure 3.1 of chapter 3. Measured data as a function of pressure difference $\left(P_H^n - p_H^n\right)$ at 523 K, 623 K, 723 K and 823 K are presented in Figures 4.28, 4.29, 4.30 and 4.31. Figures 4.28 and 4.29 present selectivity data of membranes (S2 and S3) fabricated by SIEP method whereas, Figures 4.30 and 4.31 present selectivity data of membranes (C1 and C2) fabricated by CEP method. Figures 4.28, 4.29, 4.30 and 4.31 suggest that selectivity decreases with increase in pressure but not linearly, rather exponentially. It is also clear from the Figures 4.28, 4.29, 4.30 and 4.31 that for the same pressure drop selectivity increases with increase in temperature. For all the four membranes fabricated either by SIEP or CEP method, the highest selectivity observed at 823 K and 20 psi pressure. The highest selectivity for Pd-Cu membrane (S2) fabricated by SIEP is 84.1 shown in Figure 4.28. On the other hand, selectivity of Pd-Cu membrane (C1) fabricated by CEP is 21.98 shown in Figure 4.30. Hence, in terms of selectivity, Pd-Cu membrane fabricated by SIEP method offers 4 times higher selectivity compared to Pd-Cu membrane fabricated by CEP method. Selectivity of Pd-Cu membranes fabricated by SIEP method increased after intermediate heat treatment compared to Pd-Cu membranes fabricated by CEP method, and will be discussed later in this chapter. From helium gas-tightness experiment, we concluded that Pd-Cu membrane fabricated by SIEP method was free of defects; however, heat treatment produced pinholes, which actually reduced effective thickness of perm-selective film. This might make hydrogen dissociation and adsorption a rate limiting step and could result in an increase of pressure exponent at high pressure.

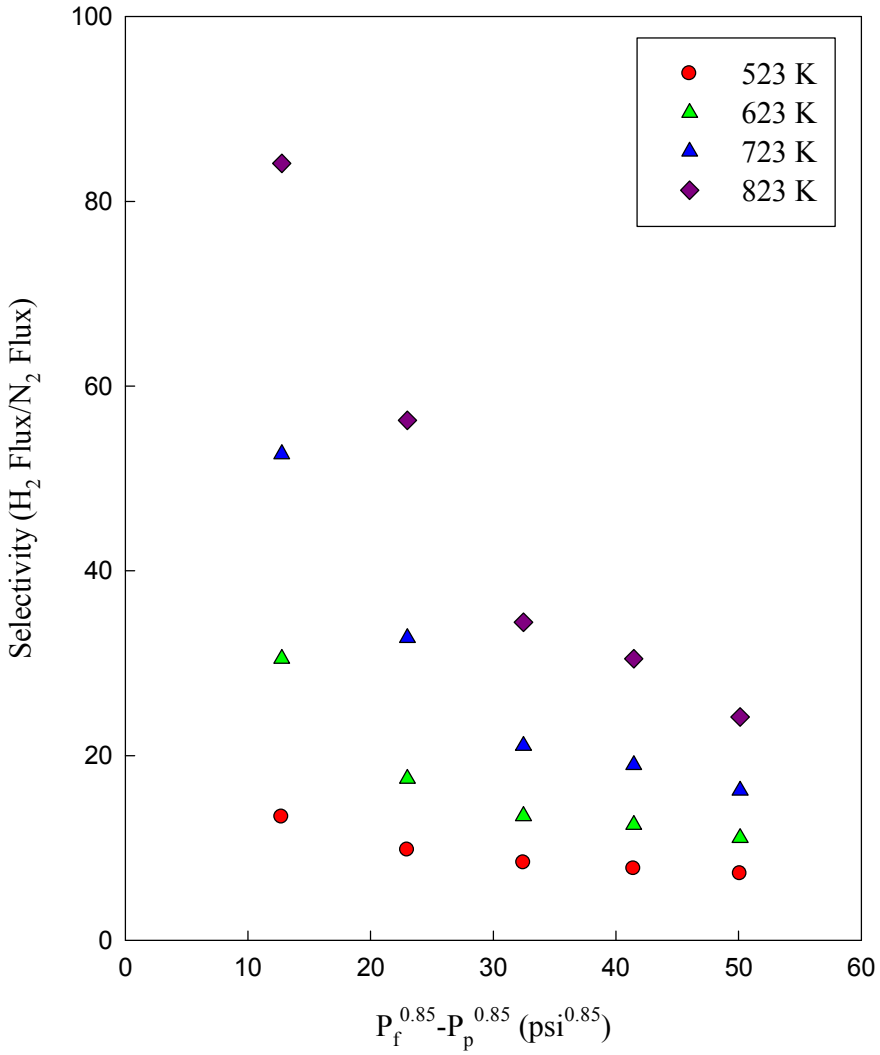

Figure 4.28. Hydrogen to Nitrogen (H_2/N_2) selectivity data of Pd-Cu membrane (S2) thickness of 16.73 µm at different temperatures fabricated by SIEP method

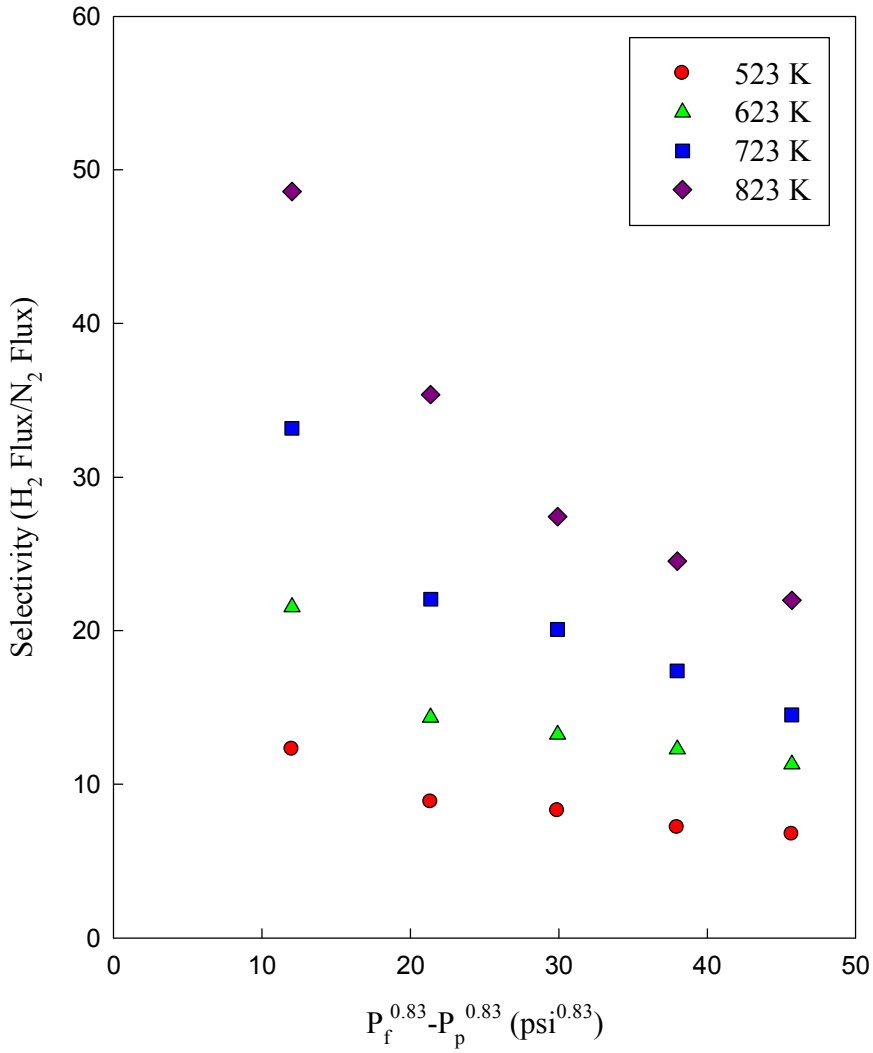

Figure 4.29. Hydrogen to Nitrogen (H_2/N_2) selectivity data of Pd-Cu membrane (S3) thickness of 14.5 µm at different temperatures fabricated by SIEP method

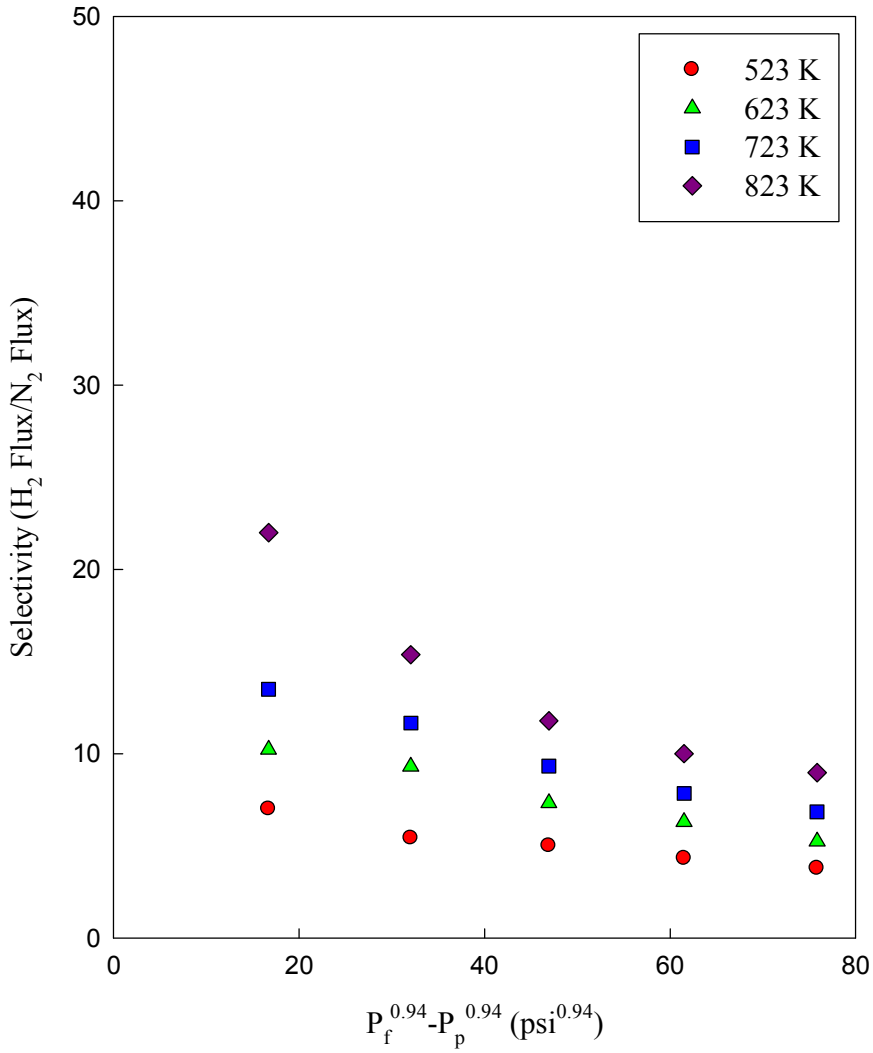

Figure 4.30. Hydrogen to Nitrogen (H_2/N_2) selectivity data of Pd-Cu membrane (C1) thickness of 19.18 µm at different temperatures fabricated by CEP method

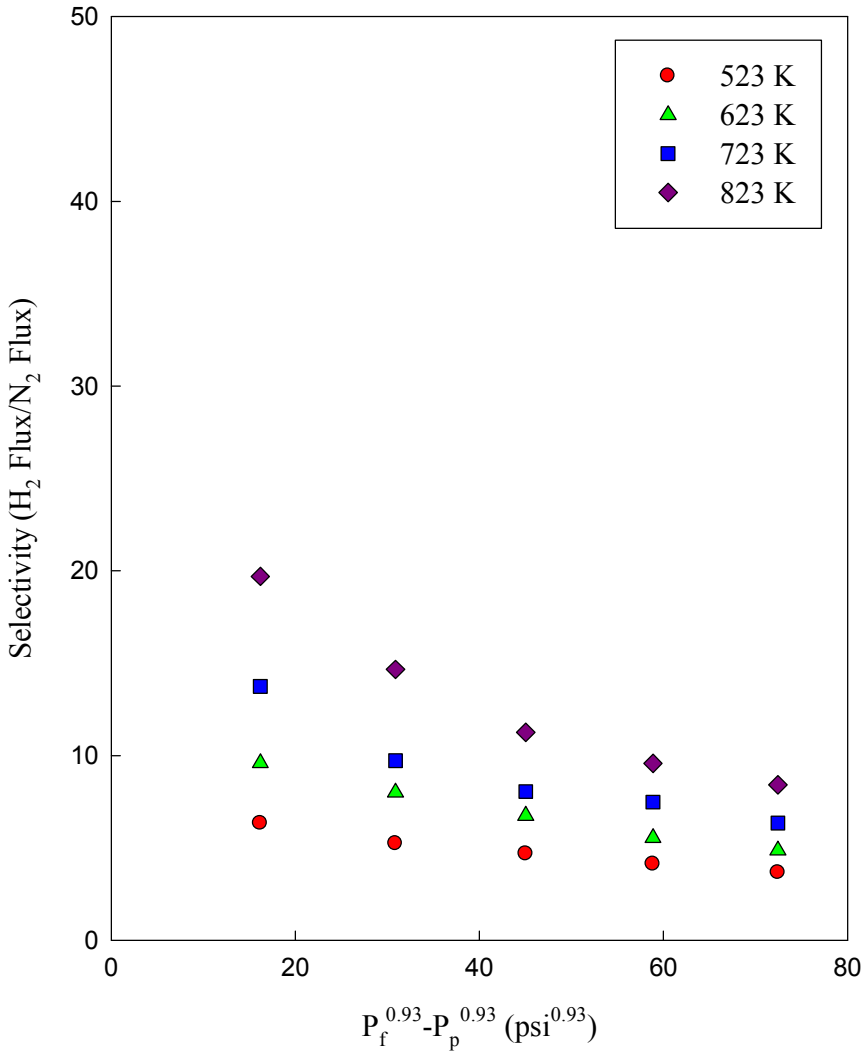

Figure 4.31. Hydrogen to Nitrogen (H_2/N_2) selectivity data of Pd-Cu membrane (C2) thickness of 20.17 µm at different temperatures fabricated by CEP method

4.3.1 Studies of Pd-Cu Membrane Flux and Selectivity after Heat Treatment

A study of intermediate heat treatment of the membrane was carried out during the fabrication process. At the end of gas tightness of each membrane, at 20 psi, 4 hours of heat treatment was carried out at 773 K under H_2 environment. After heat treatment a fresh mono layers of Pd and Cu film were deposited on the annealed Pd-Cu film as a coating to fill up pin holes of top surface, resulted from heat treatment. Figures 4.32 and 4.33 depict the effect of heat treatment on improvement of the membrane quality fabricated by SIEP process. Before the heat treatment, power index (n) was 0.85 for Pd-Cu membrane (S2), was reduced to 0.8 after heat treatment shown in Figure 4.32. Another Pd-Cu membrane (S3) fabricated by SIEP method had a power index (n) of 0.83 before heat treatment, which was reduced to 0.79 after heat treatment. The flux data for Pd-Cu membrane (S3) after heat treatment is presented in Figure 4.33. However, membranes fabricated by CEP method, the power index (n) did not change much after the intermediate heat treatment. Pd-Cu membrane (C1) fabricated by CEP method had a power index (n) of 0.94, which reduced to 0.92 after heat treatment shown in Figure 4.34. The Pd-Cu membrane (C2) fabricated by CEP method had a power index (n) of 0.93, which slightly reduced to 0.91 after heat treatment shown in Figure 4.35.

The maximum H_2 flux at 823 K and 100 psi pressure for Pd-Cu membrane (S2), with a film thickness of 16.73 μm fabricated by SIEP method is 0.6605 mol/m^2-s with a pressure exponent of 0.8 is shown in Figure 4.32. From Figure 4.33 it is clear that maximum flux of H_2 at 823 K and 100 psi pressure for Pd-Cu membrane (S3), with a film thickness of 14.5 μm fabricated by SIEP method is 0.6747 mol/m^2-s with a pressure

exponent of 0.79. On the contrary, maximum flux of H_2 at 823 K and 100 psi pressure for Pd-Cu membrane (C1), with a film thickness of 19.18 μm fabricated by CEP method is 0.4797 mol/m^2-s with a pressure exponent of 0.92 shown in Figure 4.34. Another Pd-Cu membrane (C2), with a film thickness of 20.17 μm fabricated by CEP method exhibits maximum H_2 flux at 823 K and 100 psi pressure is 0.5048 mol/m^2-s with a pressure exponent of 0.91 shown in Figure 4.35. Therefore, from the maximum flux data of all Pd-Cu membranes fabricated by SIEP and CEP methods, Pd-Cu membranes fabricated by SIEP method offers 15 to 20% higher H_2 flux compared to Pd-Cu membranes fabricated by CEP method.

In our previous work we reported detail characterization and H_2 flux data of pure Pd and Pd-Ag membranes fabricated by SIEP method [11-12]. On those study we reported maximum H_2 flux at 823 K and 100 psi pressure for Pd membrane, with a film thickness of 8.5 μm fabricated by SIEP method was 0.9044 mol/m^2-s with a pressure exponent of 0.83 and that of Pd-Ag membrane fabricated by SIEP method was 0.3838 mol/m^2-s with a film thickness of 12.63 μm and power exponent of 0.75 at 823 K and 100 psi pressure [11]. Roa et al., fabricated Pd_{80}-Cu_{20} membrane by electroless plating method on tubular porous ceramic support with a film thickness of (11±1) μm, which exhibited 0.35 mol/m^2-s H_2 flux at 773 K and 345 kPa pressure [55]. Kulprathipanja et al., reported about fabrication of Pd_{75}-Cu_{25} membrane by electroless plating on porous ceramic tubular support with a film thickness of 2 to 4 μm, which exhibited H_2 flux of (2.3±0.1) x 10^{-7} mol/s/m^2/Pa at 723 K and 430 kPa pressure [64]. In another literature, Roa et al., reported to fabricate Pd_{78}-Cu_{22} membrane by electroless plating method on

tubular porous ceramic support with a film thickness of (12.5±1) μm, which exhibited 0.17 mol/m^2-s H_2 flux at 723 K and 427 kPa pressure [65]. Yang et al., claimed to fabricate $Pd_{60}Cu_{40}$/V-15Ni membrane with a film thickness of 200 nm, which had a maximum H_2 flux of 3.72 x 10^{-8} $molm^{-1}s^{-1}Pa^{-1/2}$ at 573 K, by co-sputtering method [60, 66-67]. Hoang et al., reported to fabricate Pd-Cu alloy membrane on silicon support with a film thickness of 750 nm by dual sputtering method, which had H_2 flux of 1.6 mol/m^2-s at a temperature of 725 K [2]. Gao et al., reported to fabricate $Pd_{46}Cu_{54}/ZrO_2$ membrane with a film thickness of 10 μm on porous stainless steel support, which they claimed had a maximum H_2 flux of 1.1 x 10^{-7} mol/m^2-s^{-1}Pa at 753 K, by electroless plating technique [37]. Pomerantz and Ma reported to fabricate high permeance Pd/Cu/Pd tri-layer membrane on porous stainless steel tubular support by electroless plating method which had a film thickness of 19 μm and H_2 permeance of 22.9 m^3/m^2 $bar^{0.5}h$ at 723 K [38]. However, they fabricated this tri-layer Pd-Cu membrane using bath agitation during electroless plating. They deposited 0.4 μm of Cu with a bath agitation speed of 400 rpm on an already prepared dense Pd membrane and deposited 0.15 μm of Pd through the displacement of Cu with a bath agitation speed of 400 rpm.

Therefore, considering our previous flux data of pure Pd and Pd-Ag membranes fabricated by SIEP method and different literature reports on H_2 permeance through Pd-Cu membranes fabricated by different methods discussed above; our Pd-Cu membrane fabricated by SIEP method offers comparable and in some cases better H_2 flux data, with an average film thickness of 15.38 μm over MPSS support.

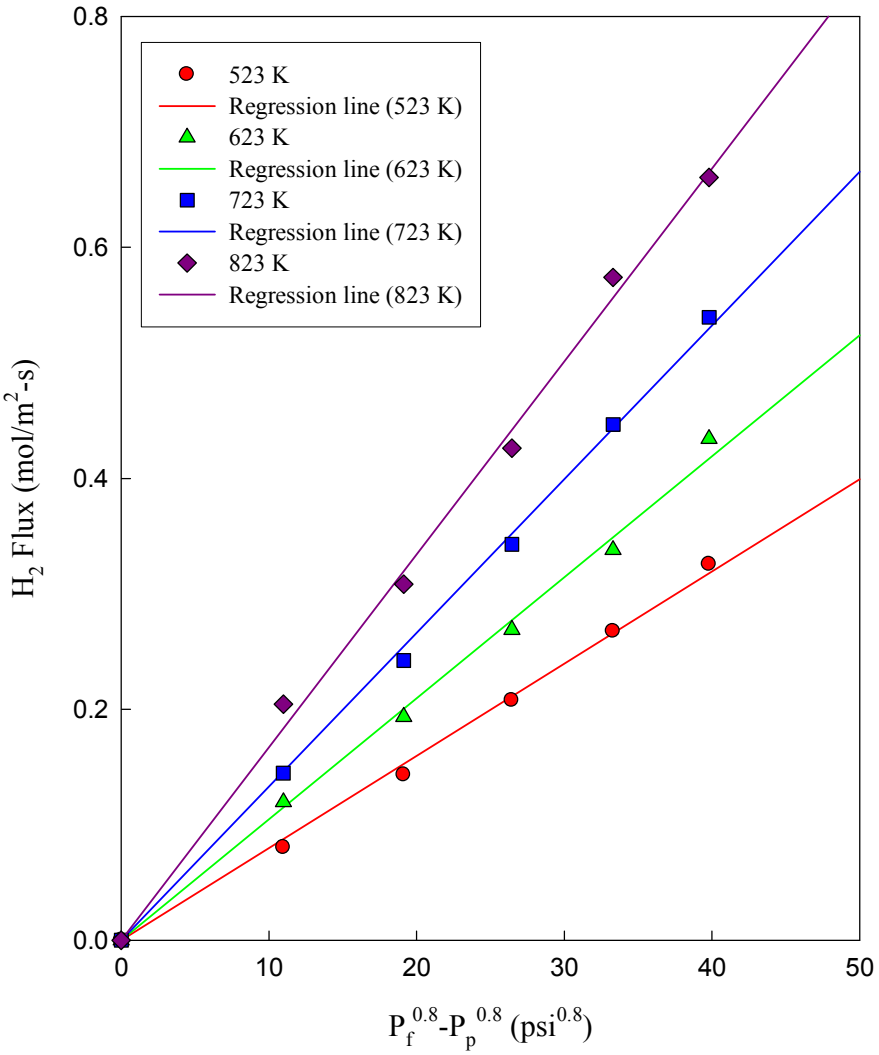

Figure 4.32. Hydrogen flux data of Pd-Cu membrane (S2) thickness of 16.73 µm after heat treatment at different temperatures fabricated by SIEP method

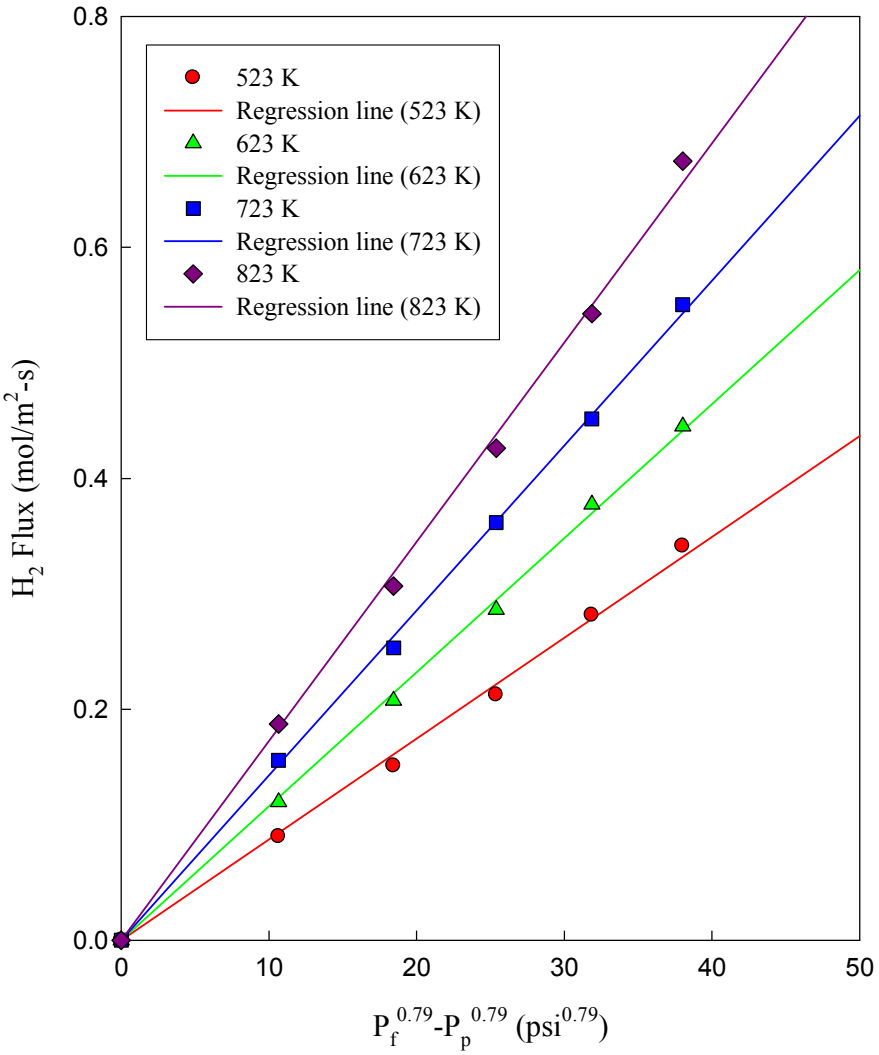

Figure 4.33 Hydrogen flux data of Pd-Cu membrane (S3) thickness of 14.5 µm after heat treatment at different temperatures fabricated by SIEP method

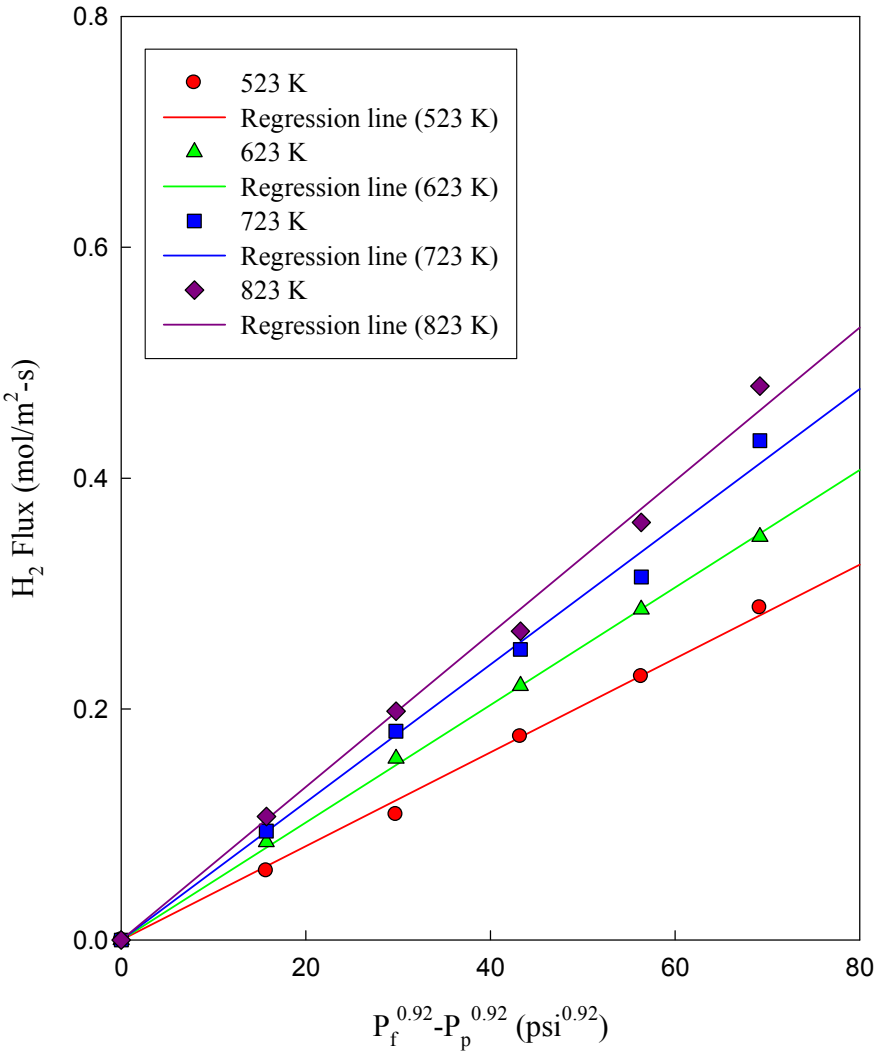

Figure 4.34. Hydrogen flux data of Pd-Cu membrane (C1) thickness of 19.18 µm after heat treatment at different temperatures fabricated by CEP method

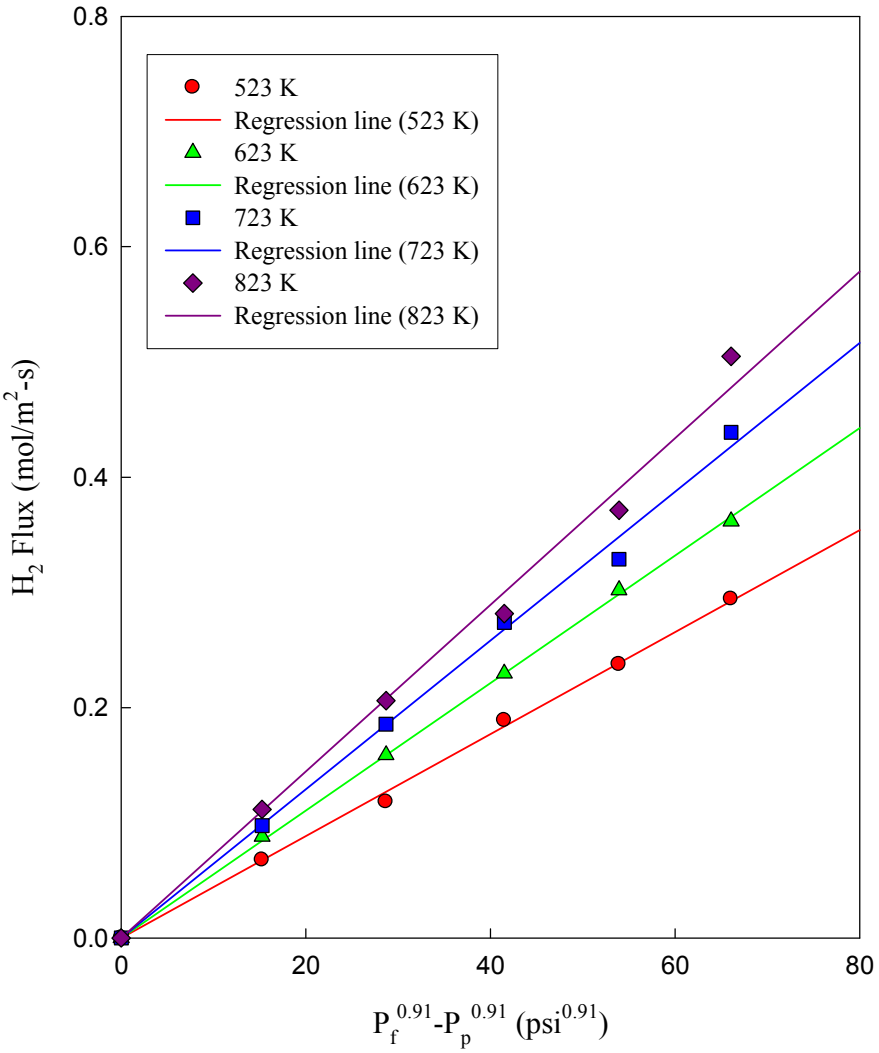

Figure 4.35. Hydrogen flux data of Pd-Cu membrane (C2) thickness of 20.17 µm after heat treatment at different temperatures fabricated by CEP method

An obvious and encouraging change was noticed while; hydrogen to nitrogen (H_2/N_2) selectivity data was compared before and after heat treatment, for each membrane fabricated by SIEP method. Hydrogen to nitrogen (H_2/N_2) selectivity increased from 84 to 186 at 20 psi and 823 K for Pd-Cu membrane (S2) fabricated by SIEP method shown in Figure 4.36. For another Pd-Cu membrane (S3), hydrogen to nitrogen (H_2/N_2) selectivity increased from 48 to 170 at 20 psi and 823 K, fabricated by SIEP method shown in Figure 4.37. Hence, the intermediate heat treatment followed by a deposition of mono layers of Pd and Cu films on top of membrane surface, caused to increase the selectivity more than double. In contrast, Pd-Cu membrane (C1) fabricated by CEP method, hydrogen to nitrogen (H_2/N_2) selectivity increased from 22 to 23 at 20 psi and 823 K, presented in Figure 4.38. Another Pd-Cu membrane (C2) fabricated by CEP method, hydrogen to nitrogen (H_2/N_2) selectivity showed no change at all at 20 psi and 823 K, after intermediate heat treatment followed by a deposition of mono layers of Pd and Cu films on top of the membrane surface, presented in Figure 4.39.

A reasonable explanation might be during heat treatment all the volatiles and oxygen entrapped inside film escaped. During cooling, most of the inter-granular spaces were plugged by the migration of metals from surrounding areas. However, some of the spaces were left open on the top surface creating channels for gases. As a result, selectivity was not high enough before heat treatment for membranes fabricated by SIEP method. There was no deep channeling from top of the film to substrate surface before heat treatment in Pd-Cu film. Plugging pin holes on top surface resulted from annealing, by deposition of mono layers of Pd and Cu films causing Pd-Cu alloy film to be free of

defects and less permeable to N_2, results increase in selectivity. However, for membranes fabricated by CEP method may have permanent channeling and pin holes inside the films before heat treatment, which ultimately not plugged; hence, did not increase selectivity of membranes after final mono layer deposition of Pd and Cu film on existing Pd-Cu films.

In our previous works we reported H_2/N_2 selectivity of pure Pd membrane fabricated by SIEP method was 312 at 823 K and 40 psi pressure, and H_2/N_2 selectivity of Pd-Ag membrane fabricated by SIEP method was 297 at 823 K and 40 psi pressure [11-12]. Roa et al., fabricated Pd_{80}-Cu_{20} membrane by electroless plating method on tubular porous ceramic support with a film thickness of (11±1) μm, which had H_2/N_2 selectivity of 70 at 773 K and 345 kPa pressure [55]. They also reported to fabricate Pd_{78}-Cu_{22} membrane with a film thickness of (12.5±1) μm, which had H_2/N_2 selectivity of 206 at 723 K and 427 kPa pressure [65]. Kulprathipanja et al., reported about fabrication of Pd_{75}-Cu_{25} membrane by electroless plating on porous ceramic tubular support with a film thickness of 2 to 4 μm, which had H_2/N_2 selectivity greater than 150 at 723 K and 430 kPa pressure [64]. Hoang et al., reported to fabricate Pd-Cu alloy membrane on silicon support with a film thickness of 750 nm by dual sputtering method, which had H_2/He selectivity of at least 500 at a temperature of 725 K [2]. Gao et al., reported to fabricate $Pd_{46}Cu_{54}/ZrO_2$ membrane with a film thickness of 10 μm on porous stainless steel support, which they claimed had an infinite separation factor for H_2 over N_2 at 753 K, by electroless plating technique [37]. This discussion suggests that we are able to fabricate Pd-Cu membrane by SIEP method which has comparable H_2/N_2 selectivity compared to other Pd-Cu membranes mentioned in literatures.

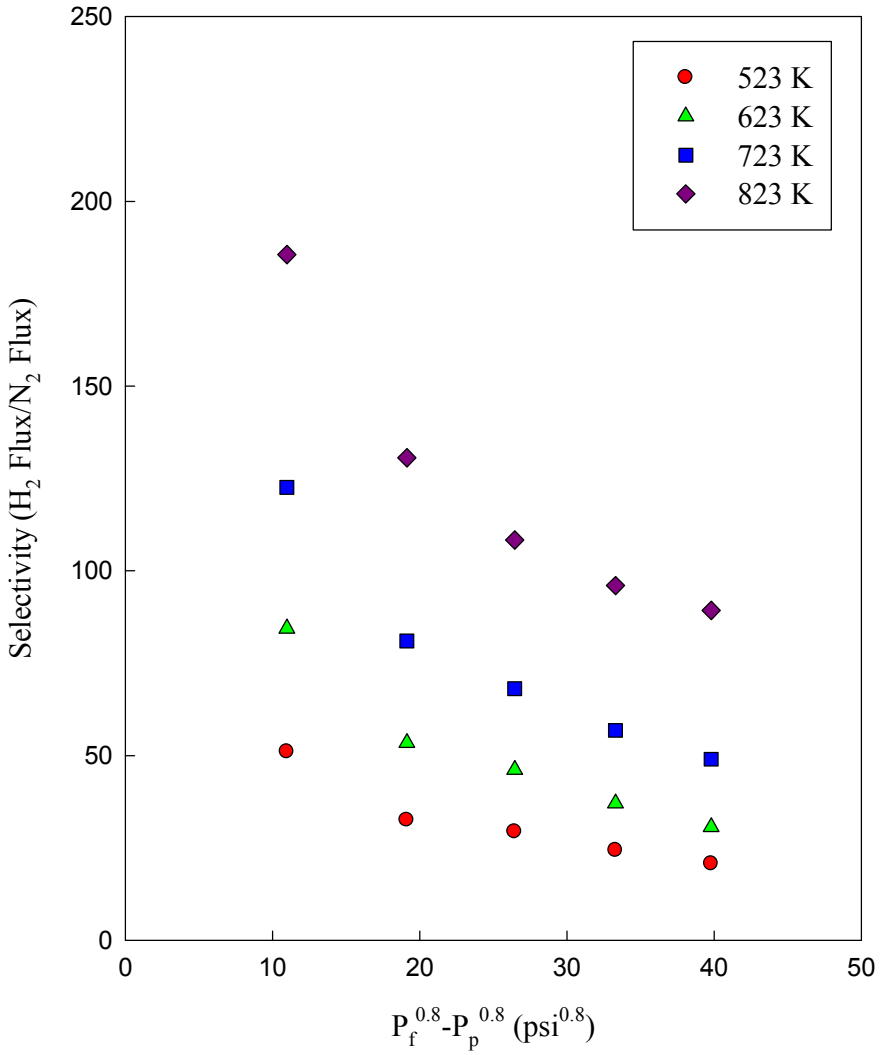

Figure 4.36. Hydrogen to Nitrogen (H_2/N_2) selectivity data of Pd-Cu membrane (S2) thickness of 16.73 µm after heat treatment at different temperatures fabricated by SIEP method

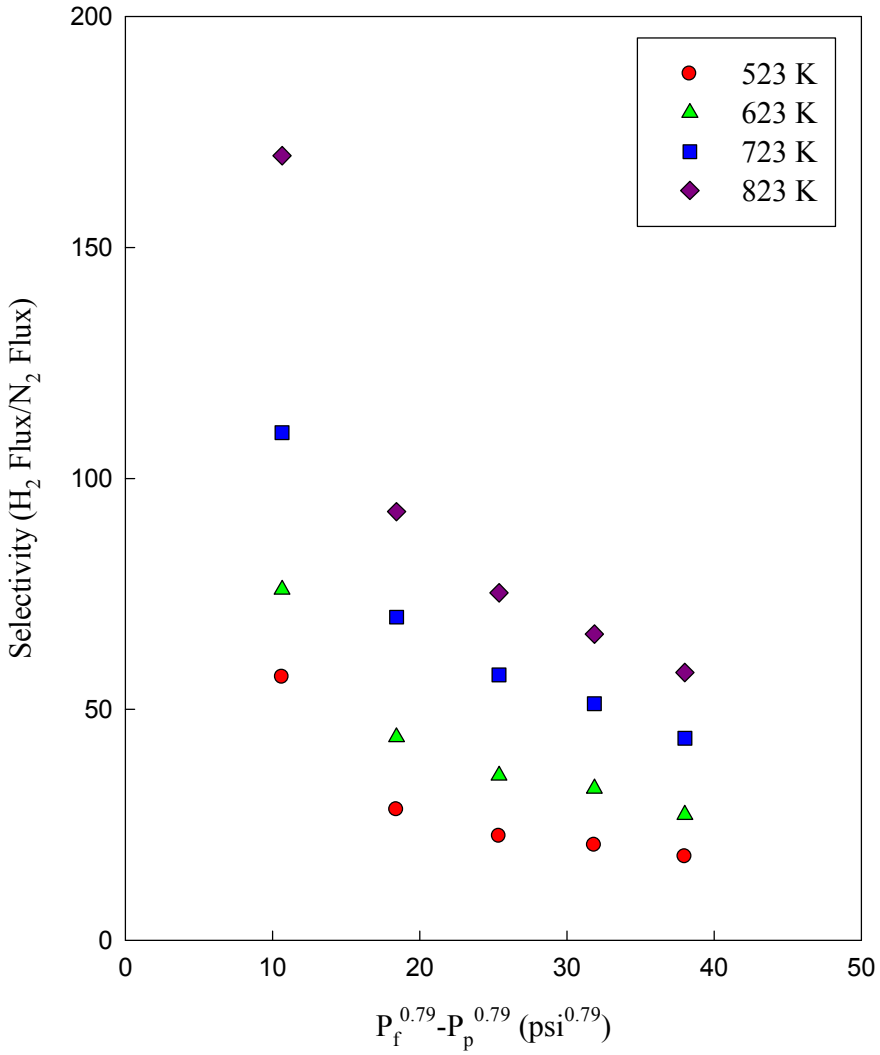

Figure 4.37. Hydrogen to Nitrogen (H_2/N_2) selectivity data of Pd-Cu membrane (S3) thickness of 14.5 µm after heat treatment at different temperatures fabricated by SIEP method

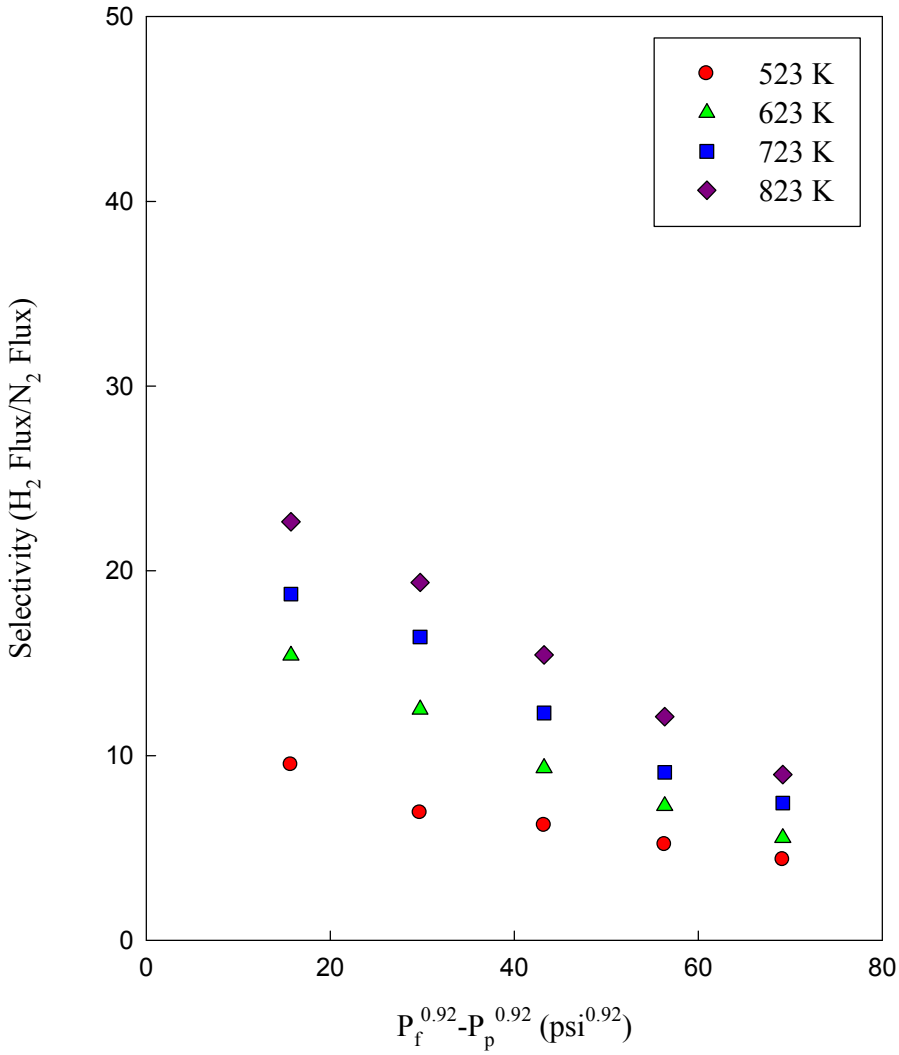

Figure 4.38. Hydrogen to Nitrogen (H_2/N_2) selectivity data of Pd-Cu membrane (C1) thickness of 19.18 µm after heat treatment at different temperatures fabricated by CEP method

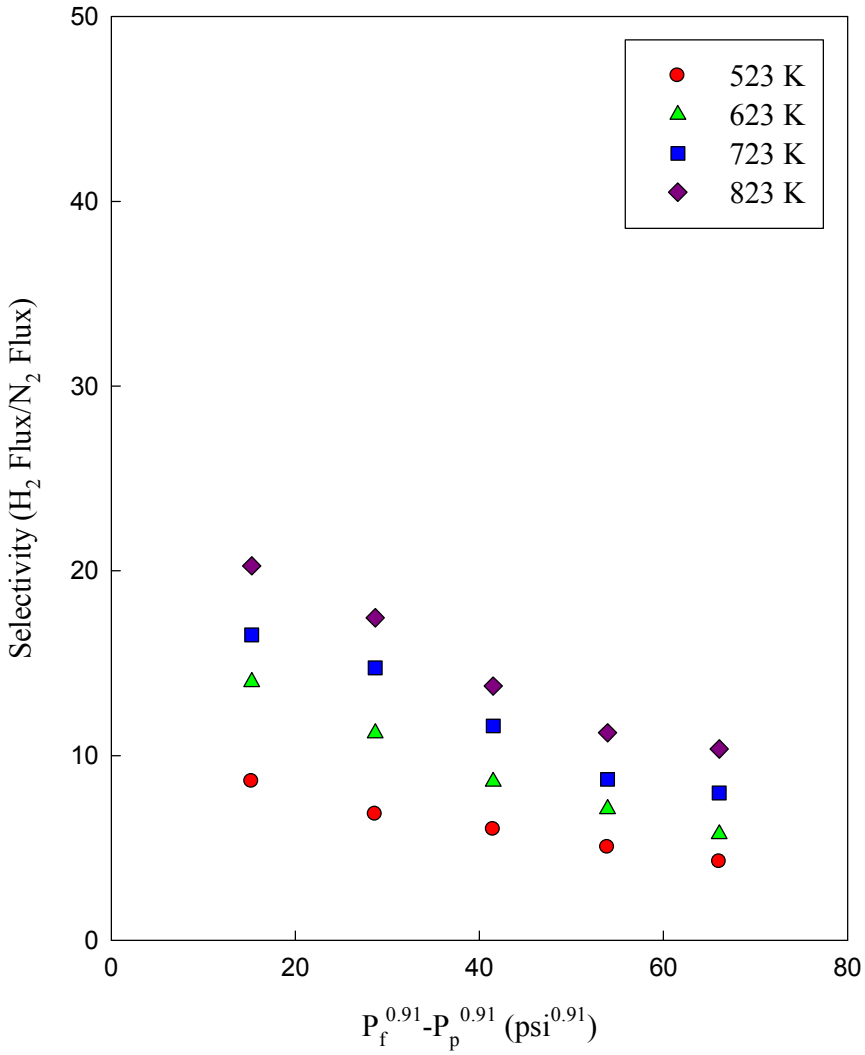

Figure 4.39. Hydrogen to Nitrogen (H_2/N_2) selectivity data of Pd-Cu membrane (C2) thickness of 20.17 µm after heat treatment at different temperatures fabricated by CEP method

It is very common that two membranes with same thickness, alloy composition, and subject to same operating temperature can exhibit very different permeance values. Therefore, to evaluate the exponent (n) of Sievert's law equation, its meaning has to be investigated in relation to the membrane properties. For example, if membrane selectivity is not infinite, effect of other diffusion mechanisms (like Knudsen-diffusion) could be relevant. Therefore, in this case, exponent (n) value cannot be used to analyze the intrinsic membrane behavior. In other works, when infinitely selective membrane are considered, some considerations about the rate-determining step can be drawn from the value of exponent (n), however, this information should be coupled and analyzed together with the overall activation energy of the permeance. A low value of the activation energy (<∼30 KJ/mol) indicates that the surface phenomena of dissociative adsorption and recombinative desorption do not provide significant influence on permeation process since they are characterized by a quite higher activation energy (∼54-146 KJ/mol) [59].

Therefore, to study the effect of diffusion mechanism on intrinsic membrane behavior we computed permeability coefficients Q_H at four different temperatures are shown in Figures 4.40 and 4.41 as Arrhenius plot (Q_H vs. $1/T$) for Pd-Cu membranes fabricated by both SIEP and CEP methods. It provides an excellent fit of the data to Arrhenius equation:

$$Q_H = Q_{Ho} \exp(-E/RT) \tag{4.2}$$

Where, Q_{Ho} is reference permeance, E is activation energy, T is absolute temperature and R is the universal gas constant. We calculated the activation energy of permeance (E) for Pd-Cu membranes fabricated by both SIEP and CEP methods from Figure 4.40 and

Figure 4.41. The activation energy (*E*) for Pd-Cu membrane fabricated by SIEP method, which had a film thickness of 13.34 μm is 8.6 KJ/mol, where as activation energy (*E*) for Pd-Cu membrane fabricated by CEP method, which had a film thickness of 20.17 μm is 5.7 KJ/mol. In our previous study we found that activation energy (*E*) for Pd membrane fabricated by SIEP method, which had a film thickness of 8.5 μm was 9.7 KJ/mol and activation energy (*E*) for Pd-Ag membrane fabricated by SIEP method, which had a film thickness of 13 μm was 8.9 KJ/mol [11]. Table 4.3 presents different parameters related to the activation energy (*E*) of different membranes. From the values of the activation energy (*E*), we see that with increase in film thickness of membranes, value of activation energy decreases, which suggests that the surface phenomena of dissociative adsorption and recombinative desorption do not provide significant influence on permeation process of our fabricated Pd and Pd alloy (Pd-Ag and Pd-Cu) membranes.

Table 4.3 Comparison of values of activation energy of different membranes fabricated by SIEP and CEP methods

Name of Membrane	Fabrication Process	Film Thickness of membrane, (μm)	Pre-exponential Factor, (Q_{Ho})	Activation Energy (*E*), (KJ/mol)
Pd	SIEP	8.5	0.65	9.7
Pd-Ag	SIEP	13	0.84	8.9
Pd-Cu	SIEP	13.34	0.79	8.6
Pd-Cu	CEP	20.17	0.91	5.7

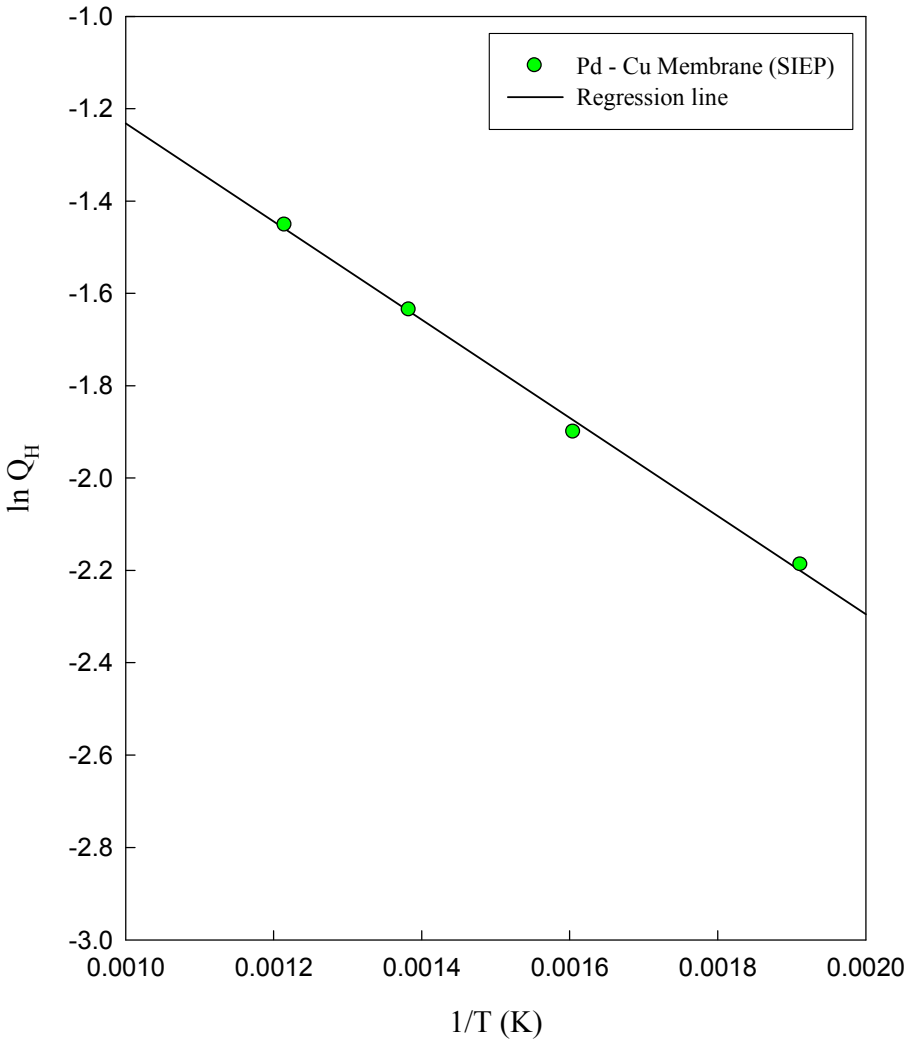

Figure 4.40. Arrhenius plot of H_2-permeability coefficients of Pd-Cu MPSS membrane fabricated by SIEP method

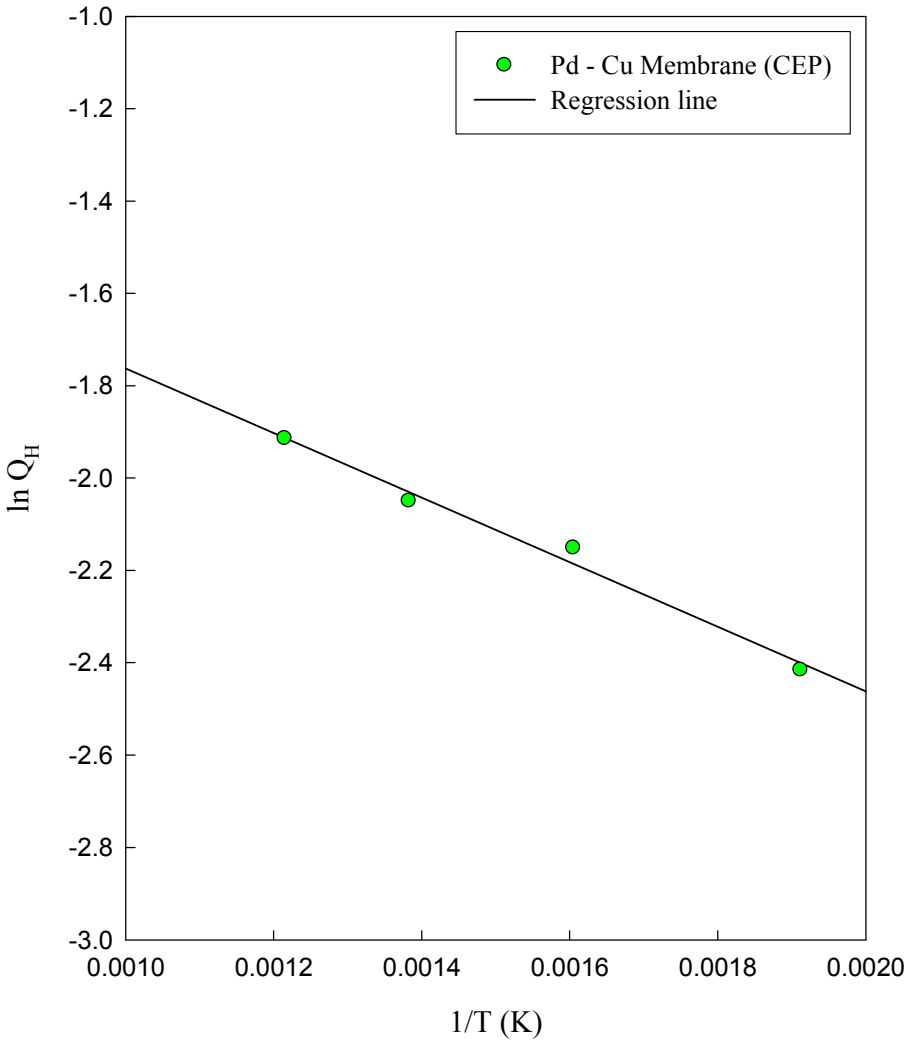

Figure 4.41. Arrhenius plot of H_2-permeability coefficients of Pd-Cu MPSS membrane fabricated by CEP method

4.3.2 Study of Thermal Stability of Pd-Cu Membrane

Finally, Pd-Cu membrane prepared by SIEP method underwent a long term thermal stability test. For a period of 90 days, the Pd-Cu membrane underwent numerous cycles of temperature changes from 573 K to 873 K and again back to 573 K, at 10 psi pressure in on and off mode (8 to 10 hours a day) and H_2 flux was measured. The membrane was tested for almost 720 hours of operation. The thermal stability test was carried out in our existing stability measurement set-up shown in Figure 3.1 of chapter 3. Each day of testing the Pd-Cu membrane fabricated by SIEP method underwent a couple of cycles of temperature from 573 K - 873 K - 573 K, and the average data of H_2 flux for each day are plotted shown in Figure 4.42. From Figure 4.42, it is clear that for first 5 to 6 days, the H_2 flux of membrane went down as we assumed that Pd and Cu metals were still diffused into the substrate layer and reorientation of these metals were taking place inside the film. Afterwards, H_2 flux increased and membrane exhibited stable H_2 flux for next 65 days. Then, H_2 flux increased a little over time. However, the membrane was still stable and good to separate H_2 from other gas mixtures. During thermal stability test Pd-Cu membrane had an average flux of 0.0922 mol/m^2-s, with a standard deviation of 1.27% at 573 K, and had an average flux of 0.13357 mol/m^2-s, with a standard deviation of 1.65% at 873 K. So, from stability study, it is clear that, Pd-Cu membrane fabricated by SIEP method showed stability under thermal cycling in between high and low temperature ranges for a period of ninety days. The thermal stability test results are very encouraging, and we believe if further test is conducted, Pd-Cu membrane fabricated by SIEP method will be stable more than ninety days.

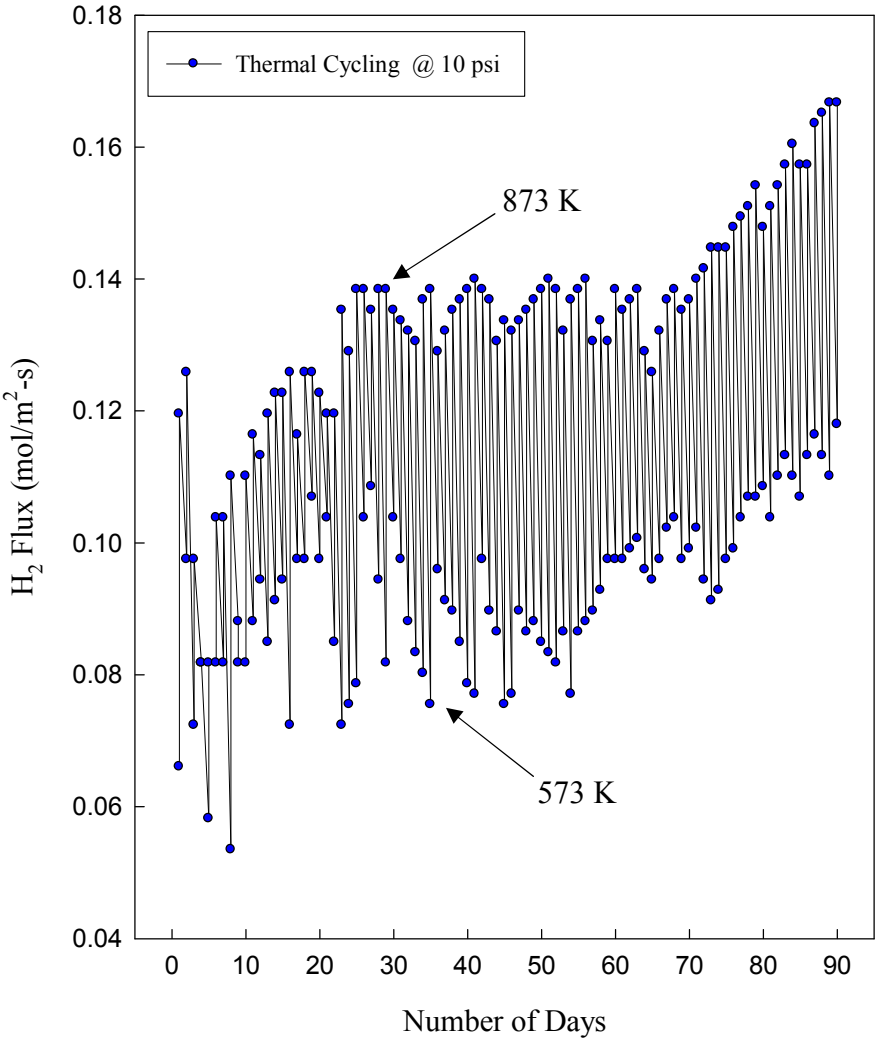

Figure 4.42: H_2 flux data of Pd-Cu MPSS membrane under thermal cycling fabricated by SIEP method

CHAPTER 5

Conclusion

The use of DTAB surfactant in SIEP process found to be efficient in fabricating Pd-Cu membrane. Consequently, grain agglomeration was observed in a larger scale in membranes fabricated by SIEP process compared to Pd-Cu membrane fabricated by CEP process. The particle size found was smaller and it was in the range of 0.65 to 1.01425 μm for Pd-Cu membrane fabricated by SIEP process. The interaction of two metals in a sequential deposition method actually reduces the grain size. The reduction of particle size basically helped to form relatively smooth and uniform Pd-Cu film. The smaller grain size and larger grain agglomeration, eventually, helped fabricating thinner films for Pd-Cu membrane in a shorter plating time. In absence of surfactant, a larger plating time and thicker film is required to make membrane helium gas-tight. Based on the previous studies of Pd membrane fabrication, four Pd-Cu membranes were fabricated by SIEP process. In every instance, all the membranes showed similar surface morphology. Actually, enhanced grain agglomeration improves hydrogen permeability which is consistent with the literature.

Heat treatment under H_2 environment at 773 K for 18 hours was sufficient to minimize MPSS constituent metals (Fe, Ni & Cr) diffusion inside the film. Studies on lattice parameter showed there was actually no or little migration of Fe into Pd-Cu alloy film. The annealing time and temperature used in these studies were sufficient to form stable Pd-Cu alloys. Heat treatment increased the grain agglomeration and formed larger

grains and in some cases a continuous film. The cross-sections of Pd-Cu film showed deep penetration of the deposited metals. But Cu deposition was found throughout the film and deep into substrate after heat treatment. It was Pd particles, which actually plugged the pores deep inside the substrate. However, the migration of Cu after annealing was found as deep as 25 μm (approximately) inside the film from top surface of the film. The EDS mapping and line scanning showed the metal distribution in the film, as well as, in the substrate. It is difficult to fabricate two different membranes having same Cu contents and with same film thickness. Also the effect of heat treatment is different in membranes having different metal composition.

The H_2 flux data and hydrogen to nitrogen (H_2/N_2) selectivity data showed that Pd-Cu membrane fabricated by SIEP method was better than the Pd-Cu membrane fabricated by CEP method. Although, H_2 permeability varies from membrane to membrane, the membranes fabricated by SIEP method showed superior selectivity data in all cases, which is very encouraging. The long term (for a period of 90 days) thermal stability data indicated that Pd-Cu membrane fabricated by SIEP method was very stable in rigorous exposure to low and high temperatures.

It can be concluded that use of surfactant in plating baths reduced the grain size, increased grain agglomeration and increased rate of deposition of Pd and Cu metals. As a result, it formed a thinner, smooth and uniform film and further heat treatment improved grain agglomeration and uniform alloy formation. This actually results a fine Pd-Cu membrane with better hydrogen transport, superior selectivity and thermally stable membrane compared to membranes fabricated by conventional electroless plating.

5.1 Future Works and Recommendations

It is required to extend the scope of SIEP to other Pd-alloys, such as, Pd-Ni and other tri-metallic membranes, as it will reduce membrane fabrication cost considerably. Additionally, SIEP process produces membrane with thinner film with higher H_2 permeability and superior selectivity. Also it is time now to identify the actual surfactant concentration which will provide the optimum surface activity. To further develop the Pd-alloy membranes and demonstrate its technical viability, we suggest the following for future works:

- Co-ordination of Pd^{+2}/EDTA could be extended to understand the actual grain growth kinetics in presences of different complexes during surfactant induced electroless process. It is also necessary to reveal the role of pH on complexation and further bath stabilization process. Study of bath kinetics for both Pd and Cu baths will give important clues how the surfactant interacts with other chemicals during deposition period. Intermediate SEM and XRD analysis of Pd-Cu membrane morphology deposited at shorter time intervals would further explain the effect of complex on in-situ grain formation and grain distribution. The development of Pd-Cu alloy using electroless plating is critically dependent upon suitable over potential and overall plating kinetics. Fundamental studies on bath kinetics would be helpful to choose suitable complexing agent, operating conditions and appropriate bath recipe during Pd-Cu membrane development, which will ultimately results a thin film Pd-Cu membrane with superior selectivity under extreme process conditions.

- Using the Pd-Cu film fabrication technique developed in this work (surfactant induced electroless plating - SIEP), other Pd-alloy films, such as, Pd-Ni and Pd-Au should be fabricated with proper alloy compositions that would be thermally stable and resist H_2-embrittlement during long-term thermal cycling operation in extreme conditions.
- Long term thermal cycling and stability study for a period of one year needs to be conducted for Pd-Cu membrane fabricated by SIEP process. This has to be conducted as a continuation of this work.
- Pd-Cu membrane fabricated by SIEP method needs to be tested in membrane reactor configuration to produce H_2. To demonstrate the use of these membranes in membrane reactors, experimental study of equilibrium limited reforming reactions, and dehydrogenation reactions of industrial significance should be conducted.
- Finally, scale up of our work has to be under taken for proto type development.

REFERENCES

[1] Bryden, K. J. and Ying, J. Y., "Nanostructured Palladium-Iron Membranes for Hydrogen Separation and Membrane Hydrogenation Reactions," *Journal of Membrane Science,* **203**, 29 (2002).

[2] Hoang, H. T., Tong, H. D., Gielens, F. C., Jansen, H. V., and Elwenspoek, M. C., "Fabrication and Characterization of Dual Sputtered Pd-Cu Alloy Films for Hydrogen Separation Membranes," *Materials Letters,* **58**, 525 (2004).

[3] Ayturk, M. E., Mardilovich, I. P., Engwall, E. E., and Ma, Y. H., "Synthesis of Composite Pd-Porous Stainless Steel (PSS) Membranes with a Pd/Ag Intermetallic Diffusion Barrier," *Journal of Membrane Science,* **285**, 385 (2006).

[4] Ayturk, M. E. and Ma, Y. H., "Electroless Pd and Ag Deposition Kinetics of the Composite Pd and Pd/Ag Membranes Synthesized from Agitated Plating Baths," *Journal of Membrane Science,* **330**, 233 (2009).

[5] Gielens, F. C., Tong, H. D., Vorstman, M. A. G., and Keurentjes, J. T. F., "Measurement and Modeling of Hydrogen Transport through High-Flux Pd Membranes," *Journal of Membrane Science,* **289**, 15 (2007).

[6] Itoh, N., Kaneko, Y., and Igarashi, A., "Efficient Hydrogen Production via Methanol Steam Reforming by Preventing Back-Permeation of Hydrogen in a Palladium Membrane Reactor," *Industrial & Engineering Chemistry Research,* **41**, 4702 (2002).

[7] Kikuchi, E., Nemoto, Y., Kajiwara, M., Uemiya, S., and Kojima, T., "Steam Reforming of Methane in Membrane Reactors: Comparison of Electroless-Plating and CVD Membranes and Catalyst Packing Modes," *Catalysis Today,* **56**, 75 (2000).

[8] Lin, Y.-M., Lee, G.-L., and Rei, M.-H., "An Integrated Purification and Production of Hydrogen with a Palladium Membrane-Catalytic Reactor," *Catalysis Today,* **44**, 343 (1998).

[9] Yeung, K. L., Sebastian, J. M., and Varma, A., "Novel Preparation of Pd/Vycor Composite Membranes," *Catalysis Today,* **25**, 231 (1995).

[10] Nam, S.-E. and Lee, K.-H., "Preparation and Characterization of Palladium Alloy Composite Membranes with a Diffusion Barrier for Hydrogen Separation," *Industrial & Engineering Chemistry Research,* **44**, 100 (2005).

[11] Rahman, M. M., "Fabrication of Pd and Pd-Ag Membranes by Surfactant Induced Electroless Plating (SIEP)," MS Thesis, Chemical and Bioengineering, North Carolina A&T State University, Greensboro, NC (2010).

[12] Islam, M. A., "The Development of Improved Electroless Plating in Fabricating Pd-Based Membrane and Membrane Reactor Application for Hydrogen Separation," PhD Dissertation, Energy and Environmental Studies, North Carolina A&T State University, Greensboro, NC (2008).

[13] Hsieh, H. P., Inorganic Membranes for Separation and Reaction, New York, NY, Elsevier, 1996.

[14] Lakshminarayanaiah, N., Equations of Membrane Biophysics, London, UK, Academic Press, 1984.

[15] Graham, T., "On the Molecular Mobility of Gases," *Philosophical Transactions of the Royal Society of London,* **153**, 385 (1863).

[16] Ilias, S. and Islam, M. A., "Methods of Preparing Thin Films by Electroless Plating," United States Patent Application 20100068391, March 18, 2010.

[17] Shu, J., Grandjean, B. P. A., Neste, A. V., and Kaliaguine, S., "Catalytic Palladium-Based Membrane Reactors: A Review," *The Canadian Journal of Chemical Engineering,* **69**, 1036 (1991).

[18] Mckinley, D. L., "Metal Alloy for Hydrogen Separation and Purification," United States Patent 3350845, 1967.

[19] Nair, B. K. R., Choi, J., and Harold, M. P., "Electroless Plating and Permeation Features of Pd and Pd/Ag Hollow Fiber Composite Membranes," *Journal of Membrane Science,* **288**, 67 (2007).

[20] Smith, D. L., Thin-Film Deposition Principles & Practices, New York, NY, McGraw Hill, 1995.

[21] Thoen, P. M., Roa, F., and Way, J. D., "High Flux Palladium-Copper Composite Membranes for Hydrogen Separations," *Desalination,* **193**, 224 (2006).

[22] Tierney, H. L., Baber, A. E., and Sykes, E. C. H., "Atomic-Scale Imaging and Electronic Structure Determination of Catalytic Sites on Pd/Cu near Surface Alloys," *The Journal of Physical Chemistry C,* **113**, 7246 (2009).

[23] Itoh, N., Niwa, S., Mizukami, F., Inoue, T., Igarashi, A., and Namba, T., "Catalytic Palladium Membrane for Reductive Oxidation of Benzene to Phenol," *Catalysis Communications,* **4**, 243 (2003).

[24] Ward, T. L. and Dao, T., "Model of Hydrogen Permeation Behavior in Palladium Membranes," *Journal of Membrane Science,* **153**, 211 (1999).

[25] Yeung, K. L., Christiansen, S. C., and Varma, A., "Palladium Composite Membranes by Electroless Plating Technique: Relationships between Plating Kinetics, Film Microstructure and Membrane Performance," *Journal of Membrane Science,* **159**, 107 (1999).

[26] Grashoff, G. J., Pilkington, C. E., and Corti, C. W., "The Purification of Hydrogen," *Platinum Metals Review,* **27**, 157 (1983).

[27] Yun, S. and Ted Oyama, S., "Correlations in Palladium Membranes for Hydrogen Separation: A Review," *Journal of Membrane Science,* **375**, 28 (2011).

[28] Lewis, F. A., The Palladium Hydrogen System, New York, Academic Press, 1967.

[29] Knapton, A. G., "Palladium Alloys for Hydrogen Diffusion Membranes," *Platinum Metals Review,* **21**, 44 (1977).

[30] Ayturk, M. E., Engwall, E. E., and Ma, Y. H., "Microstructure Analysis of the Intermetallic Diffusion-Induced Alloy Phases in Composite Pd/Ag/Porous Stainless Steel Membranes," *Industrial & Engineering Chemistry Research,* **46**, 4295 (2007).

[31] Chen, Y., Atago, T., and Mohri, T., "First-Principles Study for Ordering and Phase Separation in the Fe-Pd System," *Journal of Physics: Condensed Matter,* **14**, 1903 (2002).

[32] Hunter, J. B., *Platinum Metals Review,* **4**, 130 (1960).

[33] Darling, A. S., British Patent 827681, 1958.

[34] Darling, A. S., British Patent 956176, 1964.

[35] Massalski, T. B., Okamoto, H., Subramanian, P. R., and Kacprzak, L., Binary Alloy Phase Diagrams, 2nd ed., ASM International, 1990.

[36] Guazzone, F., "Engineering of Substrate Surface for the Synthesis of Ultra-Thin Composite Pd and Pd-Cu Membranes for H_2 Separation," PhD Dissertation, Worcester Polytechnic Institute, Worcester, MA (2005).

[37] Gao, H., Lin, J. Y. S., Li, Y., and Zhang, B., "Electroless Plating Synthesis, Characterization and Permeation Properties of Pd-Cu Membranes Supported on ZrO_2 Modified Porous Stainless Steel," *Journal of Membrane Science,* **265**, 142 (2005).

[38] Pomerantz, N. and Ma, Y. H., "Novel Method for Producing High H_2 Permeability Pd Membranes with a Thin Layer of the Sulfur Tolerant Pd/Cu FCC Phase," *Journal of Membrane Science,* **370**, 97 (2011).

[39] Nam, S.-E. and Lee, K.-H., "Hydrogen Separation by Pd Alloy Composite Membranes: Introduction of Diffusion Barrier," *Journal of Membrane Science,* **192**, 177 (2001).

[40] Nam, S.-E. and Lee, K.-H., "A Study on the Palladium/Nickel Composite Membrane by Vacuum Electrodeposition," *Journal of Membrane Science,* **170**, 91 (2000).

[41] Nam, S.-E., Lee, S.-H., and Lee, K.-H., "Preparation of a Palladium Alloy Composite Membrane Supported in a Porous Stainless Steel by Vacuum Electrodeposition," *Journal of Membrane Science,* **153**, 163 (1999).

[42] Gryaznov, V., "Metal Containing Membranes for the Production of Ultrapure Hydrogen and the Recovery of Hydrogen Isotopes," *Separation and Purification Methods,* **29**, 171 (2000).

[43] Ma, Y. H., Mardilovich, I. P., and Engwall, E. E., "Thin Composite Palladium and Palladium/Alloy Membranes for Hydrogen Separation," *Annals of the New York Academy of Sciences,* **984**, 346 (2003).

[44] Huang, T.-C., Wei, M.-C., and Chen, H.-I., "Preparation of Hydrogen-Permselective Palladium-Silver Alloy Composite Membranes by Electroless Co-Deposition," *Separation and Purification Technology,* **32**, 239 (2003).

[45] Rhoda, R. N. and Ann-Mari, M., "Palladium Plating by Chemical Reduction," United States Patent 2915406, 1959.

[46] Ma, Y. H., Akis, B. C., Ayturk, M. E., Guazzone, F., Engwall, E. E., and Mardilovich, I. P., "Characterization of Intermetallic Diffusion Barrier and Alloy Formation for Pd/Cu and Pd/Ag Porous Stainless Steel Composite Membranes," *Industrial & Engineering Chemistry Research,* **43**, 2936 (2004).

[47] Ma, Y. H., Mardilovich, P. P., and She, Y., "Hydrogen Gas-Extraction Module and Method of Fabrication," United States Patent 6152987, 2000.

[48] Mallory, G. O. and Hajdu, J. B., Electroless Plating Fundamentals and Applications, Norwich, NY, American Electroplaters and Surface Finishers Society, 2009.

[49] Souleimanova, R. S., Mukasyan, A. S., and Varma, A., "Pd-Composite Membranes Prepared by Electroless Plating and Osmosis: Synthesis, Characterization and Properties," *Separation and Purification Technology,* **25**, 79 (2001).

[50] Chen, B. H., Hong, L., Ma, Y., and Ko, T. M., "Effects of Surfactants in an Electroless Nickel-Plating Bath on the Properties of Ni-P Alloy Deposits," *Industrial & Engineering Chemistry Research,* **41**, 2668 (2002).

[51] Muller and Heinz, K., "Dependence of Thin-Film Microstructure on Deposition Rate by Means of a Computer Simulationn," *Journal of Applied Physics,* **58**, 2573 (1985).

[52] Kirchheim, R., Mütschele, T., Kieninger, W., Gleiter, H., Birringer, R., and Koblé, T. D., "Hydrogen in Amorphous and Nanocrystalline Metals," *Materials Science and Engineering,* **99**, 457 (1988).

[53] Gleiter, H., "Nanocrystalline Materials," *Progress in Materials Science,* **33**, 223 (1989).

[54] Islam, M. A. and Ilias, S., "Characterization of Pd-Composite Membrane Fabricated by Surfactant Induced Electroless Plating (SIEP): Effect of Grain Size on Hydrogen Permeability," *Separation Science and Technology,* **45**, 1886 (2010).

[55] Roa, F., Way, J. D., McCormick, R. L., and Paglieri, S. N., "Preparation and Characterization of Pd-Cu Composite Membranes for Hydrogen Separation," *Chemical Engineering Journal,* **93**, 11 (2003).

[56] Mardilovich, P. P., She, Y., Ma, Y. H., and Rei, M.-H., "Defect-Free Palladium Membranes on Porous Stainless-Steel Support," *AIChE Journal,* **44**, 310 (1998).

[57] Lin, W.-H. and Chang, H.-F., "Characterizations of Pd-Ag Membrane Prepared by Sequential Electroless Deposition," *Surface and Coatings Technology,* **194**, 157 (2005).

[58] Roa, F. and Way, J. D., "Influence of Alloy Composition and Membrane Fabrication on the Pressure Dependence of the Hydrogen Flux of Palladium-Copper Membranes," *Industrial & Engineering Chemistry Research,* **42**, 5827 (2003).

[59] Caravella, A., Scura, F., Barbieri, G., and Drioli, E., "Sieverts Law Empirical Exponent for Pd-Based Membranes: Critical Analysis in Pure H_2 Permeation," *The Journal of Physical Chemistry B,* **114**, 6033 (2010).

[60] Yang, J. Y., Komaki, M., and Nishimura, C., "Effect of Overlayer Thickness on Hydrogen Permeation of $Pd_{60}Cu_{40}$/V-15Ni Composite Membranes," *International Journal of Hydrogen Energy,* **32**, 1820 (2007).

[61] Collins, J. P. and Way, J. D., "Preparation and Characterization of a Composite Palladium-Ceramic Membrane," *Industrial & Engineering Chemistry Research,* **32**, 3006 (1993).

[62] Uemiya, S., Sato, N., Ando, H., Kude, Y., Matsuda, T., and Kikuchi, E., "Separation of Hydrogen through Palladium Thin Film Supported on a Porous Glass Tube," *Journal of Membrane Science,* **56**, 303 (1991).

[63] Caravella, A., Barbieri, G., and Drioli, E., "Modelling and Simulation of Hydrogen Permeation through Supported Pd-Alloy Membranes with a Multicomponent Approach," *Chemical Engineering Science,* **63**, 2149 (2008).

[64] Kulprathipanja, A., Alptekin, G. O., Falconer, J. L., and Way, J. D., "Effects of Water Gas Shift Gases on Pd-Cu Alloy Membrane Surface Morphology and Separation Properties," *Industrial & Engineering Chemistry Research,* **43**, 4188 (2004).

[65] Roa, F., Block, M. J., and Way, J. D., "The Influence of Alloy Composition on the H_2 Flux of Composite Pd-Cu Membranes," *Desalination,* **147**, 411 (2002).

[66] Yang, J. Y., Nishimura, C., and Komaki, M., "Preparation and Characterization of Pd-Cu/V-15Ni Composite Membrane for Hydrogen Permeation," *Journal of Alloys and Compounds,* **431**, 180 (2007).

[67] Yang, J. Y., Nishimura, C., and Komaki, M., "Effect of Overlayer Composition on Hydrogen Permeation of Pd-Cu Alloy Coated V-15Ni Composite Membrane," *Journal of Membrane Science,* **282**, 337 (2006).